

Università degli studi di Torino



PhD course in Pharmaceutical and Biomolecular  
Sciences

*Study of Gadolinium retention in  
principal organs of murine models*

*Candidate: Chiara Furlan*

*Supervisor: Prof. Eliana Gianolio*

# Contents

<b>Introduction</b>	<b>1</b>
Magnetic resonance Imaging	2
Gadolinium Based Contrast Agents	5
Gadolinium retention	7
Aim of the project	9
<b>Chapter 1: Influence of GBCAs structural variations and different formulation on Gd-retention</b>	<b>11</b>
1.1 Gd retention of Macrocyclic Lanthanide (III)-complexes with minor structural changes	13
1.2 Gd retention of GBCAs able to bind serum albumin	25
1.3 Gd retention upon the injection of a liposomal formulation of Gd-DTPABMA	35
<b>Chapter 2: Gd retention in pathology models</b>	<b>43</b>
2.1 Analysis of the Gadolinium retention in the Experimental Autoimmune Encephalomyelitis (EAE) murine model of Multiple Sclerosis	45
2.2 Inflammatory Bowel Disease (IBD-DSS)	63
<b>Chapter 3: Gadolinium retention in compartments other than Central Nervous System</b>	<b>73</b>
3.1 Gadolinium retention in Erythrocytes and Leukocytes from human and murine blood upon treatment with Gadolinium-Based Contrast Agents for Magnetic Resonance Imaging	75
3.2 In vivo study of a macrocyclic Gadolinium Based Contrast Agent and the retention in spleen, bones, and bladder	91
<b>General conclusions</b>	<b>111</b>
<b>References</b>	<b>115</b>



# INTRODUCTION

# Magnetic Resonance Imaging

Magnetic resonance imaging (MRI) is a powerful, non-invasive diagnostic medical imaging tool that is widely used for disease detection, diagnosis, and treatment monitoring.<sup>1</sup> MRI technique is based on production of images obtained through the spatial localization of water protons of observed tissues. Compared to NMR experiments, spatial information is given by the application of magnetic field gradients, so that water proton resonance depends on the position that these take up in observed tissues. To perform an MRI analysis, the body of the patient is placed in a strong magnetic field, allowing the stimulation of the atomic nuclei of hydrogens (protons) with a radio transmission, which can be detected as it returns to its pre-stimulation state<sup>2</sup>. Indeed, the excited hydrogen atoms emit a radio frequency signal, which is measured by a receiving coil.

The tissues are recognizable because contrast arises mainly from the differences in relaxation times of nuclei in different positions: the features are determined by the rate at which excited atoms return to the equilibrium state<sup>3</sup>. Indeed, the shape of the RF signal obtained depends on the number of nuclei present (a property called spin density) as well as on the time it takes for the nuclei to relax (called  $T_1$  &  $T_2$  relaxation processes)<sup>4</sup>. As mentioned before, when the protons are placed in a strong magnetic field, the nuclear spins reach their thermal equilibrium condition, which can be perturbed by an RF pulse.  $T_1$  is the time constant for regrowth of longitudinal magnetization ( $M_z$ ) to its initial maximum value ( $M_0$ ) parallel to  $B_0$ , the static magnetic field (Fig 1).

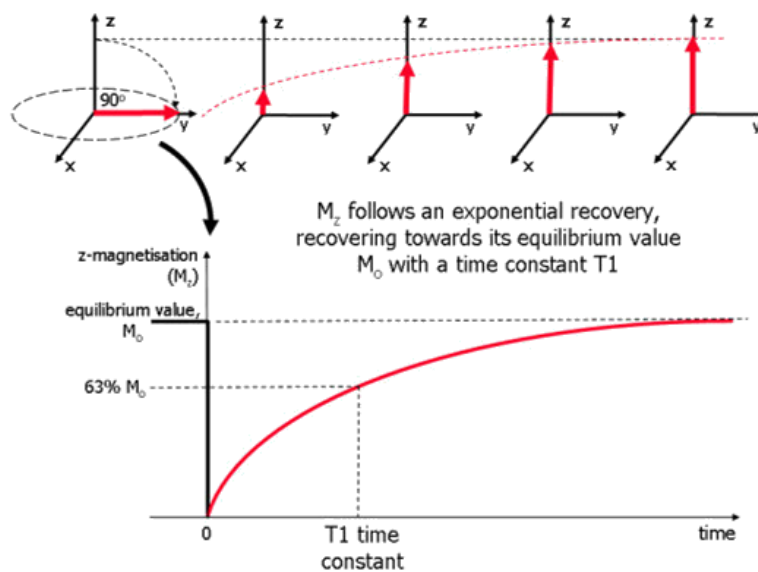


**Figure 1:** T1 relaxation process. From: Cardiovascular magnetic resonance physics for clinicians: part I J P Ridgway

$T_1$  is influenced by the chemical environment, therefore by the other atoms surrounding the nuclei.  $T_1$  relaxation is therefore also named *spin-lattice* relaxation or *longitudinal* relaxation. On the other hand,  $T_2$  relaxation is the process by which the transverse components of magnetization ( $M_{xy}$ ) decay or dephase.  $T_2$  is the time required for the transverse magnetization to fall to approximately 37% ( $1/e$ ) of its initial value (Fig 2). Synonyms for  $T_2$  relaxation are *transverse relaxation* and *spin-spin* relaxation<sup>5</sup>.

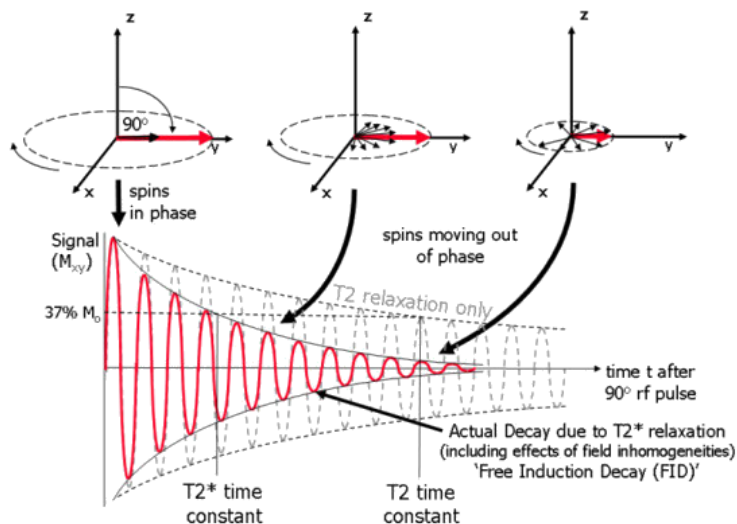


**Figure 2:** Transverse ( $T_2$  and  $T_2^*$ ) relaxation processes. From: Cardiovascular magnetic resonance physics for clinicians: part I JP Ridgway

MR signal intensity is affected by the contribution of intrinsic and extrinsic factors, among which proton spin density, longitudinal ( $T_1$ ) and transverse ( $T_2/ T_2^*$ ) relaxation times, chemical shifts of components, and instrumental parameters. Tissues generally differ in terms of endogenous signal; application of specific sequences, through modulation of instrument parameters, could emphasize this dissimilarity. The contrast can be also increased by the administration of appropriate contrast agents (CAs) that allow increasing the possibility to visualize vascular systems, inflammatory processes, the presence of tumours, etc...(Fig 3).

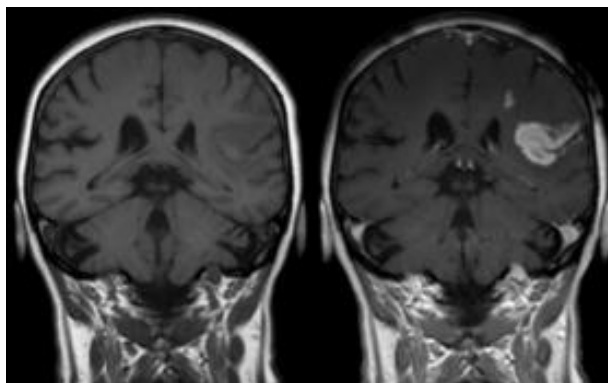


**Figure 3:** Effect of contrast agent on T1-weighted images. Left image without, right image with contrast medium administration

Numerous MRI probes, able to create or enhance the contrast, have been developed, and nowadays ca. 40% of clinical scans are commonly acquired upon their administration<sup>6</sup>. The prevalent mechanisms for contrast generation/enhancement act by shortening both longitudinal ( $T_1$ ) and transversal ( $T_2$ ) relaxation times in target tissues. Depending on whether their administration affects most  $T_1$  or  $T_2$ , these chemicals can be classified as  $T_1$  or  $T_2$  agents. The agents belonging to the  $T_1$  class are also known as positive contrast agents, as they increase the signal intensity (Fig 3). The most important representatives of this class are paramagnetic Mn- or Gd-complexes.

The presence of at least one unpaired electron makes the metal ion a paramagnetic specie able to change the relaxation time of water protons around it. The dipolar interaction between the electronic magnetic moment of the paramagnetic ion and the magnetic moment of water protons can accelerate the relaxation rate of water hydrogen atoms.  $Gd^{3+}$  has seven unpaired electrons in its 4f-orbital so it possesses a highly stable magnetic moment and can be considered the most efficient paramagnetic relaxation metal ion<sup>7</sup>.

$T_2$  or  $T_2^*$  agents are mostly represented by super-paramagnetic iron oxide (SPIO) particles, typically composed of a crystalline core, usually magnetite ( $Fe_3O_4$ ) or maghemite ( $\gamma-Fe_2O_3$ ), and surface modifying moieties (dextran or derivatives). These particles alter proton relaxation times by creating microenvironments of magnetic field inhomogeneity. Protons located in or near these particles will experience field inhomogeneity. Their spins will therefore rapidly dephase resulting in transversal relaxation time decreasing, detectable as darker regions in the image. Due to this property,  $T_2$  agents are also known as negative contrast agents<sup>8</sup>.

# Gadolinium Based Contrast Agents

Gadolinium (Gd) is a lanthanide metal with strong paramagnetic properties. The lanthanides cannot be administered as free ions since their toxicity is very high (LD 50 ~ 0.1 mmol/kg). The ionic radii of the trivalent lanthanide cations range from 1.1 Å for La<sup>3+</sup> to 0.85 Å for Lu<sup>3+</sup> while Gd<sup>3+</sup>, sitting exactly in the center of the lanthanide series, has an ionic radius of 0.99 Å, close to that one of divalent Ca<sup>2+</sup>. As a result, Gd<sup>3+</sup> can compete with Ca<sup>2+</sup> in all cellular systems that need Ca<sup>2+</sup> to function properly. When Ca<sup>2+</sup> is replaced with Gd<sup>3+</sup> in enzyme catalytic centres, the kinetics of the biological activity catalysed by that enzyme is frequently altered. To prevent this unfavorable toxicity issue, the lanthanide ions must be bound in thermodynamic stable complexes that allow for a better and safer *in vivo* use. For this reason several kinds of ligands with different structural and physico-chemical features have been designed to obtain suitable Gd(III) based contrast agents (GBCAs). There are many categories of these compounds differentiated on the basis of the clinical use, but the Gd-Based Extracellular fluid (ECF) agents are the most commonly used contrast agents and represent >98% of all employed contrast agents<sup>9</sup>. This type of GBCAs is characterized by low molecular weight and a systemic distribution after intravenous injection. They are rapidly eliminated from the body through the renal pathway. In the presence of reduced glomerular filtration, problems may arise for compounds characterized by a not sufficiently high kinetic (and/or thermodynamic) stability. Ligands utilised for clinically approved GBCAs were from the family of polyaminocarboxylates, which wrap around the paramagnetic ion as octadentate chelating moieties, leaving one position accessible for the coordination of a water molecule. The relaxation enhancement of the tissue water protons is caused by the quick exchange of the coordinated water molecule with the "bulk" water molecules<sup>10</sup>. Eight Gd-based contrast agents are currently commercially marketed and used in clinics across the United States, Europe, and Japan. (Fig 4)<sup>10</sup>.

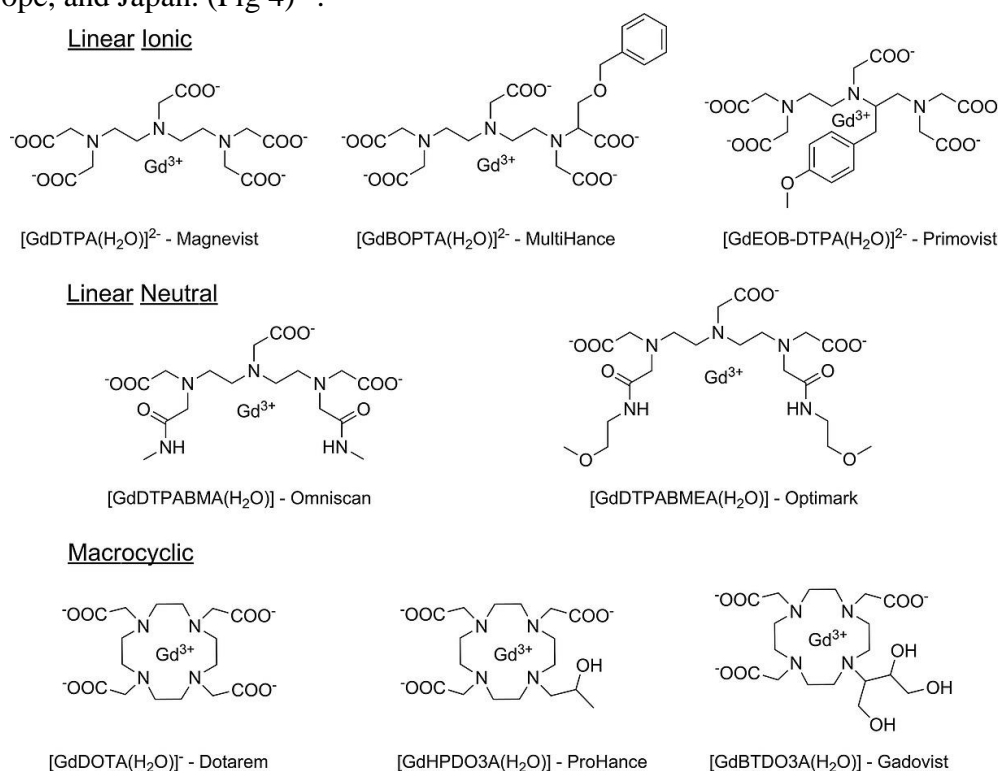


**Figure 4:** Chemical structures of clinical GBCAs.

GBCAs can be structurally divided into linear and macrocyclic agents (Fig 4). The linear ones are composed by an elongated organic molecular ligand wrapping around the metal ion, while the macrocyclic agents form a cage-like ligand structure in which Gd<sup>3+</sup> is trapped. Both GBCAs types

can be ionic or non-ionic. The  $Gd^{3+}$  complexes must be characterized by high in vivo stability which depends on both: the thermodynamic stability constant of the metal complexes and on their kinetic inertness toward transmetallation reactions in biofluids (Table 1).<sup>11</sup> The macrocyclic  $Gd^{3+}$  complexes tolerate longer excretion times because their dissociation rate is negligibly low at physiological pH.<sup>12</sup> In the case of linear  $Gd^{3+}$  complexes it was known that very small amounts of  $Gd^{3+}$  may be retained in the body, as observed in pharmacokinetic studies.<sup>13</sup> Linear GBCAs have higher dissociation rates than macrocyclic GBCAs, resulting in free Gd that can bind to endogenous compounds like phosphate, carbonate, or macromolecules, causing Gd retention in diverse organs.

**Table 1:** Stability constants of  $Gd^{3+}$ -,  $Ca^{2+}$ -,  $Zn^{2+}$ - and  $Cu^{2+}$  complexes formed with DTPA and DOTA derivatives at 25°C

	log $K_{GdL}$	log $K_{CaL}$	log $K_{ZnL}$	log $K_{CuL}$	Ref.
<b>DTPA</b>	22.03	10.63	17.58	23.40	14
<b>BOPTA</b>	21.91	9.77	17.04	22.80	14
<b>EOB-DTPA</b>	23.6	11.82	18.78	20.2	15
<b>MS-325</b>	22.06	10.45	17.82	21.3	16
<b>DTPA-BMA</b>	16.64	6.80	12.42	16.30	14
<b>DTPA-BMEA</b>	16.85	–	–	–	17
<b>DOTA</b>	24.7	16.37	18.7	22.72	18
<b>HPDO3A</b>	23.8	14.83	19.37	24.19	19
<b>BTDO3A</b>	20.8	14.3	19.0	21.1	12

**Table 2:** Kinetic parameters characterizing the dissociation ( $k_1$ ,  $k_d$  at pH=7.4,  $t_{1/2}=\ln 2/k_d$  at pH=7.4), distribution ( $k_{int}$ ,  $k_{int}=\ln 2/t_{1/2} \alpha$ ) and elimination ( $k_{el}$ ,  $k_{el}=\ln 2/t_{1/2} \beta$ ) of principal GBCAs.

	$k_1 / M^{-1}s^{-1}$	$k_d / s^{-1}$	$t_{1/2} / h$	$k_{int} \times 10^4 / s^{-1}$	$k_{el} \times 10^4 / s^{-1}$	Ref
<b>Gd-DTPA</b>	0.58	$1.5 \times 10^{-6}$ [a] $6.3 \times 10^{-7}$ [b]	127 [a] 305 [b]	9.6	1.2	12,13,20
<b>Gd-BOPTA</b>	0.41	$1.1 \times 10^{-6}$ [a]	169 [b]	23	1.6	14,21
<b>Gd-EOB-DTPA</b>	0.16	N	N	23	2.1	15,22
<b>Gd-DTPA-BMA</b>	12.7 37 (37°C)	$1.2 \times 10^{-6}$ [a] $3.9 \times 10^{-6}$ [b] $2.1 \times 10^{-5}$ [b] (37°C)	157 [a] 50 [b] 9.3 [b] (37°C)	31	1.5	11,12,23,24
<b>Gd-DOTA</b>	$1.8 \times 10^{-6}$ $2.0 \times 10^{-5}$ (37°C) $3.6 \times 10^{-5}$ (37°C)	$1.2 \times 10^{-14}$ $8.0 \times 10^{-13}$ (37°C) $1.4 \times 10^{-12}$ (37°C)	$2.6 \times 10^9$ $2.4 \times 10^8$ (37°C) $1.4 \times 10^8$ (37°C)	–	1.2 [c]	9,12
<b>Gd-HPDO3A</b>	$2.6 \times 10^{-4}$ $2.9 \times 10^{-4}$	$1.0 \times 10^{-11}$ $1.1 \times 10^{-11}$	$1.7 \times 10^7$ $1.6 \times 10^7$	–	1.2 [c]	9,12
<b>Gd-BTDO3A</b>	$2.8 \times 10^{-5}$	$1.1 \times 10^{-12}$	$1.7 \times 10^8$	–	1.1 [c]	9,25

[a] In the absence of endogenous ligands (1.0 M KCl, 25°C); [b] In the presence of endogenous ligands (0.15 M NaCl, 25°C); [c] Half-life characterizing the final excretion of Gd(DOTA), Gd(BTDO3A) and Gd(HPDO3A) are 1.60, 1.81 and 1.57 h, respectively; N – non investigated.



# Gadolinium retention

All clinically authorized GBCAs are neutral or negatively charged, and their biodistribution is almost equivalent. By fitting the plasma concentration vs. time data to the standard two-compartment open model, the pharmacokinetic parameters (clearance rate, distribution and elimination half-life, and steady state distribution volume) characterizing the distribution and elimination of the agent can be determined. GBCAs, given their extremely hydrophilic nature, are removed by renal filtration with a half-life of around 50-90 minutes in healthy individuals<sup>10</sup>, and approximately 90% of administered GBCA is excreted within 24 hours in patients with normal renal function (Table 3)<sup>26</sup>. Hepatobiliary excretion partially clears drugs with hydrophobic aromatic substituents (benzyloxymethyl or *p*-ethoxybenzyl) on the ligand framework, hence these complexes are also utilised as liver specific agents (Eovist and Multihance).

GBCAs were assumed to be safe, except for occasional allergic responses, until the discovery of Nephrogenic Systemic Fibrosis (NSF). This is an uncommon, progressive, and occasionally deadly illness characterised by skin thickening, severe joint contracture, and fibrosis of many organs including the lungs, liver, muscles, and heart<sup>27</sup>. In 2006, it was observed that there was a relationship between NSF and GBCAs assumption in individuals with end-stage renal disease<sup>28</sup>.

The pathogenesis of NSF is believed to begin with a process called transmetallation; it is the displacement of  $Gd^{3+}$  from its ligand by another metallic cation, such as  $Fe^{3+}$ ,  $Zn^{2+}$  or  $Ca^{2+}$ . It has been discovered that the released  $Gd^{3+}$  ions function as a stimulant for fibroblast development, resulting in the formation of fibrosis in the skin, joints, and internal organs<sup>29</sup>. Several findings revealed that the reduced kinetic stability of some linear GBCAs (in comparison to macrocyclic ones) was the source of the disease in individuals with severe renal impairment. The measurement of the glomerular filtration rate prior to the MRI scan allowed for the identification of patients at risk, for whom lower stability GBCAs must be avoided, and the cases of NSF-related to GBCAs have been drastically reduced since then.<sup>29</sup>

Subsequently, in 2014, it was discovered that patients that received many GBCA administrations had higher signal intensity (SI) in non-contrasted T1-weighted MR imaging of brain regions (Dentate Nucleus and Globus Pallidus), even in the absence of any renal failure.<sup>30</sup> Following this work, it was demonstrated that the observed hyperintensity can be linked to the presence of tiny amounts of Gd retained in the brain (and other tissues). Indeed, only a small fraction of the total Gd dose is found in the brain, approximately less than 0.001%. McDonald et al.<sup>31</sup> performed inductively coupled plasma mass spectroscopy analysis on postmortem brain tissue samples from 13 adult patients who had undergone at least four GBCA-enhanced MR exams<sup>32</sup>. Brain tissue samples from patients exposed to GBCA administration all contained measurable gadolinium levels, with the greatest deposition in the dentate nucleus<sup>33-35</sup>.

Apart from CNS, it has been demonstrated that even higher amounts of Gd can accumulate in other organs such as liver, spleen, kidneys and bone<sup>36</sup>. Some patients reported to have chronic, non-allergic reactions to GBCAs administration. This hypothesized syndrome has been named gadolinium deposition disease (GDD), even though it is still a proposed disease, without a clear scientific demonstration. Some of the reported symptoms are peripheral neuropathic pain, muscle spasms, fatigue, headache, distal extremity and skin substrate thickening, discoloration, and pain. It has been proposed that GDD may manifest after administration of GBCAs in a dose-dependent manner<sup>37</sup>.

After the recognition of the issues associated with  $Gd^{3+}$  retention in both healthy patients and with renal insufficiency, the European Medicines Agency (EMA) recommended suspending or restricting marketing authorizations for GBCAs based on linear chelators and warnings have been issued by the United States Food and Drug Administration (FDA)<sup>38</sup>.

**Table 3:** Pharmacokinetics in humans after intravenous administration of GBCAs; female (F), male (M)<sup>26</sup>

GBCA	Distribution half-life (min)	Elimination half-life (min)	Serum elimination half-life in renal impairment (h)	Injected dose eliminated within 24 h (%)	Elimination path	Renal clearance rate (mL/min/kg)	Plasma clearance rate (mL/min/kg)	Volume of distribution (mL/kg)	Protein binding
Magnevist (gadopentetate dimeglumine)	12 ± 7.8	96 ± 7.8	Mild: 2.6 ± 1.2 Moderate: 4.2 ± 2.0 Severe: 10.8 ± 6.9	91 ± 13	Renal	1.76 ± 0.39	1.94 ± 0.28	266 ± 43	No
MultiHance (gadobenate dimeglumine)	5.04 ± 0.72 to 36.3 ± 4.32	70.2 ± 15.6 to 121.2 ± 36	Moderate: 6.1 ± 3.0 Severe: 9.5 ± 3.1	> 80%	Renal (93%), biliary (0.6–4%)	1.37 ± 0.12 to 1.73 ± 0.65	1.55 ± 0.17 to 2.22 ± 4.5	170 ± 16 to 282 ± 79	Weak
Eovist/Primovist (gadoxetate)	–	54.6–57	–	Not detected	Renal (50%), biliary (50%)	–	–	210	< 10%
Omniscan (gadodiamide)	3.7 ± 2.7	77.8 ± 16	–	95.4 ± 5.5	Renal	1.7	1.8	200 ± 61	No
Dotarem (gadoterate meglumine)	–	84 ± 12 (F), 120 ± 42 (M)	Moderate: 5.1 ± 1 Severe: 13.9 ± 1.2	72.9 ± 17 (F), 84.4 ± 9.7 (M) (48 h elimination)	Renal	1.27 ± 0.32 (F), 1.40 ± 0.31 (M)	1.67 ± 0.17	179 ± 26 (F), 211 ± 35 (M)	No
ProHance (gadoteridol)	12 ± 2.4	94.2 ± 4.8	–	94.4 ± 4.8	Renal	1.41 ± 0.33	1.5 ± 0.35	204 ± 58	No
Gadovis/Gadovist (gadobutrol)	–	108.6 (79–127)	Mild/Moderate: 5.8 ± 2.4 Severe: 17.6 ± 6.2	> 90 (12 h elimination)	Renal	1.56 ± 0.18	1.78 ± 0.43	210 ± 20	No

# Aim of the project

The general scope of the herein reported work was to enlarge the field of view of the studies related to *in vivo* Gd-retention by using differentiated preclinical investigations, to understand the mechanisms behind the retention phenomenon. As mentioned before, the GBCAs stability in an *in vivo* system is one of the major concern regarding the metal deposition in the human body. Although it was largely demonstrated that the less stable linear GBCAs possess higher propensity to release gadolinium and undergo gadolinium retention concerning to the more stable macrocyclic ones, cases were observed with retained Gd also upon administration of macrocyclic complexes. Thus, the first aim of the thesis has been to investigate the influences of structural differences in the Gd-complexes on biodistribution and retention (Chapter 1). Another focus was set on the investigation of the extent of Gd-retention, and the related mechanisms of action, in animal models of pathologies for which extensive use of GBCAs administrations is foreseen in the clinical practice (Chapter 2). Finally, given that most of the studies reported so far are focused on the elucidation of Gd-retention phenomenon in the brain regions, the research was extended to less investigated tissues/organs where the deposition could be even higher (Chapter 3).

More in detail, the thesis is organized as follows:

In **Chapter 1**, the objective of the work was to study deeper how the structural variations of GBCAs or the differences in the formulation can change the Gd retention in the body of healthy mice. First, the influence on Gd retention of minor structural changes in the coordination cage of macrocyclic Lanthanide (III)-complexes was explored. Insights on the role of potential interactions between the Ln(III) complexes and components of the extracellular matrix (ECM) have been gained by *in vitro* relaxometric investigations. Next, we deemed it interesting to investigate if the Gd-retention phenomenon can be affected by a different elimination pathway, i.e. renal and/or hepatobiliary. Given that the *in vivo* distribution/elimination pathways of an exogenous molecule are associated to the dissimilar interactions occurring with the biomolecules of the microenvironment in which it is distributed, we analysed the extent of retained Gd in the organs of mice administered with three Gd-DTPA based complexes characterized by different abilities to bind Human Serum Albumin (i.e. the most abundant serum protein). Binding to albumin influences the blood lifetime of the investigated Gd-complexes after *i.v.* injection, and, thus, could have an effect on their biodistribution and retention. In the last part of the chapter, a study is reported aimed at the investigation of the extent of Gd-retention upon the use of a nanosized Gd-based system obtained by the encapsulation of a low molecular weight GBCA in the aqueous cavity of a liposome. The rationale behind this study was twofold: i) increasing the size of the system, and thus disadvantaging the BBB crossing of the GBCA and ii) protecting it from eventual interactions with the molecules of the microenvironment, thus, in principle, increasing its stability and decrease Gd release and retention.

In **Chapter 2**, models of pathologies where the use of contrast enhanced MRI is largely exploited in clinical diagnostic protocols were considered. The first was an immune-mediated murine model (Experimental Autoimmune Encephalomyelitis-EAE) of Multiple Sclerosis (MS), as MS patients are commonly exposed to multiple GBCAs doses within routine clinical care. The study aimed to quantitatively investigate, at the preclinical level, the extent of Gd retention in the central nervous system, and peripheral organs, of immune-mediated murine models of MS compared to control animals. The second model of pathology considered during my thesis was a murine model of Inflammatory Bowel Disease (IBD) induced through the administration to mice of dextran sulfate sodium (DSS) in drinking water. This model was chosen because a strong relationship between gastrointestinal tissue and nervous system have been recently reported. Is known that the gut

microbiota forms a complex network along with the central nervous system (CNS), which is called the microbiota- gut-brain axis. In this study we investigated whether the occurrence of a strong gastrointestinal inflammation performed on a well-established murine model of colitis leads, upon administration of GBCA, to an enhanced Gd retention in CNS system, excretion organs and bones.

**Chapter 3** is focused on a deeper investigation of Gadolinium retention in other compartments other than those of the Central Nervous System. First, we deemed interesting to study the Gd behaviour in the blood, because it is the tissue that MRI GBCAs mostly encounter, being administered intravenously. Herein, it has been investigated how much Gd is internalized by cellular blood components upon the in vitro incubation of GBCAs in human blood or upon intravenous administration of GBCAs to healthy mice. Next, the investigation was extended to organs which have been poorly investigated by the scientific community up to now, such as the bladder, the spleen and the bones, but potentially able to accumulate high amounts of metal.

According to previous studies, the spleen is one of the tissues characterized by very high concentration of metal retained; we aimed at elucidating if Gd mainly accumulates in the fibrous or in the cellular districts. On the other hand, bones are renowned in literature to be a secondary deposit of metal ions, thus we strived for understanding whether Gd accumulates to higher extent in the matrix or in the bone marrow. Lastly, it was decided to analyse the bladder since GBCAs are almost completely excreted through urine therefore we hypothesized that some Gd could accumulate in this district. Indeed, it is known from literature that some xenobiotics and toxic substances contained in the urine could possibly be retained in the bladder leading to concerning consequences.



# CHAPTER 1

Influence of GBCAs structural variations and different formulation on Gd-retention



# 1.1

Gd retention of Macrocyclic Lanthanide (III)-  
complexes with minor structural changes

## Introduction

Recently, great attention has been dedicated to observations reporting that tiny amounts of Gadolinium based contrast agents (GBCAs) (administered by i.v. injection) evade the blood circulation bed being retained in body districts, possibly, for long times<sup>31,39–41</sup>. Less stable (thermodynamically and kinetically) complexes may eventually form deposits, likely of composite nature, that are detected, basically unaltered, over one year time in healthy animals. The more stable macrocyclic-based GBCAs are expected to flow intact along the glymphatic pathway although their transit time may differ markedly from agent to agent. For instance, it was reported that, in healthy mice, 5 weeks after the administration, the Gd concentration in the cerebellum was roughly three-times lower for Gd-HPDO3A than for Gd-BTDO3A (mean, 0.19 vs. 0.63 nmol/g, respectively)<sup>42,43</sup>. Both complexes are neutral and of very similar structure, and differ only for the presence of two additional hydroxyl moieties on the external surface of the BTDO3A ligand. Recently, to get more insight into the understanding of the issues related to Gd-retention, we suggested to compare the in vivo behavior of complexes with different Lanthanide(III) ions simultaneously administered to the same animal.<sup>44</sup> Analogously, the Yttrium-86 positron emitter has been proposed as surrogate of gadolinium, as it is endowed with very similar properties, for the in vivo whole-body quantification of GBCAs through PET imaging<sup>45</sup>.

We deemed interesting to compare the longitudinal water proton relaxation rate of Gd-BTDO3A, Gd-HPDO3A and Gd-DOTA (used as control compound lacking any OH group) in water and in the presence of the main extracellular matrix Glycosaminoglycans (GAGs). The measurement has provided some insights on the molecular interactions that these macrocyclic complexes can establish with the macromolecules present along the “transit” pathways in the extracellular, extravascular space. On this basis, we performed a medium-term (21 days) in vivo experiment to study the amount of retained metal ions upon the simultaneous administration of Gd-BTDO3A and the analog of Gd-HPDO3A in which gadolinium was substituted with europium (Eu-HPDO3A). In this way any interindividual difference between mice is avoided and the number of used animals is considerably reduced. Moreover, to evaluate the possibility that Eu-HPDO3A could have been retained to a different extent with respect to Gd-HPDO3A was checked (and excluded) by carrying out an independent experiment where Gd-HPDO3A, Eu-HPDO3A and Tb-HPDO3A were compared. Besides, the experiment was conceived to assess whether the different isomeric composition of the three complexes (present in solution as mixture of Square Anti Prismatic and Twisted Square Anti Prismatic structure) may eventually affect their biodistribution and retention behavior.



## Material and methods

### Chemicals and cells

The following clinical Gadolinium based contrast agents were employed in this study: i) gadoteridol (Prohance®, Bracco Imaging, Gd(HPDO3A)), ii) gadobutrol (Gadovist®, Bayer S.p.A, Gd-BTDO3A), iii) gadoterate (Dotarem®, Guerbet, Gd-DOTA). Gadoteridol and HPDO3A ligand were kindly provided by Bracco Imaging S.p.A. Gadobutrol and Gadoterate were purchased from Bayer and Guerbet, respectively. All other chemicals were purchased from Sigma–Aldrich.

J774A.1 cell line (murine macrophages) was obtained from American Type Culture Collection (ATCC, Manassass, VA, USA). Cells were grown in Dulbecco's modified Eagles's medium (DMEM). The medium was supplemented with 10% (v/v) heat-inactivated fetal bovine serum, 2mM L-Glutamine, 100 U/ mL<sup>-1</sup> penicillin and 100 mg mL<sup>-1</sup> streptomycin. DMEM, fetal bovine serum, and penicillin– streptomycin mixture were purchased from Lonza (Lonza Sales AG, Verviers, Belgium). Cells were seeded in 75 cm<sup>2</sup> flasks at density of *ca.* 2×10<sup>4</sup> cells/cm<sup>2</sup> in a humidified 5% CO<sub>2</sub> incubator at 37 °C. When J774A.1 cells reached confluence, they were gently detached by means of a scraper.

### Synthesis of Eu-HPDO3A and Tb-HPDO3A

The 10-(2-hydroxypropyl)-1,4,7,10-tetraazacyclododecane-1,4,7-triaceticacid (HPDO3A) (1 g; 24 mmol) was dissolved in water (15 mL) and an excess of the lanthanide oxide (14 mmol) was added; the suspension was heated at 90°C.<sup>11</sup> After cooling, the excess of lanthanide oxide was filtered away and a new aliquot of ligand (≤ 0.1% of the initial amount) was added maintaining pH 7 with NaOH 0.1N. The absence of residual free metal in the solution was assessed by the orange xylenol UV method. The product was freeze-dried.

The lyophilized products were then re-dissolved in water to obtain the solution to be injected. After mixing Eu-HPDO3A with Gd-BTDO3A (for the first animal study) and Tb-HPDO3A and Eu-HPDO3A with Gd-HPDO3A (for the second animal study) in 1:1 ratio the total Gd, Tb and Eu concentrations were checked by inductively coupled plasma mass spectrometry (ICP-MS) analysis.

### Animals

Ten-week-old male Balb/c mice (Charles River Laboratories, Calco, Italy), bred at the Molecular Biotechnology Center of the University of Torino, were used for the *in vivo* experiments (n = 5 for each study, mean weight 24 ± 1 g). Mice were kept in standard housing with standard rodent chow and water available *ad libitum*, and a 12h light/dark cycle. Experiments were performed according to national rules and policies on animal handling and authorized by the Italian Ministry of Health (authorization number: 808/2017-PR in 19/10/2017). Before the injection of the metal complexes, mice were anesthetized by intramuscular injection of tiletamine/zolazepam (Zoletil 100; Virbac, Milan, Italy) 20 mg/kg *plus* xylazine (Rompun; Bayer, Milan, Italy) 5 mg/kg.

### Animal study setup

Two animal studies were carried out:

1. 5 healthy BALB/C mice were administered, by *IV* injection, with 10 doses containing Eu-HPDO3A and Gd-BTDO3A in 1:1 molar ratio (0.3 mmol/Kg of each complex) every second day. Then the mice were sacrificed by cervical dislocation 21 days after the last administration and cerebrum, cerebellum, spleen, liver, kidney, eyes, a portion of bone, skin and muscle were recovered. Each specimen was weighted, mineralized and underwent Eu and Gd determination by ICP-MS analysis.

- 5 healthy BALB/C mice were administered, by IV injection, with 10 doses containing Eu-HPDO3A, Tb-HPDO3A and Gd-HPDO3A in equimolar ratio (0.3 mmol/Kg of each complex) every second day. Then the mice were sacrificed by cervical dislocation 21 days after the last administration and the same organs/tissues of study 1 were harvested and analyzed for Eu, Tb and Gd quantification by ICP-MS analysis.

### ICP-MS quantification of metal content

The Gd, Eu and Tb content of the excised organs and tissues was measured by ICP-MS analysis (Element-2; Thermo-Finnigan, Rodano (MI), Italy) and the results expressed as nmol/g of wet tissue weight. The preparation of the samples for ICP-MS analysis has been carried out as follows: 1 mL of concentrated HNO<sub>3</sub> (67%) (2 mL in the case of liver tissues) was added to the samples. After 3-5 days, the completely dissolved materials were further mineralized under microwave heating at 180°C for 40 minutes (Milestone ETHOS UP High performance Microwave digestion system equipped with an optical fiber, temperature control and SK-15 high-pressure rotor, Bergamo, Italy). After mineralization, the volume of each sample was brought to 3 mL with ultrapure water and the samples were analysed by ICP-MS. The calibration curve was obtained using eight absorption standard solutions (Sigma-Aldrich) containing equimolar concentrations of Eu and Gd or Tb and Gd in the range 0.001–0.1 µg/mL. The detection limit in our ICP-MS analyses was determined to be 0.00005 µg/mL (10 times higher than blank solution). Considering the mean weights of the organs/tissues recovered from mice and the dilutions made in the preparation of the samples for ICP/MS, the LOQ of the method with respect to the respective tissues/organs were calculated and reported in the following table.

**Table 1:** Limits of quantification (LOQ) in the selected organs/tissues calculated considering the detection limit of the ICP-MS measures (0.00005 µg/mL, i.e. 10 times higher than blank solution), the mean weights of the organs/tissues and the dilutions made in the dilutions made in the preparation of the samples

Organ/tissue	LOQ (nmol/g of tissue)		
	Eu	Gd	Tb
Cerebrum	0.0034	0.0033	0.0033
Cerebellum	0.0098	0.0094	0.0093
Eye	0.025	0.023	0.023
Muscle	0.0032	0.0031	0.0031
Skin	0.0103	0.010	0.0099
Liver	0.0035	0.0034	0.0034

Spleen	0.0078	0.0075	0.0075
Kidney	0.0052	0.005	0.0049
Bone	0.0066	0.0064	0.0063

### Water proton relaxation measurements

The longitudinal water proton relaxation rates of Gd-DOTA, Gd-HPDO3A and Gd-BTDO3A (0.1 mM), with and without the addition of Hyaluronic Acid (HA) sodium salt from rooster comb, Chondroitin sulfate (CS) sodium salt from bovine cartilage or Heparan Sulfate (HS) (Sigma-Aldrich) were measured at 25°C by using a Stelar Spinmaster (Stelar, Mede, Pavia, Italy) spectrometer operating at 0.5 T (21.5 MHz Proton Larmor Frequency), by means of the standard inversion-recovery technique. All solutions were prepared in physiological salt concentration (NaCl 150 mM).

Binding parameters (the affinity constant,  $K_A$ , and the relaxivity of the supramolecular adduct,  $r_{1b}$ ) toward Hyaluronic acid were determined using the proton relaxation enhancement (PRE) method, which considers the relaxation enhancement due to the formation of a slowly moving macromolecular, adduct. The water proton relaxation rate ( $R_1 = 1/T_1$ ; 21.5MHz and 25 °C) of solutions containing the Gd-complexes (at concentration of 0.086mM Gd-BTDO3A, 0.087 mM Gd-HPDO3A, or 0.089 mM Gd-DOTA) was measured as a function of the concentration of hyaluronic acid (in the range 1-5 mg/mL corresponding to a concentration of disaccharide units 0.0024-0.012M). The analysis of the experimental data, according to simple equations for isotherm binding curves,<sup>12</sup> afforded the values of  $K_A$  (toward each single disaccharide unit of the hyaluronic acid polymer) and  $r_{1b}$  (relaxivity of the Gd-complexes in the supramolecular framework) reported in table 2.

### Cellular uptake in J774 macrophages

Briefly,  $5 \times 10^5$  J774A.1 cells were seeded on 6 cm Petri dishes. After one day, cells were incubated for 4 h at 37°C in 3mL of cell culture medium in presence of Gd/Tb/Eu HPDO3A at different concentrations (i.e. 1, 3, 5 mM). After the incubation, cells were extensively washed by using fresh PBS, detached by scraper and collected in fresh PBS. At the end of each experiment, cells were lysed by sonication by using a Bandelin Sonoplus Sonicator (20 kHz, power 30%, 20 s). Then cell lysates (0.2 mL) were mineralized by adding 0.2 mL of concentrated HNO<sub>3</sub> (67%) by using microwave heating (Milestone MicroSYNTH, Microwave lab station equipped with an optical fiber temperature control and HPR-1000/6M six position high-pressure reactor, Bergamo, Italy). After digestion, the volume of each sample was brought to 2 mL with ultrapure water and analysed by ICP-MS, (as mentioned above) for quantification of the total amount of internalized Gd/Tb/Eu metals. The total number of cells in each specimen was assessed by quantification of protein content, as measured by the Bradford method (1 mg of protein is equal to  $2.5 \times 10^6$  cells).

### Statistical Analysis

All data are expressed as the mean values of at least three independent experiments  $\pm$  standard deviation (SD). Between group differences with respect to the mean Ln concentration were assessed using unpaired t test or two-way ANOVA followed by the Bonferroni's multiple comparison post-hoc test. Graph-Pad Prism 7.00 software was used for data analysis. Overall, statistical significance was defined as follows: \*p < 0.05, \*\*p < 0.01, \*\*\*p < 0.001; unless differently specified.

## Results

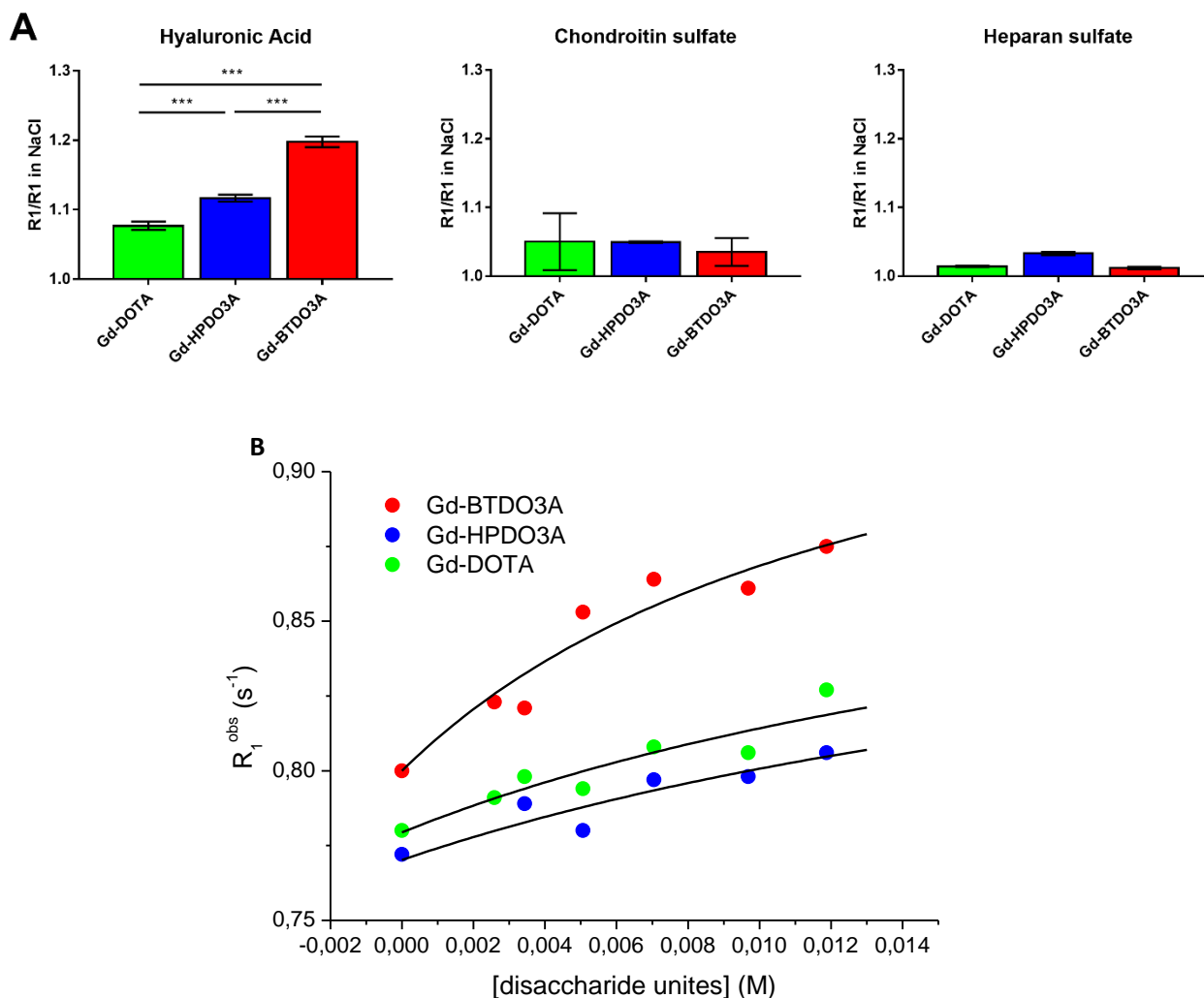
### Relaxometric study of Gd-BTDO3A, Gd-HPDO3A and Gd-DOTA in the presence of selected ECM components

Figure 1A reports the ratio of the proton longitudinal relaxation rates of solutions of Gd-HPDO3A, Gd-BTDO3A and Gd-DOTA (concentration ca. 0.1 mM) measured in the presence of the Glycosaminoglycans (GAGs) (at 5 mg/mL concentration) and in NaCl 150 mM at 25°C and 21.5 MHz. Hyaluronic acid, already at very low concentration (< 2 mg/mL), is characterized by having an extensive secondary and tertiary structure which stiffens the molecule and give rise to very viscous jelly solutions<sup>46</sup>. On the contrary, the presence of sulfates in Chondroitin and Heparan sulfate derivatives, confers an electrostatic repulsion between these molecules preventing aggregation and the formation of ordered tertiary structures, if not at very high concentration. Results reported in figure 2a were obtained by using Glycosaminoglycans (GAGs) at 5 mg/mL, where only Hyaluronic acid was under the form of gel. In the presence on Hyaluronic acid, an increase in the observed relaxation rate was observed with respect to NaCl 150 mM for all three investigated GBCAs. The increase in relaxation rate was in the order Gd-BTDO3A > Gd-HPDO3A > Gd-DOTA with significative differences between each other. Chondroitin and Heparan sulfate addition did not yield any significative increase in the observed relaxation rates.

The extent of the interaction of the three Gd-complexes with Hyaluronic acid was further investigated by measuring the variation of the observed longitudinal relaxation rate as a function of increasing HA concentration. The obtained binding curves (Fig 1B) have been fitted allowing to determine  $K_A$  and  $r_{1b}$  values reported in table 2. As the molecular weight of the hyaluronic acid was unknown, data were fitted by reporting the observed relaxation rates versus the molar concentration of disaccharide units, thus  $K_A$  values reported in table 3 are referred to the affinity toward each disaccharide unit composing the polymer. The affinity constants of Gd-BTDO3A, Gd-HPDO3A and Gd-DOTA are very low, to indicate a non-specific weak interaction between the Gd-complexes and the polymer. Nevertheless, the affinity shown by Gd-BTDO3A is ca. twice that observed for Gd-HPDO3A and Gd-DOTA.

**Table 2:** Binding parameters ( $K_A$  and  $r_{1b}$ ) of Gd-BTDO3A, Gd-HPDO3A and Gd-DOTA toward Hyaluronic acid. The affinity constants were calculated for each disaccharide unit of the hyaluronic acid polymer.

	<b>Gd-BTDO3A</b>	<b>Gd-HPDO3A</b>	<b>Gd-DOTA</b>
$K_A(M^{-1})$	$72 \pm 6.7$	$37 \pm 3.9$	$30 \pm 3.2$
$r_{1b}(mM^{-1}s^{-1})$	$6.9 \pm 0.84$	$5.9 \pm 1.9$	$6.3 \pm 1.5$



**Figure 1:** A) Ratio of the proton longitudinal relaxation rates of solutions of Gd-HPDO3A, Gd-BTDO3A and Gd-DOTA measured in the presence of the Glycosaminoglycans (GAGs) (at 5 mg/ml concentration) and in NaCl 150 mM at 25°C and 21.5 MHz; B) Water proton relaxation rates of aqueous solutions of 0.086mM Gd-BTDO3A, 0.087 mM Gd-HPDO3A, or 0.089 mM Gd-DOTA upon addition of increasing amounts of hyaluronic acid. (2.15MHz, 25°C, NaCl 150mM)

### Eu and Gd retention upon the administration of a mixture of Eu-HPDO3A and Gd-BTDO3A

Ten repeated injections consisting of a 1:1 mixture of Gd-BTDO3A and Eu-HPDO3A (0.3 mmol/Kg each, for a total dose of 3 mmol/Kg of each complex) were performed on healthy mice. After 21 days from the last administration, the animals were sacrificed and the organs resected to determine, by ICP-MS, the amounts of Eu and Gd. The amount of Gadolinium found in all organs, except eye and muscle, was significantly higher than that of Europium (Fig 2 and Table 3), suggesting that Gd-BTDO3A is retained to a greater extent than Eu-HPDO3A.

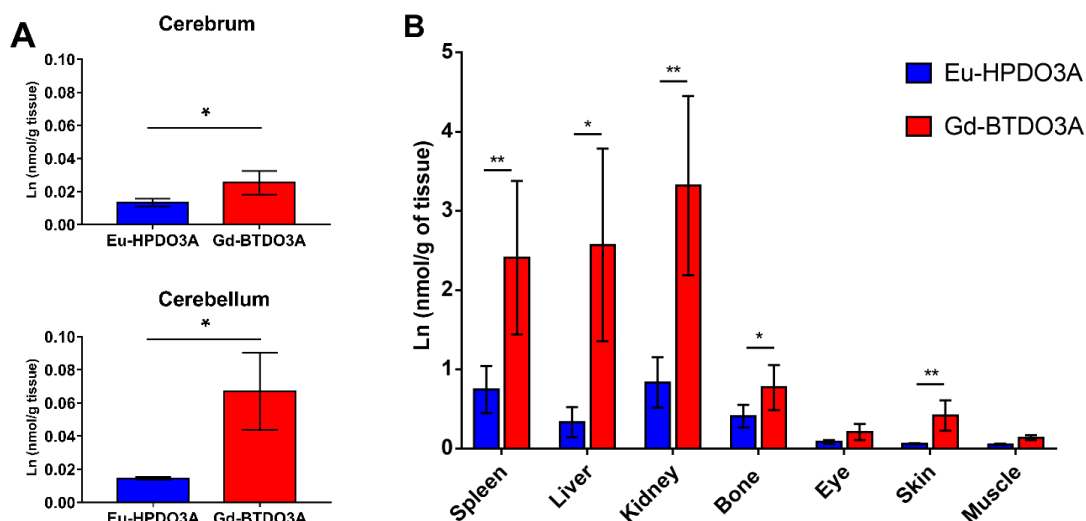


**Figure 2:** Amounts of Eu and Gd determined in cerebrum and cerebellum (a) and in other organs/tissues (b) upon the administration of ten doses of a mixture of Eu-HPDO3A/Gd-BTDO3A (0.3 mmol/Kg each) 21 days after the last injection.

**Table 3:** Metal concentrations (in nmol/g of wet tissue) for the various tissues/organs determined by ICP-MS analysis upon administration of Eu-HPDO3A and Gd-BTDO3A. (Mean values  $\pm$  SD).

Tissue/organ	Eu (from Eu-HPDO3A) (nmol/g)	Gd (from Gd-BTDO3A)	P
Cerebrum	0.0153 $\pm$ 0.0021	0.0253 $\pm$ 0.0032	<0.05 *
Cerebellum	0.0209 $\pm$ 0.00393	0.0515 $\pm$ 0.0121	<0.05 *
Liver	0.333 $\pm$ 0.191	2.57 $\pm$ 1.21	<0.05 *
Spleen	0.746 $\pm$ 0.297	2.41 $\pm$ 0.968	<0.01 **
Kidney	0.836 $\pm$ 0.318	3.32 $\pm$ 1.13	<0.01 **
Muscle	0.0538 $\pm$ 0.0083	0.138 $\pm$ 0.0303	ns
Bone	0.408 $\pm$ 0.143	0.771 $\pm$ 0.284	<0.05 *
Eye	0.084 $\pm$ 0.0242	0.209 $\pm$ 0.101	ns
Skin	0.0604 $\pm$ 0.0071	0.418 $\pm$ 0.192	<0.01 **

### Gd, Tb and Eu retention upon the administration of equimolar solutions of Gd-HPDO3A and Tb-HPDO3A and Eu-HPDO3A

Ten repeated injections of an equimolar mixture of Gd-HPDO3A, Tb-HPDO3A and Eu-HPDO3A (0.3mmol/Kg each, for a total dose of 3 mmol/Kg of each complex) were performed on healthy mice. After 21 days from the last injection, the animals were sacrificed and the organs resected to determine, by ICP-MS, the amounts of Gd, Tb and Eu (Fig 3B). Figure 3 reports the amount of Lanthanides found in cerebrum and cerebellum (A) and in the other resected organs (B) upon the administration of Eu-HPDO3A, Gd-HPDO3A and Tb-HPDO3A. No significant differences were observed in all the

investigated organs with the exception of liver and spleen were Tb concentration resulted to be doubled with respect to amounts of Eu and Gd.

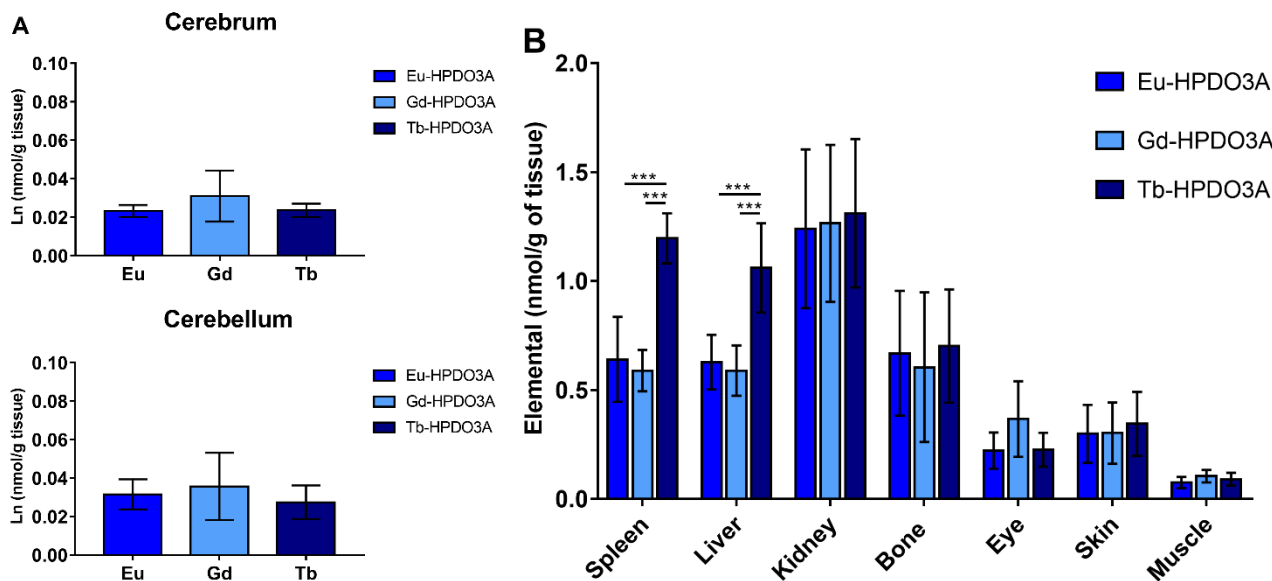


**Figure 3:** Amounts of Eu, Gd and Tb found in cerebrium and cerebellum (A), and in the other organs (B) upon the administration of ten doses of a mixture of Eu-HPDO3A/Gd-HPDO3A/Tb-HPDO3A (0.3 mmol/Kg each) 21 days after the last injection.

### Cellular uptake in J774 macrophages

Incubation of J774 macrophages with Gd-HPDO3A, Tb-HPDO3A and Eu-HPDO3A in the concentration range 1-5 mM afforded the results reported in figure 4. Whereas, the amount of Gd, Tb and Eu internalized by the cells followed an increasing trend as a function of the concentration of the corresponding Ln(III)-complex in the incubation medium, no significant differences were observed in the uptake efficiency of the three different Ln(III)-HPDO3A complexes.

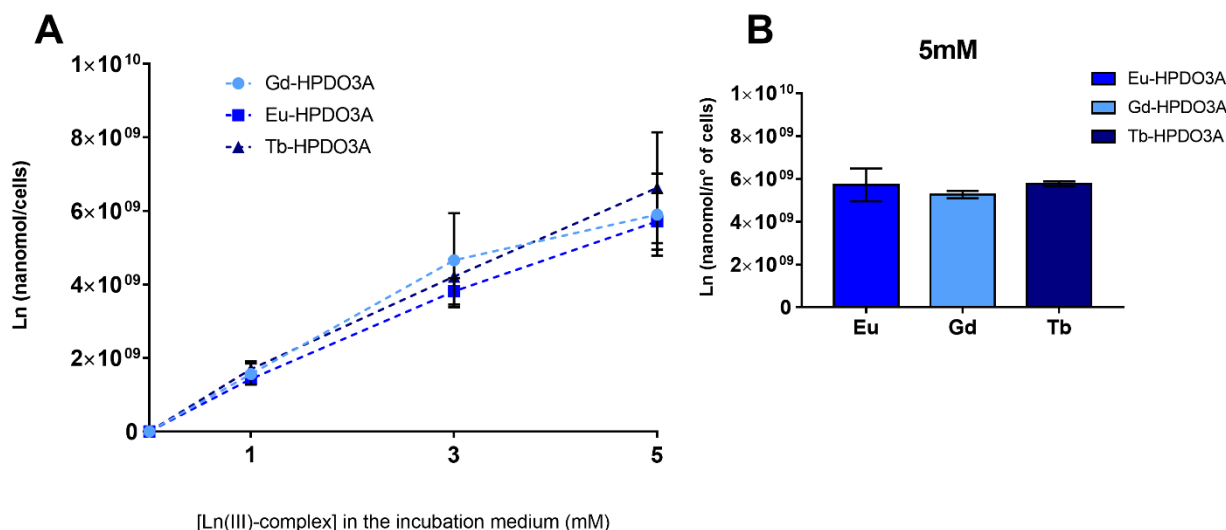


**Figure 4:** Amounts of Eu, Gd and Tb found in J774 macrophages incubated for 4h at 37°C with increasing concentration of Eu-HPDO3A, Gd-HPDO3A or Tb-HPDO3A.

## Discussion

### What do differences in behaviour between lanthanide compounds suggest?

It is known that the paravascular space in the brain through which the glymphatic excretion is suggested to take place, contains Glycosaminoglycans (GAGs) based fibers that act as a kind of sieving system for the xenobiotics and wastes along their excretion pathway<sup>48</sup>. GAGs are a family of negatively charged chains with repeating disaccharide units. GAGs include Chondroitin sulfate (CS), Heparan sulfate (HS) and Hyaluronic acid (HA). Except for HA, GAGs are sulfated on the sugar residues and attached to the core proteins forming the proteoglycans. We surmise that the GAGs structures may offer reversible anchoring sites for the formation of H-bonds to the GBCAs. Thus, in vitro water protons relaxation enhancements were used for the determination of binding affinity to the principal GAGs. The results (Fig 1a) showed that, upon the addition of HA, the relaxation enhancement is significantly higher for Gd-BTDO3A and Gd-HPDO3A with respect to Gd-DOTA. Indeed, the enhancement is larger for Gd-BTDO3A with respect to Gd-HPDO3A. The observed behavior suggests that the relaxation enhancement increases with increasing the number of hydroxyl groups on the surface of the complex. As the relaxation enhancement at 20MHz is strictly dependent upon the molecular correlation time of the GBCA, it is straightforward to say that the motion of Gd-BTDO3A is slowed down more than that of Gd-HPDO3A by the reversible formation of molecular interactions with the HA-containing macromolecules. Yet, in a study where the relaxivity was used to measure the diffusion of Gd-based contrast agents in cartilage<sup>49</sup>, it was reported that the diffusivity (a parameter that describes the transport of the contrast agent into a given material) of Gd-HPDO3A in cartilage (rich of GAGs) was 15% slower than that of Gd-DTPA. In the same paper an enhancement of ca 50% in the relaxivity of Gd-HPDO3A in cartilage with respect to saline was observed.

The assessment of the binding capability of a given CA toward a macromolecular substrate can be conveniently carried out in vitro by exploiting the proton relaxation enhancement (PRE) method which allows to obtain reliable values for the thermodynamic binding constant ( $K_A$ ), the number of binding sites ( $n$ ), and the relaxivity of the macromolecular adduct ( $r_{1b}$ ). To support data reported in figure 1a, binding affinity for HA calculated from data reported in figure 1b follows the order of Gd-BTDO3A > Gd-HPDO3A > Gd-DOTA.

The addition to Gd-complexes solutions of CS and HS at 5 mg/mL concentration did not yield a significant increase in the relaxation rate for all three complexes. Likely, the extensive hydration of the  $SO_3^-$  groups hampers the approach of the neutral Gd-HPDO3A and Gd-BTDO3A molecules thus not allowing the set-up of any H-bonding between the hydroxyl moieties present at the macromolecules and the surface of the complexes.

### What do differences in retention among organs tell us?

We examined how HPDO3A- and BTDO3A- complexes behave when they are simultaneously administered to the same animal by using both  $Eu^{3+}$  and  $Gd^{3+}$  complexes, respectively. The absolute mean values of Eu and Gd retained in the investigated organs are in agreement with those reported by Bussi et al.<sup>47</sup> in a study where Gd-DOTA (Gadoterate), Gd-HPDO3A (Gadoteridol) and Gd-BTDO3A (Gadobutrol) were compared in terms of Gd retention, taking into consideration that, in their study, the total administered dose (12 mmol/Kg) was 4 times higher than that used in this study. As shown in figure 2, the retained Eu/Gd ratio differs significantly from the 1:1 ratio of the administered mixture. In the cerebellum, the relative ratio between Gd-BTDO3A and Eu-HPDO3A is close to 3:1 (Fig 2A). In Fig 2B) the Eu/Gd amounts determined for the other tissues are also reported. In the excretion organs (spleen, liver and kidneys), the actual amounts of Eu or Gd are about two order of magnitude higher than the values found in the brain. This behavior confirms previous observations in animal models. Interestingly, the Eu/Gd ratios maintain the analogous behavior



shown by the brain regions, probably due to the presence of extracellular matrix, inclusive of GAGs, in these three specific organs

Indeed, from these results, it can be hypothesized that the sieving effects in the extravascular, extracellular matrix in the brain, as well in other organs, cause an enhanced retention of Gd-BTDO3A than Eu-HPDO3A. Given that the charge of the two complexes is the same and the thermodynamic and kinetic stability is very high for both, one may speculate that the different behavior may be associated to the presence of the two additional hydroxyl moieties on the ligand's surface in the case of Gd-BTDO3A. The exposed hydroxyl functionalities may represent anchoring sites for the formation of H-bonding with the macromolecular structures present in the extracellular space.

Finally, we explored whether the simple substitution of the lanthanide(III) ion, by maintaining the same ligand, may affect the transit of the complexes in their wash-out processes. For this study, a third lanthanide, Tb, was considered in order to better explore the influence of metal substitution; indeed, Eu(III) and Tb(III) flank Gd(III) in the Lanthanide series.

Therefore, their thermodynamic and kinetic stabilities are very similar and definitively very high to guarantee that no transmetallation can occur during the *in vivo* experiment. Each complex is present under two interconverting isomers defined by the Squared AntiPrismatic (SAP) geometry and the Twisted Square AntiPrismatic (TSAP) one. From previous work it has been ascertained that the SAP/TSAP ratio is equal to 1.5 for Eu-HPDO3A, 2.3 for Gd-HPDO3A and 4 for Tb-HPDO3A, respectively.<sup>50</sup>

We did not observe any significant difference in the retention of the three complexes in cerebrum and cerebellum to confirm that the differences in the solution structures of the complexes of HPDO3A with the three lanthanides do not affect their transit time in the brain. Quite surprisingly, a difference in metal retention was observed in the spleen and liver (Fig 3b), being the amount of retained Tb ca. doubled with respect to Eu and Gd. We investigated if this result could be related to a different uptake capacity of circulating macrophages of the three Ln(III)-HPDO3A complexes by studying the cellular uptake in J774 Mouse BALB/c monocyte macrophages (Fig 4). We didn't observe any different internalization behavior by comparing the three Ln(III)-complexes.

Actually, today we do not have any explanation for this experimental evidence and further investigations will have to be carried out to better elucidate this aspect.

The principal limitation of this study is that the amount of retained metal-complexes was investigated only at one medium-term time point (21 days after the last administration). For a better comparison between the investigated complexes, a long-term sacrifice time point (i.e. 3 or 5 months) should have been considered. Nevertheless, it was already known and reported<sup>42</sup> that the differences in retained Gd for the three commercial macrocyclic GBCAs are canceled at long analysis time (i.e. 5 months or 1 year). However, in this work, we were interested into the understanding of the molecular interactions these complexes can establish once they are administered and distribute in the body at relatively short and medium-time points, before they are completely eliminated.

## Conclusions

Results here presented demonstrate how the use of complexes of different Lanthanide ions enables a direct comparison of the biodistribution of different complexes, hence eliminating the uncertainties associated with the variability of the animal model. The behavior of the macrocyclic complexes studied herein suggests that slight structural alterations are sufficient to cause major changes in molecular interactions with the macromolecules present throughout the wash-out process from the extracellular, extravascular environment. Although our study has been limited to macrocyclic complexes (in order to avoid the complications associated to the de-chelation events), it is expected that analogous behaviors occur also for linear systems. Yet, the behavior of every GBCA during its passage through the extracellular matrix must be evaluated precisely, since simple oversimplifications may be not exhaustive.

# 1.2

Gd retention of GBCAs able to bind serum albumin

## Introduction

Recent works put relevance on the specific Gadolinium retention in the organs of the Central Nervous System (CNS). Renal impairment has been shown to disturb homeostasis and the function of the Blood Brain Barrier (BBB) or the Blood Cerebrospinal Fluid Barrier (BCSFB).<sup>51</sup> The BBB is intact in healthy patients, and only small molecules can flow across it physiologically. However, it is known in the literature that Gd can be retained in the CNS. By crossing the BCSFB, all GBCAs appear in the cerebrospinal fluid (CSF) within a few minutes after an intravenous injection.<sup>52</sup>

However, this is a very static system that experiences few and moderate changes in the adult human life: the wash-out taking place in these tissues, even if it occurs, is very slow. The most accredited hypothesis behind the phenomenon of Gd retention is that the GBCA, after injection in the patient, is almost completely excreted from the body through the renal route in relatively short times, indeed a very small amount remains in the circulation for a longer period, possibly undergoing dechelation and transmetallation. In this way, the free ion could be retained in different amount and in different organs.<sup>53</sup>

The aim of this study is to investigate if the Gd-retention phenomenon can be affected by a different elimination pathway, i.e. renal and/or hepatobiliary. The distribution/elimination pathways that an exogenous molecule experiences *in vivo* are related to the different interactions occurring (or not) with the molecules of the microenvironment in which it is distributed, i.e. the blood which is the first district GBCAs experience once they are intravenously injected in the patients.

Among clinically available GBCAs, two Gd-complexes (i.e. Gd-BOPTA, gadobenate dimeglumine, MultiHance and Gd-EOB-DTPA, gadoxetic acid, Primovist) have a hydrophobic moiety in their structure, which enables the agent to reversibly interact with human serum albumin (HSA) protein. These agents have higher *in vivo* relaxivities than those lacking this substituent thanks to the interaction with serum proteins.<sup>54</sup>

In the case of MultiHance and Primovist, this substituent also allows these agents to be taken up by functioning hepatocytes and eliminated via the hepatobiliary pathway (3–5% for MultiHance; 50% for Primovist).<sup>9</sup>

Moreover, binding to serum albumin (a protein of ca 6 nm in size and a molecular weight of 66.5 kDa)<sup>55,56</sup> could, in principle, reduce the amount of GBCAs that could pass the BBB and thus reduce the metal retained in the CNS, in particular in brain and cerebellum.<sup>57</sup> The study was focused on the analysis of Gd-retained in the organs of mice administered with three Gd-DTPA based complexes characterized by different abilities to bind HSA. Namely, Gd-DTPA (Magnevist), with no-HSA binding, Gd-BOPTA (MultiHance), with moderate binding, and a Gd-DTPA covalently functionalized with a cholic acid (B22956/1), with high HSA binding affinity.<sup>58</sup>

Binding to albumin, which is the most abundant serum protein, influences the blood lifetime of the investigated Gd-complexes after *i.v.* injection, and, thus, could have an effect on their biodistribution and retention.

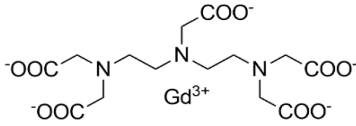
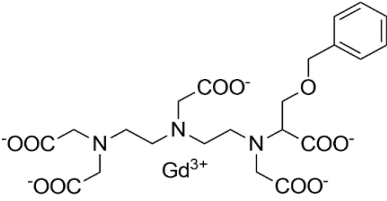
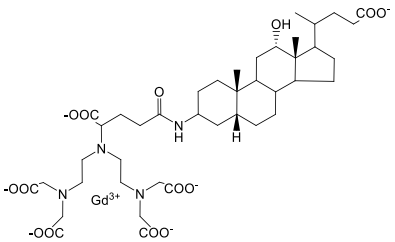
## Methods

### Materials, Chemicals and animals

The following clinical Gadolinium based contrast agents were employed in this study: i) B22956/1, a new preclinical contrast agent for MRI kindly supplied by Bracco Imaging, ii) gadobenate dimeglumine (MultiHance®, Bracco Imaging, Gd-BOPTA), and iii) gadopentetate dimeglumine (Magnevist®, Bayer, Gd-DTPA) (Scheme 1). The last GBCA is used as a control not able to bind HSA.

The experiments have been carried out in accordance with the European Community Parliament and Council Directives of 24 November 1986 (86/609/EEC) and 22 September 2010 (2010/63/EU). Mice were housed with a 12 hours light/dark cycle and free access to food/water. Adequate measures were taken to minimize pain and discomfort. 6–8 week-old-male mice used for all the experimental procedures were purchased from Charles River. 15 male Balb/C mice were divided into three groups, each one administered with a different GBCA: B22956/1, MultiHance and Magnevist. Mice were administered with 12 intravenous injections, at the dose of 0.3 mmol/Kg. The sacrifice was performed 21 days after the last injection. The day of the sacrifice, mice were deeply anesthetized (Zoletil 60 mg/kg and Rompun 5 mg/kg) and underwent cervical dislocation. Next, cerebrum, cerebellum, spleen, liver, kidneys, eyes, skin, a portion of bone and muscle were collected. Each specimen was weighted, mineralized and underwent Gd determination by ICP-MS analysis.

**Table 1** Chemical structures of the Gd-complexes investigated in the study. Affinity constants for human serum albumin,<sup>59</sup> octanol-water ripartition coefficients<sup>59</sup> and thermodynamic stabilities<sup>60</sup>

 <p>[GdDTPA(H<sub>2</sub>O)]<sup>2-</sup> - Magnevist</p> <p>no HSA binding  <math>\log P_{(\text{octanol-water})} = -3,16</math>  <math>\log K_{\text{therm}} = 22,1</math></p>	 <p>[GdBOPTA(H<sub>2</sub>O)]<sup>2-</sup> - MultiHance</p> <p><math>K_a(\text{HSA}) = 3.5 \times 10^2 \text{ M}^{-1}</math>  <math>\log P_{(\text{octanol-water})} = -2,23</math>  <math>\log K_{\text{therm}} = 22,6</math></p>	 <p>B22956/1</p> <p><math>K_a(\text{HSA}) = 4.5 \times 10^4 \text{ M}^{-1}</math>  <math>\log P_{(\text{octanol-water})} = -1,59</math>  <math>\log K_{\text{therm}} = 21,5</math></p>
---	--	---

### Inductively Coupled Plasma-Mass spectrometry (ICP-MS) quantification of Gd content

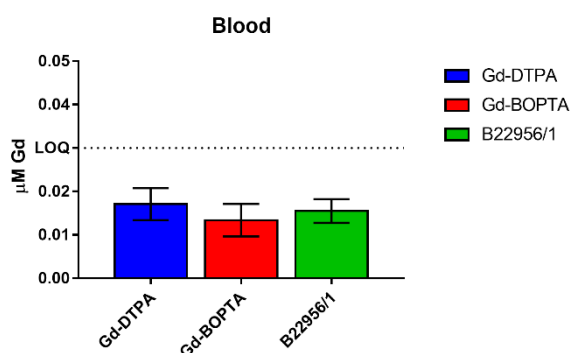
The total amount of Gd in the collected organs and tissues was measured by ICP-MS analysis. The analysis were performed as showed in the previous chapter.

### Statistical Analysis

All data were expressed as the mean values of at least three independent experiments  $\pm$  standard deviation (SD). The statistical analysis were performed using one-way ANOVA followed by the Bonferroni's multiple comparison post-hoc test. The mean of each data set was compared to the group of mice administered with Gd-DTPA (no HSA binding affinity), used as a control group. The statistical significance was defined as follows: \* $p < 0.05$ , \*\* $p < 0.01$ , \*\*\* $p < 0.001$ ; unless differently specified.

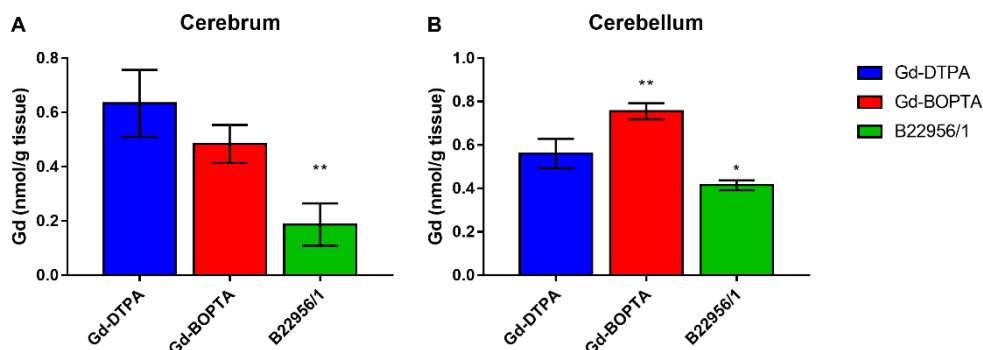
## Results

Gd-DTPA, Gd-BOPTA and B22956/1 were administered to three different groups of mice; after 21 days, mice were sacrificed and the tissue were collected for the quantification of the amount of retained gadolinium. Analysis performed on blood samples collected from each group of mice 21 days after the last injection, shows that most of the GBCAs were correctly excreted by the mice: as shown in figure 1, the whole amount of Gd is under the Limit of Quantification (LOQ) in all the three groups of mice.



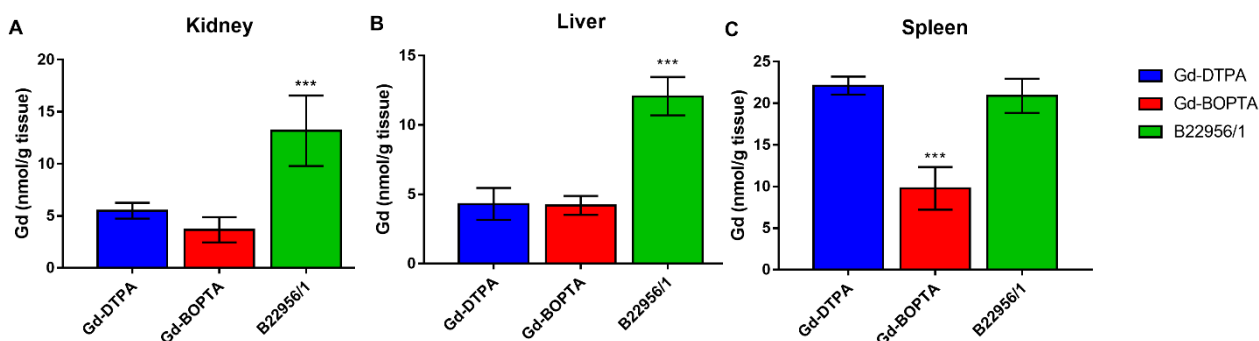
**Figure 1:** Amount of gadolinium (nanomol Gd/mg of tissue) in blood after the exposure to Gd-DTPA, Gd-BOPTA and B22956/1. Mice were administered with 12 intravenous injection, at the dose of 0.3 mmol/Kg and sacrifice after 21 days.

Figure 2 reports total gadolinium retained in the CNS organs: the metal is less retained in cerebrum and cerebellum of mice administered with B22956/1, which is the GBCA with the highest affinity toward albumin, with respect to mice administered with Gd-DTPA and Gd-BOPTA.



**Figure 2:** Amount of gadolinium (nanomol Gd/mg of tissue) in brain (A) and cerebellum (B) after the exposure to gadopentetate dimeglumine, gadobenate dimeglumine and B22956/1. Mice were administered with 12 intravenous injection, at the dose of 0.3 mmol/Kg and sacrifice after 21 days.

Interestingly, the amount of total metal found in the other tissues is significantly higher in the case of tissues derived from mice administered with B22956/1. In particular (Fig 3), kidneys and liver from mice administered with this GBCA retain metal in concentration more than doubled with respect to organs collected from the groups administered with Gd-DTPA and Gd-BOPTA. The total amount of Gd retained in the spleens follows a distribution which is not of easy interpretation. In fact, the group administered with Gd-BOPTA retained an amount of gadolinium which is significantly lower compared to the other two groups, without a clear dependence on the albumin binding ability.



**Figure 3:** Amount of gadolinium (nanomol Gd/mg of tissue) in kidney (A), liver (B) and spleen (C), muscle (E) and bones (F) after the exposure to Gd-DTPA, Gd-BOPTA and B22956/1. Mice were administered with 12 intravenous injection, at the dose of 0.3 mmol/Kg and sacrifice after 21 days.

In figure 4, ICP-MS analysis performed on a portion of muscle, bones and skin shows similar results to kidney and liver. Bones shows smaller differences between the groups, even if the amount retained from bones of mice administered with B22956/1 is still significantly higher than in the other two groups; the portion of skin analysed, shows the same trend as the bones, but the differences are more statistically significant.

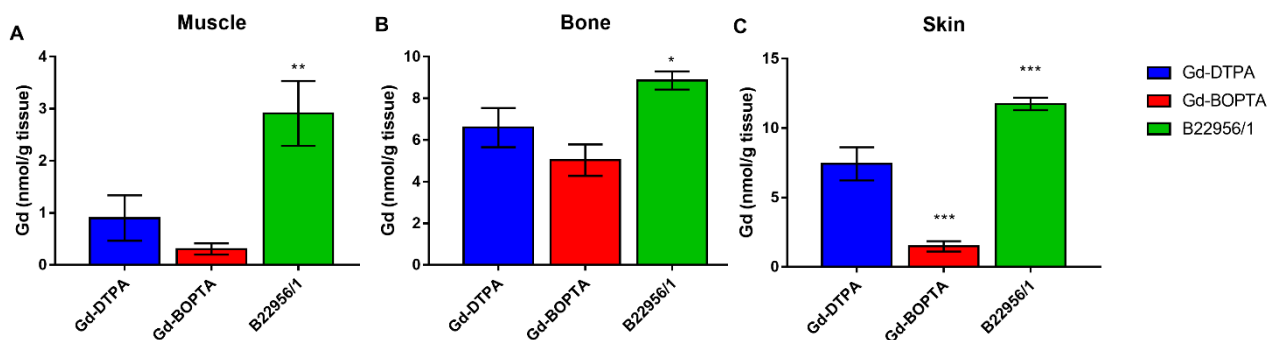


**Figure 4:** Amount of gadolinium (nanomol Gd/mg of tissue) in muscle (A), bone (B) and skin (C) after the exposure to gadopentetate dimeglumine, gadobenate dimeglumine and B22956/1. Mice were administered with 12 intravenous injection, at the dose of 0.3 mmol/Kg and sacrifice after 21 days.

**Table 1:** Metal concentrations (in nmol/g of wet tissue) for the various tissues/organs determined by ICP-MS analysis upon administration of Gd-DTPA, Gd-BOPTA and B222956/1 (Mean values  $\pm$  SD). The P value is related to the difference between the two group administered with Gd-BOPTA and B222956/1 and the control group Gd-DTPA.

Tissue/organ	Gd-DTPA (nmol/g)	Gd-BOPTA (nmol/g)		B222956/1 (nmol/g)	
Cerebrum	0.633.7 $\pm$ 0.1236	0.4844 $\pm$ 0.07001	ns	0.1871 $\pm$ 0.0782	*** P<0.001
Cerebellum	0.561 $\pm$ 0.06759	0.7559 $\pm$ 0.03717	** P<0.01	0.415 $\pm$ 0.02303	* P<0.05
Kidney	5.498 $\pm$ 0.7567	3.671 $\pm$ 1.207	ns	13.18 $\pm$ 3.384	*** P<0.001
Liver	4.305 $\pm$ 1.151	4.198 $\pm$ 0.6855	ns	12.07 $\pm$ 1.383	*** P<0.001
Spleen	22.12 $\pm$ 1.081	9.777 $\pm$ 2.561	*** P<0.001	20.9 $\pm$ 2.052	ns
Muscle	0.9001 $\pm$ 0.4367	0.3057 $\pm$ 0.1091	ns	2.911 $\pm$ 0.6213	** P<0.01
Bone	6.595 $\pm$ 0.9417	5.03 $\pm$ 0.7543	ns	8.855 $\pm$ 0.4355	* P<0.05
Skin	7.426 $\pm$ 1.197	1.48 $\pm$ 0.3721	*** P<0.001	11.75 $\pm$ 0.449	*** P<0.001



## Discussion

The purpose of this research was to investigate the correlation between the total Gd retained in murine tissues and the ability of the GBCA to form, once administered *in vivo*, macromolecular adducts with high molecular weight substrates such as proteins. Mice were administered with GBCAs with specific characteristics in order to understand how much the binding with the HSA is significant in the Gd retention in brain and other organs tissue. Three different compounds were taken into consideration (Scheme 1):

1. gadopentetate dimeglumine (Magnevist®, Bayer, Gd-DTPA), a linear ionic GBCA used as a control without binding affinity for albumin;
2. gadobenate dimeglumine (Multihance®, Bracco Imaging, Gd-BOPTA), a linear ionic GBCA already used in clinics for liver MRI, having a  $K_a(\text{HSA})=2-4.9 \times 10^2 \text{ M}^{-1}$ ; <sup>61</sup>
3. gadocoletic acid trisodium salt (B22956/1; Bracco Imaging), a gadolinium-based contrast agent formulated to be used as a blood-pool agent, whose potential has been assessed in detail in preclinical and clinical (phase I) trials. <sup>59,62,63</sup> The compound is a derivative of gadopentetate to which a bile acid like lateral chain has been linked to increase the binding to the plasma protein and so its circulation lifetime. This molecule has a  $K_a(\text{HSA})= 4.5 \times 10^4 \text{ M}^{-1}$ . <sup>59</sup>

GBCAs with similar stability characteristics but different HSA binding ability were compared. Indeed, the three tested Gd-complexes are derived from DTPA ligand without modification of the coordination ability of the ligand and the same overall charge. Actually, the relative thermodynamic stability constants reported in Scheme 1, are very similar.

On the other hand, the structures of the three complexes are rather different, in that Gd-DTPA is a linear ionic hydrophilic complex lacking any substituent able to establish any kind of hydrophobic interaction with serum albumin, while Gd-BOPTA, and even more B22956/1, are provided with hydrophobic substituents allowing non-covalent binding to plasma proteins.

The affinity order shown by the three GBCAs toward HSA,  $\text{Gd-DTPA} < \text{Gd-BOPTA} < \text{B22956/1}$ , follows the same trend found for their lipophilicity values (Scheme 1).

The insertion of the bile acid lateral chain takes to an increase in logP value of almost one unit. The increase in the lipophilic character of the Gd-complexes fosters the binding affinity for serum proteins leading to an increase in their circulation half-life and to a different elimination pathway from the body. Significant hepatobiliary excretion has been reported for B22956/1 <sup>64,65</sup> and, to a lesser extent, for Gd-BOPTA.

This reversible binding slows the molecule's tumbling and increases gadolinium's paramagnetic efficacy, allowing for lower contrast agent doses when compared to typical extravascular contrast agents. Gd-BOPTA has an *in vivo* blood relaxivity approaching twice that obtained in aqueous solution because it weakly binds to plasma proteins. B22956/1, with its strong binding, can provide high T1-relaxivity ( $\sim 27 \text{ mM}^{-1} \text{ s}^{-1}$  at 20 MHz Larmor frequency in human serum), which is almost six-fold higher than that of conventional extravascular contrast agents ( $4.9 \text{ mM}^{-1} \text{ s}^{-1}$  at 20 MHz Larmor frequency in human serum). In preclinical trials, B-22956/1 was able to maintain blood T1 below 100 ms for 25 min in pigs. <sup>66</sup>

Therefore, according to this premise, the amount of metal found in the organs of mice administered with the three GBCAs, can be, in principle, correlated with their ability to bind albumin and thus with pathway of albumin distribution through the body. To better highlight eventual relationships, the amounts of retained Gd in the principal organs were correlated with the binding association constant ( $K_a$ ) of the three Gd-complexes towards HSA and with their lipophilicity (logP) (Fig 5).

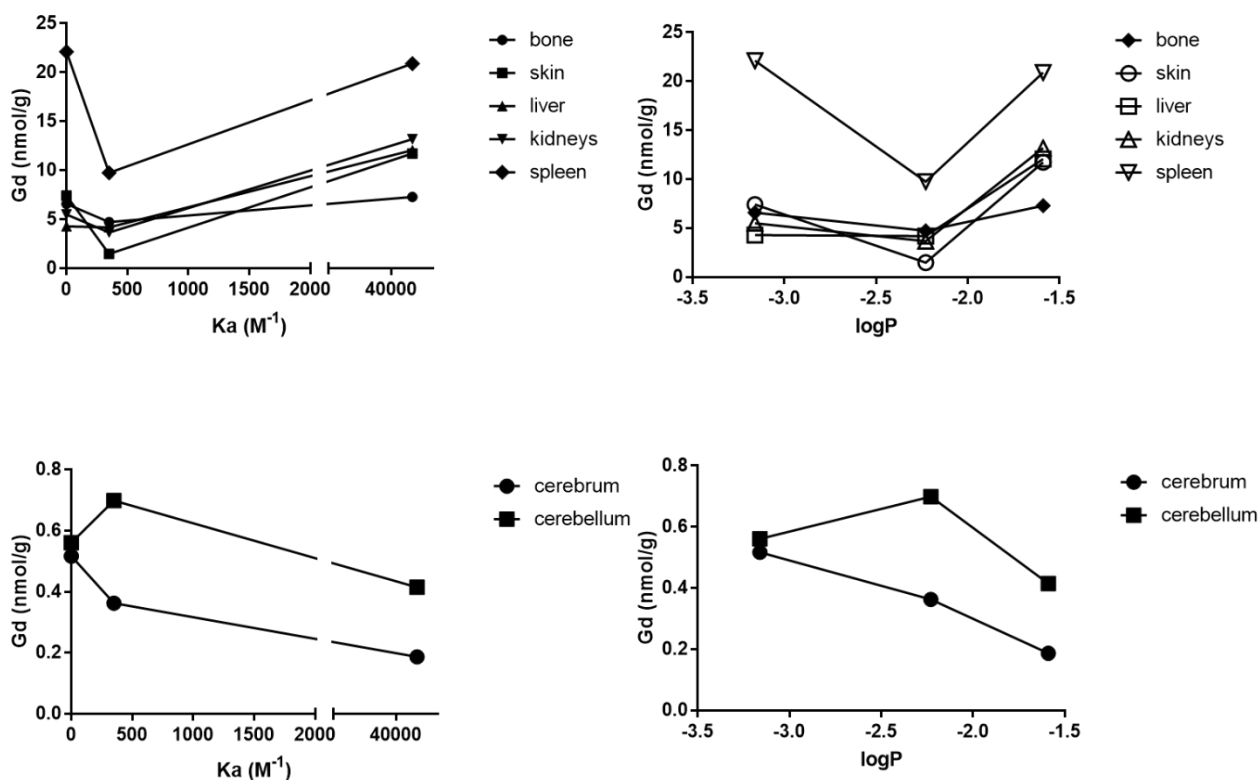


**Figure 5:** Amount of retained Gd in bone, skin, liver, kidneys, spleen, cerebrum and cerebellum of mice administered with Gd-DTPA, Gd-BOPTA or B22956/1 as a function of their binding affinity constant towards HSA or their lipophilicity ( $\log P$ ).

We found that the whole quantity of Gd in cerebrum and cerebellum are significantly lower in mice administered with B22956/1, which has the higher binding affinity for albumin. These results suggest that the reduced extravasation from the blood vessels due to the higher size of the protein-bound Gd-complex leads to a decrease of the metal retained in the CNS.

Conversely, the analysis of Gadolinium retained in the other organs shows an opposite trend. In mice administered with B22956/1, the gadolinium amount found in liver, kidneys and muscle is more than twofold that found in the same organs of mice administered with Gd-DTPA or Gd-BOPTA. The metal concentrations determined in mice administered with Gd-BOPTA are similar to those obtained in mice treated with Gd-DTPA. In particular, despite the fact that Gd-BOPTA is used as GBCA specific for liver imaging<sup>67</sup> only the liver of mice injected with B22956/1 shows an amount of Gd twice the metal found in the livers of the other mice groups.

Lastly, in bones, the difference in Gd retained by each group of mice is less pronounced. This is not surprising, as bones are considered one of the main important deposit of Gd for many metal complexes, which remains almost at the same level for long period.<sup>38</sup> However, when B22956/1 is used, the metal concentration is statistically greater compared to the other groups. The skin shows similar outcomes from the group of mice administered with B22956/1, but not in the tissue from the group administered with Gd-BOPTA, where the amount of metal retained is lower.

In general, the higher gadolinium retention experienced by mice injected with B22956/1, is likely to be related to the longer residence lifetime of this Gd-complex in the blood stream, which, in turn, relies on its higher binding affinity towards serum albumin. Being retained in the blood for longer time, B22956/1 travels through the body districts for longer and thus the probability to go towards dechelation/transmetallation phenomena or interaction with endogenous macromolecules of the tissues matrices increases.

## Conclusions

This work gives some insights about the Gd retention in the different organs/tissues as a function of the GBCA ability to bind serum proteins. It was found that, while increasing the size of the paramagnetic complex through non covalent albumin binding takes to a reduced deposition of gadolinium in the CNS organs (cerebrum and cerebellum), the amount of gadolinium retained in the other investigated organs (liver, kidneys, muscle and bones) is significantly increased. These results assume particular importance for the evaluation of the Gd-retention issue in the case of use of blood-pool GBCAs for angiographic applications. The prolonged circulation time characteristic for these contrast agents could raise, in principle, concerns related to an increased Gd retention in the principal body organs.



# 1.3

Gd retention upon the injection of a liposomal formulation of Gd-DTPA-BMA

## Introduction

Medical imaging is one of the most important branch in clinical diagnosis, and it is characterized by a wide diversity of techniques. Depending on the needs, one imaging modality is chosen instead of another, based on the invasiveness, resolution, deep tissue penetration, and so on. In general, Magnetic Resonance Imaging becomes a preferable choice to access in-depth anatomical details<sup>8,68-70</sup>, but suffers from low intrinsic contrast sensitivity. For this reason, the contrast can be enhanced with the use of compounds, such as Gadolinium-Based Contrast Agents (GBCAs). Regardless of the improvements, sometimes insufficient contrast is observed during the acquisition, presumably due to the insufficient CAs at the intended site.<sup>68,70-72</sup> In the years, to avoid this problem, nanosized system were used in association with the CAs, allowing a better localization of the compound and minimizing the administered Gd dose.<sup>73</sup>

As evidenced in the second part of this chapter (1.2), a Gd-complex able to strongly bind the high-molecular weight serum albumin is also less retained in the CNS: indeed, this is a protein of ca 6 nm in size and has a molecular weight (MW) of 66.5 kDa,<sup>55,56</sup> which extravasation is reduced. The aim of that study was to investigate if Gd retention in the CNS can be reduced, through the increasing of the size of the used GBCA. The obtained results confirmed this assumption, but the Gd retention in other districts was dramatically increased compared to that obtained in control mice treated with GBCAs endowed with no- or low binding to HSA.

The work reported in this chapter, is an extension of the study reported in the previous chapter and was aimed at the investigation of the extent of Gd-retention upon the use of a Gd-based nanosized system obtained by the encapsulation of a low molecular weight GBCA in the aqueous cavity of a liposome. Liposomes are self-assembling spherical structures composed by a lipid bilayer enclosing an internal aqueous cavity. Based on the composition of the used lipids and on the structure of other possible components, the size of the liposomal nanoparticles varies from nanometers to micrometers.<sup>74</sup> For this project, the linear neutral gadodiamide (Omniscan®, GE Healthcare, Gd-DTPABMA), GBCA was chosen: the Gd-based compound, being a hydrophilic molecule, can be incorporated in the aqueous core of the liposome.

In order to better appreciate eventual differences between the free GBCA and its liposomal formulation, the choice of the GBCA intentionally fell on the least robust and stable of the available commercial contrast agents, namely gadodiamide.

A second rationale was behind the design of the present study: beside increasing the size of the system, and thus disadvantaging the BBB crossing of the GBCA, the encapsulation of Gd-DTPABMA in the liposomal cavity could, in principle, protect the GBCA from eventual interactions with the molecules of the microenvironment, thus, in principle, increase its stability and decrease Gd release and retention.

## Methods

### Liposome preparation

Large unilamellar vesicles (LUV) were prepared by following the lipidic thin film hydration method. Briefly, the lipids (30 mg/mL in total including 75% of POPC PM, 5% of MetossiPEG and 20% of cholesterol) were dissolved in chloroform and the organic solution was slowly evaporated to remove the solvent until a thin film was formed. The film was then hydrated at 55°C with neutral aqueous solutions containing 300 mM Gd-DTPA-BMA. The resulting suspension of multilamellar vesicles was extruded (Lipex extruder, Northern Lipids Inc., Canada) two times through polycarbonate filters of 400 nm and four times through 200 nm filters. The final suspension of LUV was purified from not encapsulated Gd-complex by exhaustive dialysis carried out at 25°C against an iso-osmolar NaCl solution. For size measurement, the vesicles dispersions were diluted 100 times and investigated by dynamic light scattering (Zetasizer NanoZS, Malvern, UK) in order to assess the mean hydrodynamic diameter and the polydispersity (PDI) of the system which were determined to be 160 nm and 0.05, respectively.

### Animals

Mice were randomized in two groups (n=4 each): the first one was administered with a total of 3 intravenous injections of liposomal gadodiamide at a dose of 0.1 mmol Gd/kg every 2 days; the second group was administered with an aqueous solution of gadodiamide at the same dose of 0.1 mmol Gd/kg every 2 days, as a control. The sacrifice was performed after 7 days since the last administration. The day of the sacrifice, mice were deeply anesthetized (Zoletil 60 mg/kg and Rompun 5 mg/kg) and underwent cervical dislocation. After sacrifice, blood, cerebrum, cerebellum, spleen, liver, kidneys, eyes, skin, and a portion of bone and muscle were collected. Each specimen was weighted, mineralized and underwent Gd determination by ICP-MS analysis.

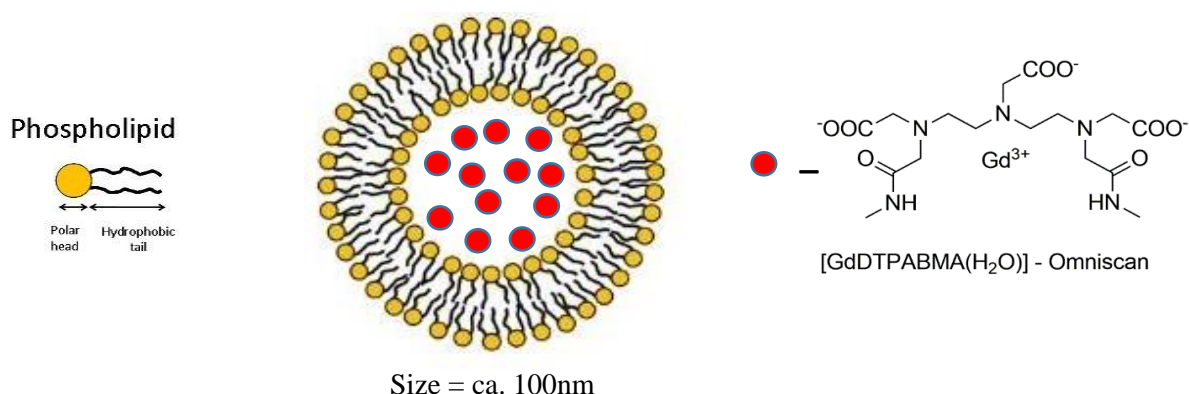


**Figure 1:** Scheme of Gd-DTPA-BMA encapsulated in the nanosized structure.

### Inductively Coupled Plasma-Mass spectrometry (ICP-MS) quantification of Gd content

The Gd content of the collected organs and tissues was measured by ICP-MS analysis. The analysis were performed as showed in the previous chapters.

### Statistical Analysis

All data are expressed as the mean values  $\pm$  standard deviation (SD). The group of mice administered with Gd-DTP-BMA is used as a control group. Between group differences with respect to the mean Gd concentration were assessed using unpaired t test followed by the Bonferroni's multiple comparison post-hoc test, as seen in the previous chapters. Graph-Pad Prism 7.00 software was used for data analysis. Overall, statistical significance was defined as follows: \* $p < 0.05$ , \*\* $p < 0.01$ , \*\*\* $p < 0.001$ ; unless differently specified.



## Results

The amount of total Gd found in the cerebrum and cerebellum of mice administered with three doses of gadodiamide 0.1 mmol/kg or with the same dose of gadodiamide encapsulated in the liposome (Fig 2) is almost equal between the two groups.

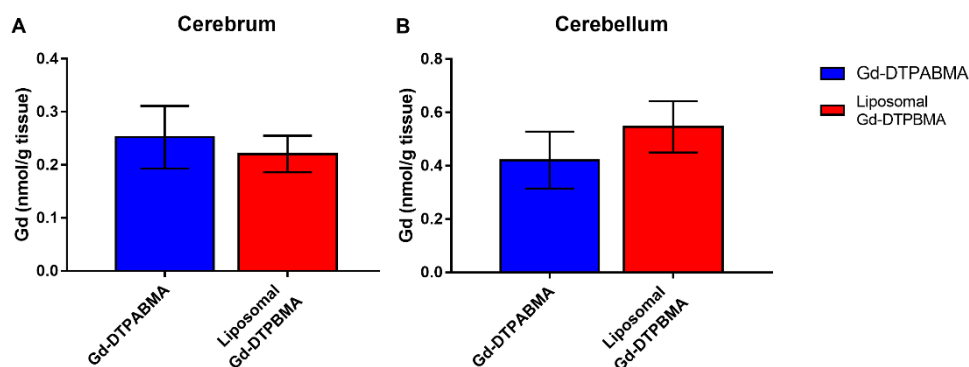


**Figure 2:** Amount of gadolinium (nanomol/g of tissue) in cerebrum (A) and cerebellum (B) after the administration of three doses of gadodiamide encapsulated and non-encapsulated in the liposome, at the dose of 0.1mmol/kg.

On the contrary, the results obtained analysing the other tissues are consistently different. Indeed, in the organs usually deputy to the excretion of exogenous substances, after 7 days, the amount of Gd retained upon the administration of the liposomal formulation is incredibly higher. Specifically, in kidneys and liver (Fig 3A and 3B) the metal concentration in the group of mice treated with the liposome, is greater than 10 and 100 times, respectively, when compared with the control group. In the spleen the difference is even higher as the amount of retained gadolinium (Fig 3C), is 1000 times higher than the metal found in the control group.

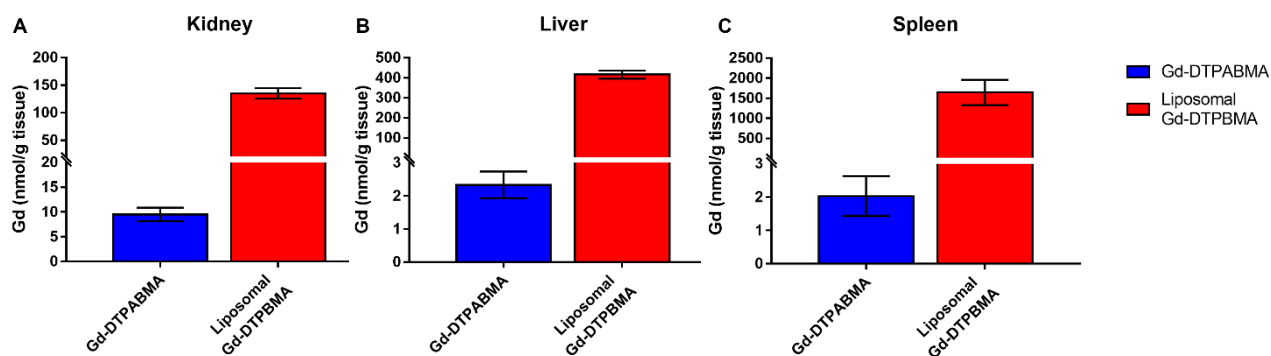


**Figure 3:** Amount of gadolinium (nanomol/g of tissue) in kidney (A), liver (B) and spleen (C), after the administration of three doses of gadodiamide encapsulated and non-encapsulated in the liposome, at the dose of 0.1mmol/kg.

Following the same trend, in muscle, bones and skin the amount of metal found in the mice administered with the liposome is extremely higher, almost 10 folds, than the quantity found in the control group of mice (Fig 4).

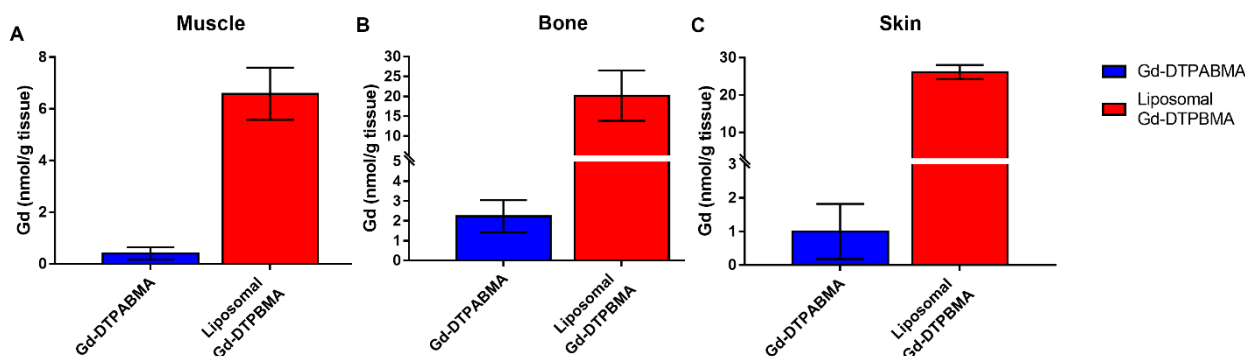


**Figure 4:** Amount of gadolinium (nanomol Gd/mg of tissue) in muscle (A), bones (B) and skin (C), after the administration of three doses of gadodiamide encapsulated and non-encapsulated in the liposome, at the dose of 0.1 mmol/kg.

In the end, an aliquot of blood from each mice was collected and analysed to determine the Gd content (Fig 5). Again, 7 days after the last administration, the amount of Gd found in the blood of mice administered with gadodiamide encapsulated in the liposomes is tremendously higher than the amount in the blood of mice injected with free gadodiamide.

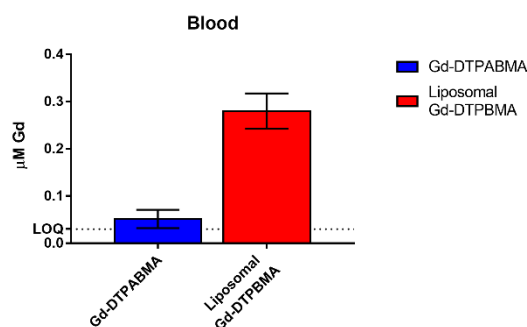


**Figure 5:** Concentration of gadolinium (µM) in blood after the administration of three doses of gadodiamide encapsulated and non-encapsulated in the liposome, at the dose of 0.1 mmol/kg.

**Table 2:** Gd concentrations (in nmol/g of wet tissue) for the various tissues/organs determined by ICP-MS analysis upon administration of Gd-DTPABMA and its liposomal formulation (Mean values ± SD).

Tissue/organ	Gd-DTPABMA (nmol/g)	Liposomal Gd-DTPABMA	P value
Cerebrum	0.2523 ± 0.05898	0.2206 ± 0.03448	ns
Cerebellum	0.421 ± 0.1066	0.5459 ± 0.09647	ns
Kidney	9.487 ± 1.358	135.1 ± 9.485	***P<0.001
Liver	2.332 ± 0.4002	415.7 ± 19.7	***P<0.001
Spleen	2.032 ± 0.5965	1643 ± 315.3	***P<0.001
Muscle	0.402 ± 0.2413	6.585 ± 1.01	***P<0.001
Bone	2.229 ± 0.8207	20.17 ± 6.339	***P<0.001
Skin	1.323 ± 0.8509	26.15 ± 1.861	***P<0.001
Blood	0.05124 ± 0.01927	0.2797 ± 0.03747	***P<0.001

## Discussion

This project was carried out on the basis of the results obtained in the previous chapter: a negative correlation was demonstrated between the size of the administered gadolinium based-compound and the Gd retained in cerebrum and cerebellum. As mentioned before, the reduced extravasation from the blood vessels, due to the larger size of the non-covalent adduct of the GBCA with serum albumin, leads to a decrease of the Gd retained in the CNS. Unfortunately, the observed decrease in Gd retained in the brain was accompanied by a higher accumulation in other compartments of the murine body such as liver, kidney, muscle and bones.

The work described in this chapter was carried out contextually to the work reported in Chapter 1.2, and based on the same purpose.

Unfortunately, in this work it was not possible to administrate to mice the same dose of Gd as the previous work, due to the resulting challenges in encapsulating in the liposome cavity a very high concentration of Gd-DTPABMA. Moreover, the sacrifice of mice was carried out at a relatively short time (7 days) after the last GBCA injection, due to the necessity to recover a quantifiable amount of retained Gd even upon injection of a very low dose. Nevertheless, the main objective of the present study was to compare the amount of retained Gd upon the administration of the liposomal formulation of gadodiamide with that retained injecting free gadodiamide at the same dose. We found that the amount of Gadolinium retained in the CNS is not different between the two groups. On the contrary, as already observed in the previous chapter, looking at other body districts an extremely large difference was observed. Actually, the amount of Gd found in some of the analysed tissues is the highest ever seen even in other works. In kidney, liver and spleen, the metal concentration is 10, 100 and 1000 times higher in the group of mice administered with gadodiamide loaded liposomes with respect of the free gadodiamide. In bones and skin, known in literature to be tissues of preferential Gadolinium deposition,<sup>38</sup> the metal concentration found when the GBCA was encapsulated is almost 20 times higher.

We hypothesized that the tremendous enhancement in Gd retention experienced by mice administered with liposomal Gd-DTPABMA must be found in the longer circulation time of the nanosized liposomes with respect to the small free GBCA. In fact, in blood, 7 days after the last administration, the amount of residual Gd is near to the LOQ value in the group of mice injected with free Gd-DTPABMA while it is five times higher in the liposomal group.

This last result has also to be considered a bias of this study, in fact, since liposomes are retained in the blood circulation after 7 days and the mice were sacrificed by means of cervical dislocation without a prior systemic perfusion to clear the circulatory system of the intravascular blood, a gross percentage of the Gd detected in the spleen, kidney and liver can be explained by the liposomal-Gd present within the intravascular space of those organs rather than the tissutal parenchyma itself.

However, the high metal concentration found in blood cannot completely justify the terribly high quantity of total Gd retained in kidney, spleen and liver tissues.

## **Conclusions**

In summary, the results reported in this chapter clearly indicate that the size of the administered Gd-based compound has an enhancing effect on the extent of Gd retention, in particular in the organs deputed to the contrast agent excretion, that are kidney, liver and spleen.

The only districts where the amount of retained Gd is not enhanced upon the use of a nanosized Gd-based system, are those of the CNS (cerebrum and cerebellum), likely due to a higher hindrance in BBB crossing. Anyway, the initial hypothesis of a possible reduction of Gd retention due to the trick of protecting/masking the GBCA in the internal cavity of a liposome is not supported by the obtained results, thus it cannot be thought as successful.



# CHAPTER 2

## Gadolinium retention in pathology models



## 2.1

# Analysis of the Gadolinium retention in the Experimental Autoimmune Encephalomyelitis (EAE) murine model of Multiple Sclerosis

*Based on Furlan C, Montarolo F, Di Gregorio E, et al. Analysis of the Gadolinium retention in the Experimental Autoimmune Encephalomyelitis (EAE) murine model of Multiple Sclerosis. J Trace Elem Med Biol. 2021;68:126831. doi:10.1016/j.jtemb.2021.126831*

## Introduction

Multiple sclerosis (MS) is the most prevalent chronic inflammatory disease of the central nervous system (CNS), affecting >2 million people worldwide, and currently incurable. MS is a demyelinating disease that causes neuronal damage and the creation of lesions, also known as plaques, when self-reactive immune cells enter the CNS, causing myelin destruction and neuronal damage. The increased permeability of the blood-brain barrier facilitates the invasion of immune cells from the peripheral blood into the CNS (BBB). Many factors contribute to the development of MS, including exogenous, environmental, and genetic factors, but the disease's aetiology is still unknown. MRI is an important tool in the diagnosis of MS and has been part of the diagnostic criteria since 2001<sup>75,76</sup> and it has a fundamental role in the monitoring of disease and in the assessment of treatment efficacy. Clinical protocols for conventional MRI typically include a variety of image acquisitions and approaches. Among them, T<sub>1</sub> contrast-enhanced MRI (CE-MRI) is used to visualize blood–brain barrier breakdown, which represents active lesions, and it is important for the assessing disease dissemination in time to allow for the early MS diagnosis. The disruption of the BBB allows low-molecular-weight MRI contrast agents to extravasate, resulting in a local increase in signal intensity in T<sub>1</sub>-weighted imaging. Enhancement lasts for an average of three weeks before disappearing. The most often used contrast agents for positive MR imaging are gadolinium-based contrast agents (GBCAs). The clinically used GBCAs are considered unable to cross the intact BBB. Indeed, they are very efficient molecules for the MRI detection of any kind of blood-brain barrier disruption of the CNS. Moreover, in the past they were considered very safe products on the basis of more than 300 million administrations, with a very low frequency of acute adverse events. However, in the previous ten years, both renal and non-renal adverse responses have been documented following administration to individuals with or without pre-existing kidney disease.<sup>30–32,77–79</sup>

Patients with MS are subjected to many contrast-enhanced MR exams, resulting in several GBCA injections throughout the life course. In general, no clinical impact associated with Gd retention in the brain has yet been recorded in the field of MS patients; indeed, investigations imply that Gd retention in the brain does not alter clinical deterioration<sup>80</sup>. Nonetheless, some studies have found long-term increases in T<sub>1</sub>-signal in the dentate nucleus (DN) following administration of linear<sup>81–83</sup> and, although to a less extent, macrocyclic GBCAs<sup>84–86</sup>. Actually, it was demonstrated that massive gadobutrol exposure did not induce significant grey and white matter signal intensity or DN relaxometry changes in patients with clinically isolated syndrome<sup>87</sup> or relapsing-remitting MS<sup>88</sup>. More work appears necessary to shed light on this matter that remains the source of great concern among the MS patients.

A recent pre-clinical<sup>89</sup>, study on an immune-mediated murine model of MS, known as Experimental Autoimmune Encephalomyelitis (EAE), found that after repeated administrations of Gd-DTPA, EAE mouse brains retained higher levels of Gd than healthy controls, implying that ongoing inflammation may facilitate Gd retention in brain tissue. However, because of the small number of animals used in the studies, a quantitative analysis of the data was not possible. Notably, the well-defined EAE model is an excellent tool for studying Gd retention in various organs and tissues in a systematic method. Specifically, the invasion of immune cells from peripheral blood into the CNS is facilitated by the increased permeability of the BBB function, which represents a hallmark of MS and is also characteristic for EAE<sup>90</sup>.

Herein, our aim is to quantitatively assess, at the preclinical level in the mice models of MS (EAE mice), the amounts of Gd retained with particular attention to the regions of CNS. The results obtained in the EAE mice are compared to two groups of control mice:<sup>90,91</sup> (I) the sham-immunized control group (SHAM), to confirm that the effects observed in induced EAE mice are attributable to an immune response generated against myelin antigens capable of causing demyelination; and (II) the healthy control group (h-CTRL), to compare the results with a physiological healthy condition. Gadodiamide was administered following several protocols during the disease course. The applied



experimental design allows for the systematic evaluation of potential Gd deposition under controlled and reproducible conditions.

## Methods

### Animals

All experimental procedures were carried out at Neuroscience Institute Cavalieri Ottolenghi (NICO), approved by the Ethical Committee of the University of Torino and authorized by the Italian Ministry of Health (authorization number: 808/2017-PR in 19/10/2017 and following integration in 18/03/2020). The experiments have been carried out in accordance with the European Community Parliament and Council Directives of 24 November 1986 (86/609/EEC) and 22 September 2010 (2010/63/EU). Mice were housed with a 12 hours (h) light/dark cycle and free access to food/water. Adequate measures were taken to minimize pain and discomfort. Female C57BL/6J mice used for all the experimental procedures were purchased from Envigo RMS srl (Udine, Italy).

### EAE induction and clinical evaluation

As reported in <sup>92,93</sup>, to induce EAE, 6–8 week-old-female C57BL/6 mice were immunized by subcutaneous injection under the rostral part of the flanks and at the base of the tail with 300  $\mu$ L of 200  $\mu$ g/mouse of myelin oligodendrocyte glycoprotein (MOG<sub>35–55</sub>; Espikem, Florence, Italy) in incomplete Freund's adjuvant (IFA; Sigma-Aldrich, Milan, Italy) containing 8 mg/mL Mycobacterium tuberculosis (strain H37Ra; Difco Laboratories Inc., Franklin Lakes, NJ, USA). A sham-immunized control group (SHAM) was immunized with the previous emulsion containing IFA and Mycobacterium tuberculosis in which the MOG<sub>35–55</sub> peptide is replaced by phosphate-buffered saline (PBS), as suggested in <sup>90,91</sup>. In addition, a control group of healthy mice (h-CTRL) was included in the study. EAE and SHAM mice were treated with two intravenous injections of 500 ng of Pertussis toxin (Duotech, Milan, Italy) on the immunization day and 48 h later. Body weight and clinical score (0=healthy; 1=limp tail; 2=ataxia and/or paresis of hind limbs; 3=paralysis of hind limbs and/or paresis of forelimbs; 4=tetraplegia; 5=moribund or dead) were recorded daily by an investigator blind to group identity.

### Gadolinium Based Contrast Agent (GBCA) administration protocols

In this study, a total of 3 intravenous injections of gadodiamide (Omniscan®, GE Healthcare, Gd(DTPA-BMA)), a linear neutral GBCA, were administered at a dose of 1.2 mmol/kg every 2 days to three different groups of mice: i) healthy (h-CTRL), ii) SHAM and iii) EAE mice. In mice the dose of 1.2 mmol/Kg is considered equivalent to the usual human dose of 0.1 mmol/kg of GBCA upon adjusting for body surface area as recommended by the FDA (Food and Drug Administration) guidelines<sup>94</sup>. The GBCA administration and the sacrifice were performed following four different protocols based on the development of the disease:

- i. Mice (n=6 per group) were injected during the pre-symptomatic phase of the disease (i.e. at days 4, 6 and 8 post immunization, dpi). The sacrifice time was set to 21 days after the last administration (29 dpi).
- ii. Mice (n=6 per group) were injected in the time range between the onset and the peak of the disease (i.e. at 11, 13 and 15 dpi). The sacrifice time was set to 21 days after the last administration (36 dpi).
- iii. Mice (n=6 per group) were injected during the chronic phase of the disease after the onset (i.e. at 19, 21 and 23 dpi). The sacrifice time was set to 21 days after the last administration (44 dpi).

- iv. Mice (n=6 per group) were injected during the chronic phase of the disease after the onset (i.e. at 19, 21 and 23 dpi). The sacrifice time was set to 39 days after the last administration (62 dpi).

The day of the sacrifice mice were deeply anesthetized (Zoletil 60 mg/kg and Rompun 5 mg/kg) and underwent cervical dislocation. After sacrifice, cerebrum, cerebellum, spinal cord, spleen, liver, kidneys and a portion of bone and muscle were collected. Each specimen was weighted, mineralized and underwent Gd determination by ICP-MS analysis.

### Inductively Coupled Plasma-Mass spectrometry (ICP-MS) quantification of Gd content

The Gd content of the collected organs and tissues was measured by ICP-MS analysis (Element-2; Thermo-Finnigan, Rodano (MI), Italy) and the results expressed as nmol/g of wet tissue weight. Mineralization of samples and ICP-MS analysis were carried out as described in the previous chapters. Considering the mean weights of the organs/tissues recovered from mice and the dilutions made in the preparation of the samples for ICP/MS, the LOQ of the method with respect to the respective tissues/organs were calculated and reported in the following table:

**Table 1:** Limits of quantification (LOQ) in the selected organs/tissues calculated considering the detection limit of the our ICP-MS measures (5 times higher than responses of blank organs from not injected control mice), the mean weights of the organs/tissues and the dilutions made in the preparation of the samples.

<b>Organ/tissue</b>	<b>LOQ (nmol/g of tissue)</b>
Cerebrum	0.021
Cerebellum	0.038
Spinal cord	0.022
Muscle	0.046
Liver	0.0025
Spleen	0.010
Kidney	0.015
Bone	0.158

### Transmission Electron Microscopy (TEM)

TEM was carried out in h-CTRL (n=3) and EAE (n=3) mice. EAE mice were injected during the chronic phase of the disease after the onset (i.e. at 19, 21 and 23 dpi). The sacrifice time was set to 21 days after the last administration (44 dpi).

Conventional TEM was carried out as in ref<sup>95</sup>. Mice were deeply anesthetized (Zoletil 60 mg/kg and Rompun 5 mg/kg) and trans-cardially perfused with 2% paraformaldehyde and 2.5% glutaraldehyde in 0.12 M phosphate buffer, pH 7.2–7.4. The cerebellum and the spinal cord were removed and immersed in the same fixative at 4 °C for 24 h. Vibratome transversal sections (250 µm thick) were cut, and post-fixed with 1% osmium tetroxide for 1 h at 4 °C, then stained with uranyl acetate replacement stain (Electron Microscopy Sciences, USA). After dehydration in ethanol, samples were

cleared in propylene oxide and embedded in Araldite (Fluka, Saint Louis, USA). Semithin sections (1  $\mu\text{m}$  thick) were obtained at the ultramicrotome (Ultracut UCT, Leica, Wetzlar, Germany), stained with 1% toluidine blue and 2% borate in distilled water and then observed under a light microscope for precise location. Ultrathin sections (70–100 nm) were examined under a transmission electron microscope (JEOL, JEM-1010, Tokyo, Japan) equipped with a Mega-View-III digital camera and a Soft-Imaging-System (SIS, Münster, Germany) for computerized acquisition of the images.

### Magnetic Resonance Imaging

MR images of the brain were acquired for healthy control mice (h-CTRL, n=5) not injected with gadodiamide and for four groups of mice 21 days after the last gadodiamide injection:

- I, II: SHAM mice (n=3) or EAE mice (n=3) injected during the pre-symptomatic phase of the disease;
- III, IV: SHAM mice (n=3) or EAE mice (n=3) injected during the time range between the onset and the peak of the disease.

Animals were deeply anesthetized (Zoletil 60 mg/kg and Rompun 5 mg/kg). MR images were acquired at 7.1 T on a Bruker Avance 300 spectrometer equipped with a Micro 2.5 microimaging probe at room temperature (*ca.* 21 °C).

High resolution  $T_{2w}$  images were acquired by using a high-resolution RARE (Rapid Acquisition with refocused Echoes) sequence with the following parameters: TR = 4000 ms, TE = 36 ms, RARE factor = 8, flip angle = 180°, number of averages = 8, FOV = 30 mm  $\times$  30 mm, slice thickness = 0.5 mm, matrix size 384  $\times$  384, spatial resolution = 0.078 mm/pixel  $\times$  0.078 mm/pixel.  $T_{1w}$  images were acquired by using a standard MSME (multi-slice multi-echo) sequence with the following parameters: TR = 200 ms, TE = 3.4 ms, number of average = 6, FOV = 30 mm  $\times$  30 mm, slice thickness = 1 mm, matrix size 128  $\times$  128, spatial resolution = 0.273 mm/pixel  $\times$  0.273 mm/pixel. A glass tube containing a standard solution (ProHance 0.5 mM in water) was placed close to the mouse body as signal reference. Regions of Interest (ROIs) were manually drawn in the cerebellum and the cerebrum: in particular, the deep cerebellar nuclei in the cerebellum, and cerebral cortex, mid brain, hippocampus and hypothalamus, in the cerebrum, were considered.

### Statistical Analysis

All data are expressed as the mean values of at least three independent experiments  $\pm$  standard deviation (SD). Between group differences with respect to the mean Gd concentration were assessed using unpaired t test or two-way ANOVA followed by the Bonferroni's multiple comparison post-hoc test. Graph-Pad Prism 7.00 software was used for data analysis. Overall, statistical significance was defined as follows: \* $p < 0.05$ , \*\* $p < 0.01$ , \*\*\* $p < 0.001$ ; unless differently specified.

## Results

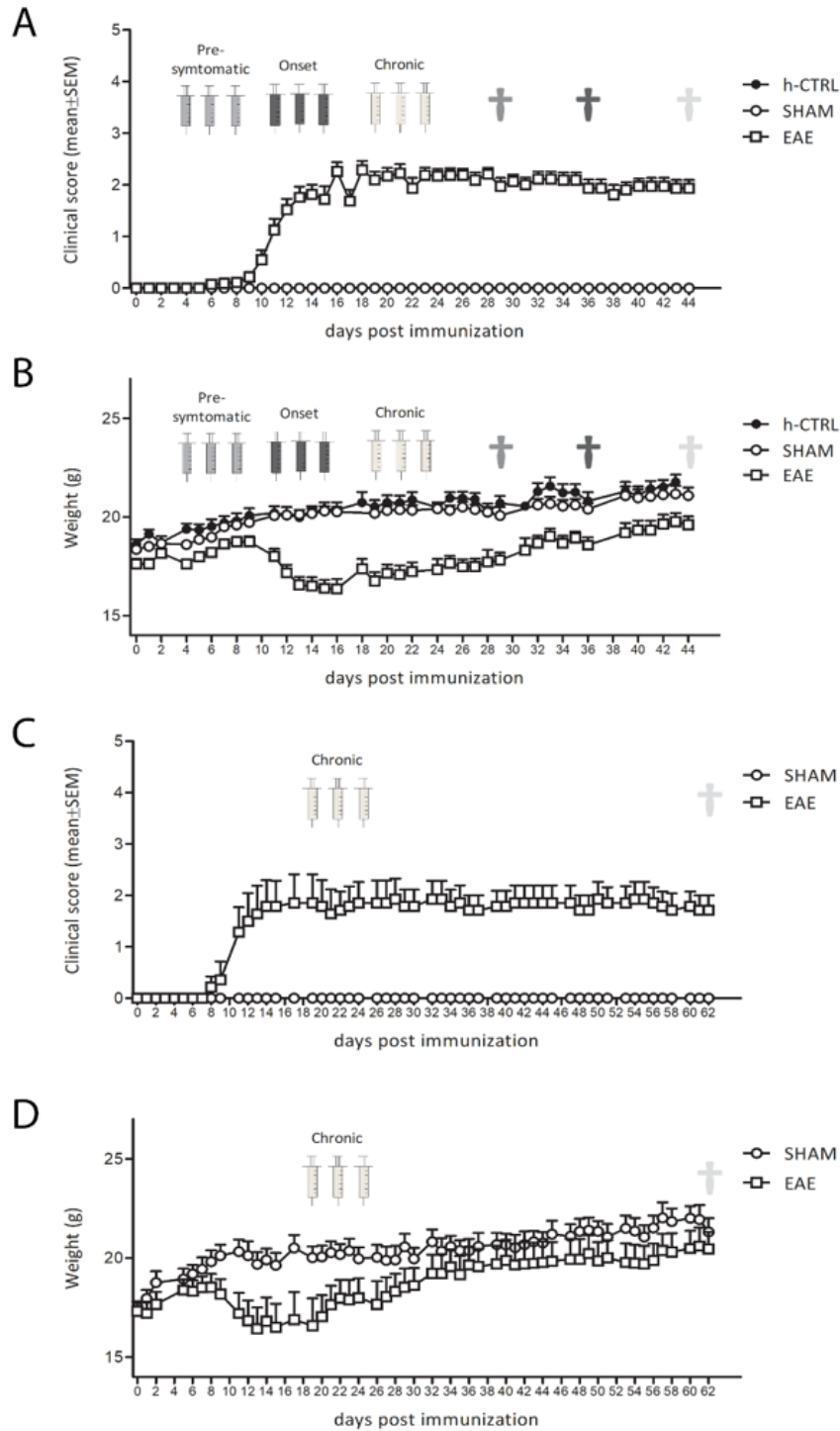
### ICP-MS quantification of retained Gd in healthy control, SHAM and EAE mice upon injection of gadodiamide in different disease phases

Figure 1 shows the clinical course (A, C) and the body weight loss (B, D) during time in h-CTRL, SHAM and EAE mice. All EAE mice had an onset of disability and weight loss. The h-CTRL and SHAM mice rightfully showed no disability and weight loss.

Figure 2 and Table 2 report the amounts of retained Gd in the CNS organs (spinal cord A, cerebrum B and cerebellum C) of EAE mice, injected with 3 doses (1.2 mmol/kg each) of gadodiamide either during the pre-symptomatic, the onset and the chronic phases of the disease model development. The experimental group of EAE mice was compared with the group of healthy mice (h-CTRL) and a third group of inflamed but not demyelinated sham-immunized control group (SHAM).

**Table 2:** Quantitative total gadolinium concentrations in the CNS organs of EAE, SHAM and h-CTRL mice determined by ICP-MS analysis. Data are reported as mean (in nmol/g of tissue)  $\pm$  standard deviation

	<b>Group</b>	<b>Pre-Symp (21 d)</b> nmol/g tissue	<b>Onset (21 d)</b> nmol/g tissue	<b>Chronic (21 d)</b> nmol/g tissue	<b>Chronic (39 d)</b> nmol/g tissue
<b>Spinal cord</b>	EAE	0.553 $\pm$ 0.40	1.32 $\pm$ 0.57	3.05 $\pm$ 0.78	0.111 $\pm$ 0.04
	SHAM	0.516 $\pm$ 0.10	0.428 $\pm$ 0.05	0.464 $\pm$ 0.09	0.03 $\pm$ 0.007
	h-CTRL (21 d)	0.484 $\pm$ 0.16			
<b>Cerebrum</b>	EAE	0.586 $\pm$ 0.11	0.584 $\pm$ 0.13	0.377 $\pm$ 0.06	0.257 $\pm$ 0.09
	SHAM	0.587 $\pm$ 0.10	0.438 $\pm$ 0.10	0.330 $\pm$ 0.05	0.29 $\pm$ 0.08
	h-CTRL (21 d)	0.301 $\pm$ 0.04			
<b>Cerebellum</b>	EAE	1.60 $\pm$ 0.26	1.45 $\pm$ 0.25	1.09 $\pm$ 0.42	0.479 $\pm$ 0.07
	SHAM	1.59 $\pm$ 0.21	1.39 $\pm$ 0.18	0.918 $\pm$ 0.20	0.497 $\pm$ 0.11
	h-CTRL (21 d)	0.741 $\pm$ 0.17			



**Figure 1:** The clinical score (A, C) and body weight (B, D) of healthy control (h-CTRL), SHAM and EAE mice were daily measured and reported. (A-D) Syringes indicate the days when mice were injected with doses corresponding with 1.2 mmol/Kg Gd. Specifically, Gadodiamide was intravenously administered in the pre-symptomatic phase (4, 6 and 8 days post immunization), in the onset (11, 13 and 15 days post immunization) and in the chronic phase (19, 21 and 23 days post immunization). Crosses indicate the sacrifice time. (A-B) In the short experiment the sacrifice of h-CTRL (n=16), SHAM (n=27) and EAE (n=27) mice occurred 21 days after the last administration. In the long experiment only the Gd administration in the chronic phase (19, 21 and 23 days post immunization) is performed and the sacrifice of SHAM (n=5) and EAE (n=7) mice occurred 39 days after the last administration (A-B).

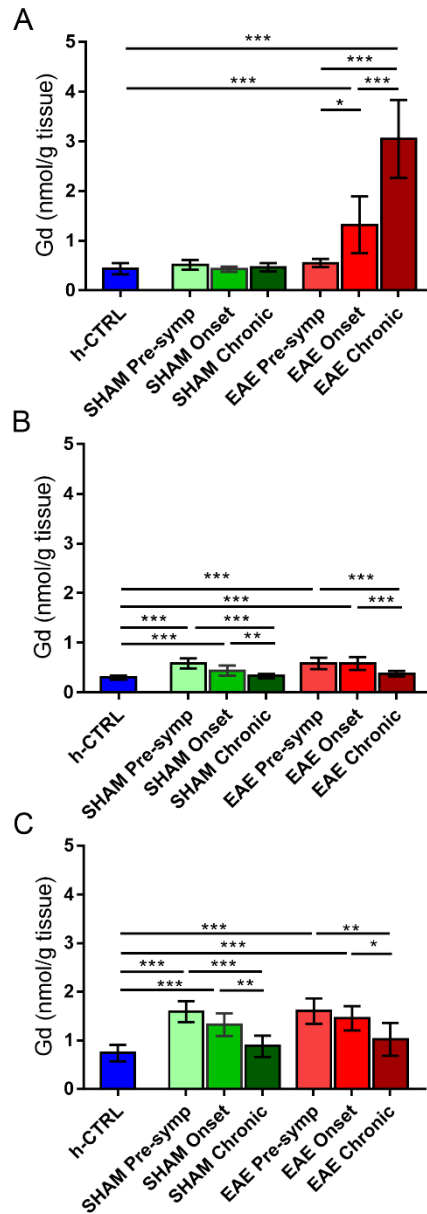


**Figure 2:** Amounts of retained Gd in spinal cord (A), cerebrum (B) and cerebellum (C) of h-CTRL, SHAM and EAE mice administered with three doses of gadodiamide at days 4, 6, 8 p.i. (pre-symptomatic), 11, 13, 15 p.i. (onset) and 19, 21, 23 p.i (chronic). Mice from all experimental groups were sacrificed 21 days after the last GBCA injection.

In the spinal cord (Fig 2A), a low Gd retention was observed in the h-CTRL, in the whole SHAM group and in the EAE mice administered with GBCA in the pre-symptomatic phase. Conversely, upon the GBCA injection in the onset and chronic phase of the model, in EAE group, a significantly higher and progressive accumulation of Gd was detected (six times higher than in h-CTRL, in the chronic group). In the SHAM group, the Gd retention was not significantly different from that of h-CTRL mice.

Conversely, in cerebrum (Fig 2B) and cerebellum (Fig 2C), a lower amount of Gd retention was reached. Notably, a similar behaviour was observed for EAE and SHAM mice. For both groups of mice, a modest but significantly higher retention of Gd was observed, with respect to h-CTRL mice, when animals were injected with the GBCA in the pre-symptomatic phase and on the onset of the disease course but not in the chronic phase.

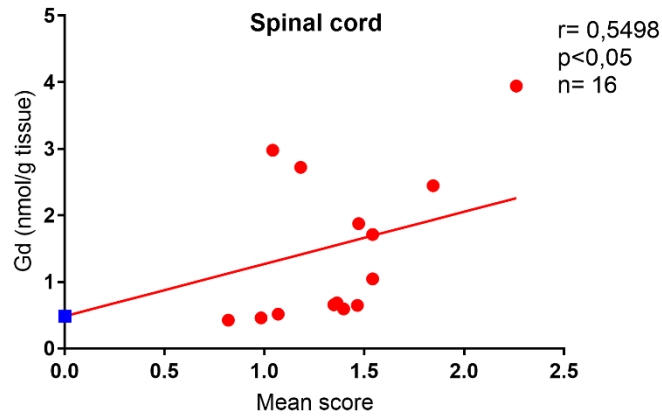


**Figure 3:** Correlation line of the amounts of retained Gd in the spinal cord of each EAE mouse as a function of its mean clinical score (calculated as the ratio between the respective cumulative score and the days of life between immunization and sacrifice) (n= 16, p<0.05). The blue square represents the mean quantity of Gd detected in each spinal cord of the h-CTRL mice group.

Figure 3 reports the amounts of retained Gd in the spinal cord of each EAE mouse as a function of its mean clinical score (calculated as the ratio between the respective cumulative score and the days of life between immunization and sacrifice). A positive correlation was observed with an r-value of 0.5498. The same correlation analysis was carried out in cerebrum and cerebellum without finding any significant correlation (data not shown).

The assessment of the amounts of retained Gd was extended to other organs beside those of the CNS, namely to muscle, spleen, kidneys, liver and bone, (Fig 4).

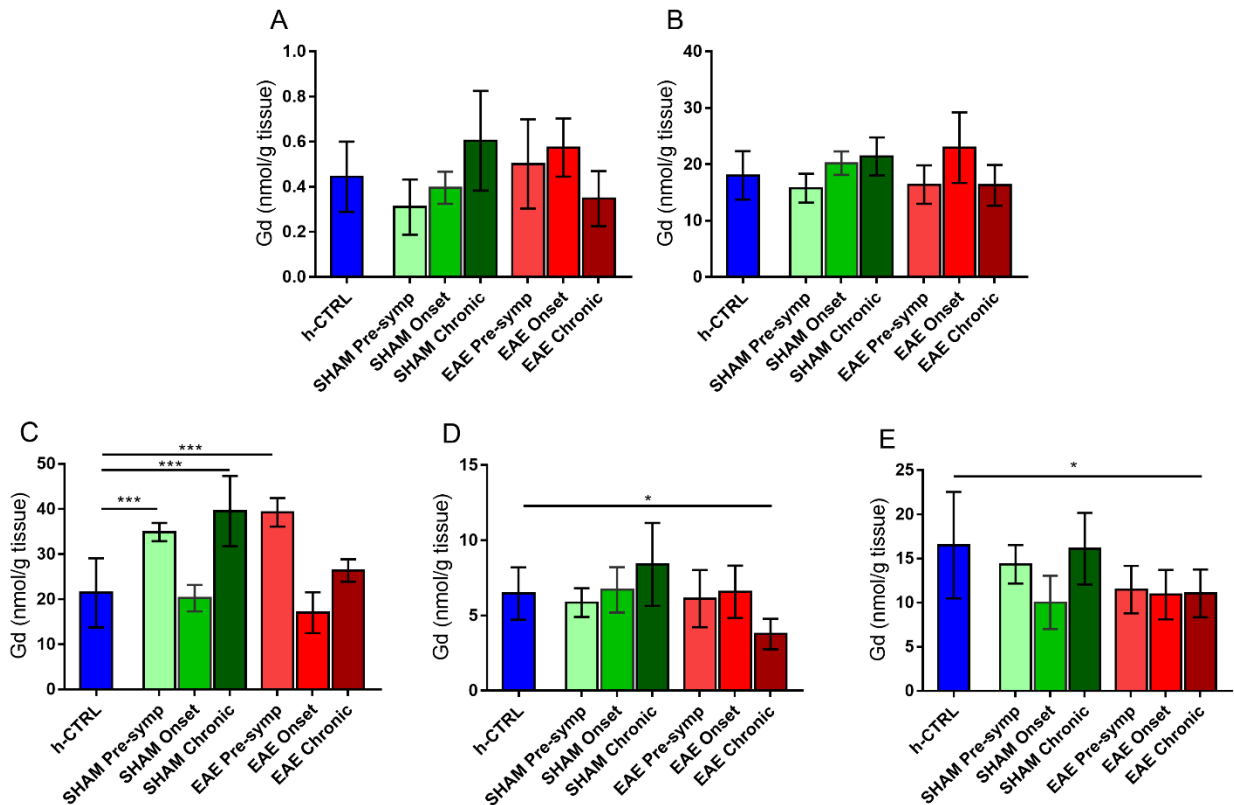


**Figure 4:** Amounts of retained gadolinium in muscle (A), spleen (B), kidney (C), liver (D), and bone (E) of EAE and Sham mice 21 days after the last administration of three doses of gadodiamide in the pre-symptomatic phase (4, 6 and 8 dpi), in the onset (11, 13 and 15 dpi) and in the chronic phase (19, 21 and 23 dpi).

In muscle (Fig 4 A) and spleen (Fig 4 B), no differences emerged in the amounts of retained Gd either comparing the three groups (h-CTRL, SHAM and EAE) or the disease phases when mice were



injected. In the kidneys (Fig 4 C), a significantly higher concentration of Gd was observed with respect to control mice, for SHAM mice injected in the pre-symptomatic and chronic phases and for EAE mice injected in the chronic phases. In the liver (Fig 4 D) and bone (Fig 4 E), a significantly lower concentration of Gd was observed for EAE mice injected in the chronic phase with respect to h-CTRL mice. In addition, a negative correlation was observed ( $r = -0.4748$ ) between the amounts of retained Gd in the bone of each EAE mouse as a function of its mean clinical score (Fig 5). The same correlation analysis was carried out in all the other investigated organs without finding any significant correlation (data not shown).

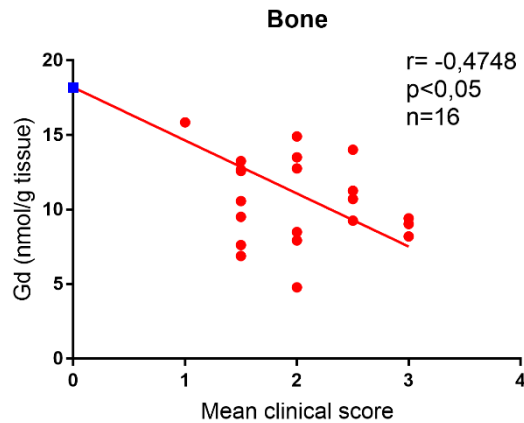


**Figure 5:** Correlation line of the amounts of retained Gd in the bone of each EAE mouse as a function of its mean clinical score (calculated as the ratio between the respective cumulative score and the days of life between immunization and sacrifice) ( $n = 16$ ,  $p < 0.05$ ). The blue square represents the mean quantity of Gd detected in each spinal cord of the h-CTRL mice group.

### Time dependence of Gd retention in EAE and SHAM mice

In figure 6 the time dependence of Gd retention in spinal cord (A), cerebrum (B) and cerebellum (C) of EAE and SHAM mice injected with 3 doses (1.2 mmol/kg each) of gadodiamide during the chronic phase of the disease development were compared. In all the CNS analysed regions a decrease of Gd retention is observed extending the time after the last GBCA injection.

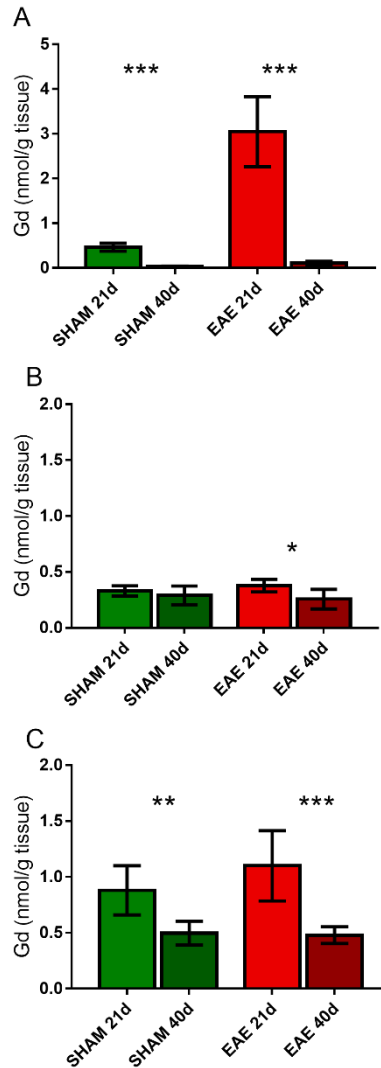


**Figure 6:** Amounts of retained Gd in spinal cord (A) cerebrum (B) and cerebellum (C) of EAE and SHAM mice administered with three doses of gadodiamide at 19, 21, 23 p.i (chronic phase) and sacrificed 21 or 39 days after the last GBCA injection.

Specifically, the decrease of retained Gd is particularly evident in the spinal cord of EAE mice and, to a lesser extent, in SHAM mice. However, 39 days after the last gadodiamide injection, the amount of detected Gd remains well above the LOQ values reported in Table 1, in all the CNS organs. Still, the preferential accumulation is in the spinal cord.

### TEM analysis

To qualitatively validate the presence of Gd in CNS, TEM was applied. Specifically, TEM analysis showed Gd-spheroidal deposits with typical sea urchin-shaped in the basal lamina of blood vessels (Fig 7A and F) and intracellular inclusions (Fig 7A, B, D, F and G), in form of small electron-dense dots in dental cerebellar nuclei (Fig 7A-D) and in spinal cord (Fig 7E-F). Here, Gd-depositions have been shown in a not-damaged area of the cerebellum as indicated in the low magnification image (Fig 7A) and in a demyelinated region of the spinal cord (Fig 7F). Demyelination in the spinal cord is demonstrated by the marked reduction of myelin ensheathment (Fig 7F) in comparison to a not-demyelinated area (Fig 7E).

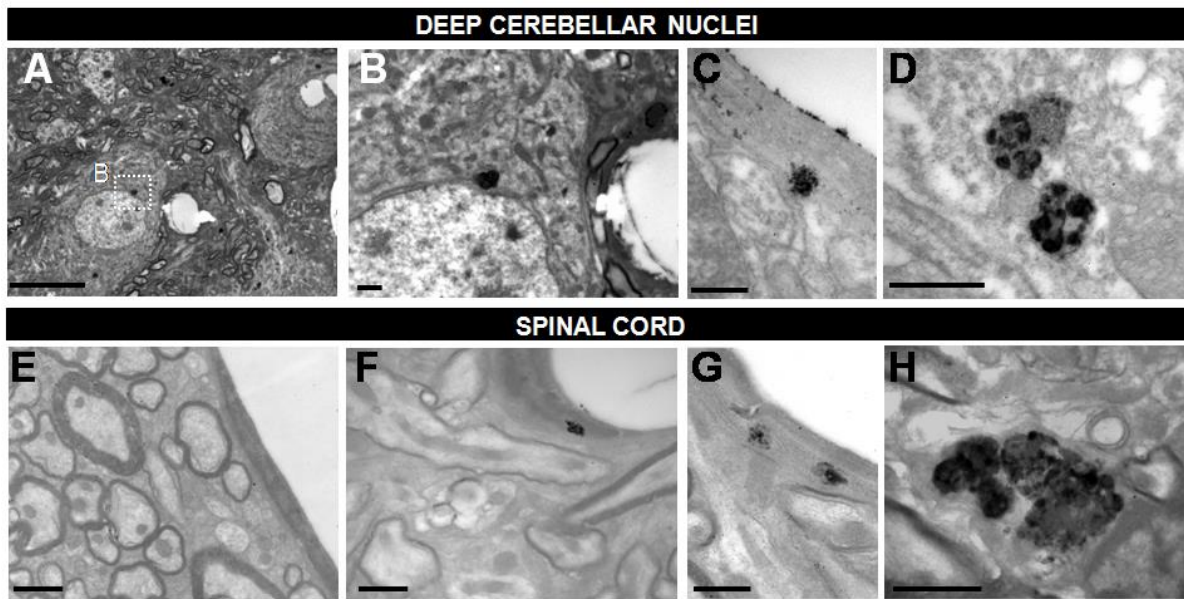


**Figure 7:** TEM tissue localization of Gd-containing deposits in the dentate cerebellar nuclei (A-D) and in the spinal cord (E-G) of EAE mice that received Gd. TEM evaluation showed Gd-containing deposits with typical sea urchin-shaped in the basal lamina of blood vessels (A and F) and intracellular inclusions of Gd (A, B, D, F and G), in form of small electron-dense dots. Representative low magnification images showed not-damaged areas of the cerebellum (A) and spinal cord (E) and a demyelinated regions of the spinal cord (F). Scale bars 10  $\mu\text{m}$  (A), 1  $\mu\text{m}$  (B, E and F) and 500 nm (C, D, G and H).

### Magnetic Resonance Imaging

MR images of the brain were acquired before the sacrifice (i.e. 21 days after the last gadodiamide injection) at 7.1T on groups of mice which received GBCA injection in the pre-symptomatic phase and in the onset of disease progression compared to those of healthy control mice not injected with gadodiamide (Fig 8). No significant difference in signal intensities (reported as the ratio between the signal intensities of each region and the signal intensity of the reference tube) was observed in all investigated groups of mice in cerebrum and cerebellum regions (Fig 9). We did not observe hyper-intense signals even in the dentate nuclei of all groups of mice.

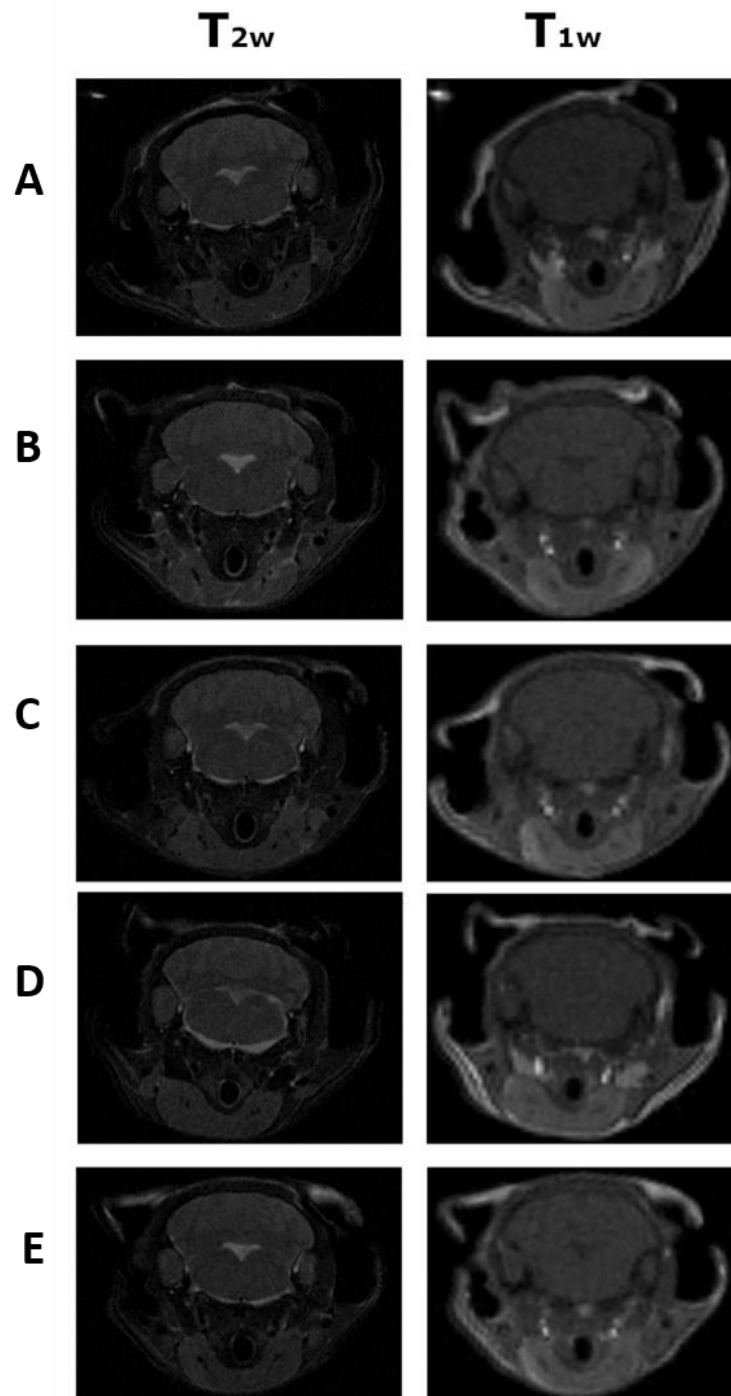


**Figure 8:** T<sub>2</sub> (left) and T<sub>1</sub> (right) weighted MR-images of brains of not injected h-CTRL (A), SHAM (B,C) and EAE (D,E) mice injected with gadodiamide in the pre-symptomatic phase (4, 6 and 8 dpi) (B,D) and at the onset (11, 13 and 15 dpi) (C,E) of the disease. Images were acquired at 7.1 T.

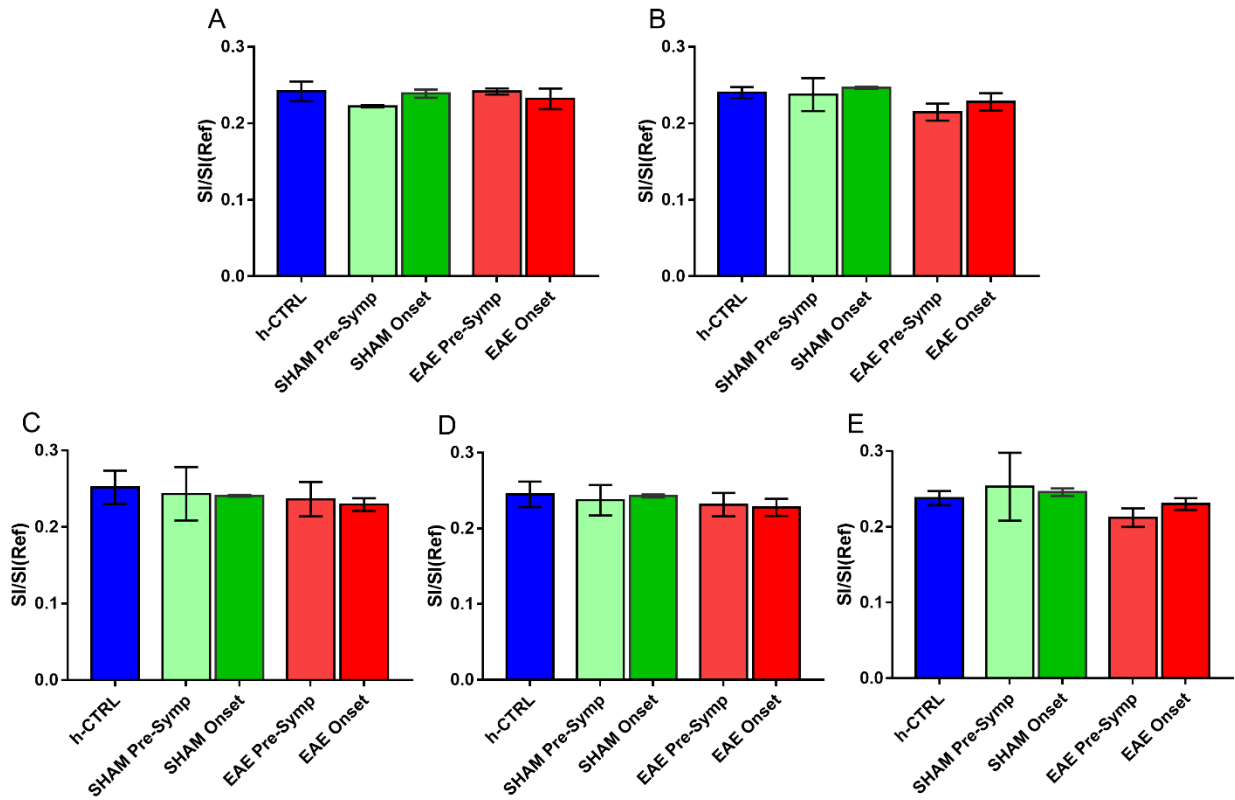


**Figure 9:** Signal intensities (reported as the ratio between the signal intensities of each region and the signal intensity of the reference tube) in  $T_1$  weighted MR images of brains of not injected healthy control and EAE and SHAM mice injected with gadodiamide in the pre-symphomatic phase (4, 6 and 8 dpi) and at the onset of the disease (11, 13 and 15 dpi): (A) deep cerebellar nuclei, (B) cerebral cortex, (C) mid brain, (D) hippocampus and (E) hypothalamus.

## Discussion

The primary goal of this work was to see if the particular circumstances associated with MS pathology (i.e. BBB disruption, inflammation, plaque development) played a role in the retention of Gd after repeated injections of a GBCA in a mouse MS model. The used murine model caused persistent EAE and is regarded as the best option for studying MS pathophysiology.<sup>96</sup> In our study, the model allowed us to assess the role of GBCA injections during the pre-symptomatic, onset and chronic disease stage on the amount of retained Gd. Indeed, the course of the pathology in the model is characterized by an initial inflammatory peak (acute stage) followed by a chronic phase (chronic stage).<sup>97</sup>

The BBB is a continuous endothelial membrane within brain microvessels that has sealed cell to cell contacts and is coated by mural vascular cells and perivascular astrocyte end-feet. The BBB shields neurons from species in the systemic circulation and maintains the highly controlled internal milieu of the CNS, which is necessary for normal synaptic and neuronal functioning.<sup>98</sup> MS neuropathology is characterized by BBB breakdown which plays a crucial role on the pathogenesis of MS disease.<sup>99</sup> In fact, BBB disruption allows influx into the brain of neurotoxic blood-derived debris, cells and microbial pathogens and is associated with inflammatory and immune responses.

Despite the fact that various research have been conducted on Gd deposition in healthy animals, there is a lack of data on animal models that mirror human neurodegenerative disorders or BBB impairment.

We are dealing with a systematic and repeatable animal research that allows for a comparison of healthy and diseased patients, elucidating the level of Gd-retention and comparing it to what was seen in healthy animals. With respect to the study published by Wang et al.<sup>89</sup> several improvements were pursued on a closely related EAE model, including: i) increasing the number of analysed mice in order to achieve statistical significance of results, ii) increasing the sacrifice time after the last administration in order to report on the amount of Gd effectively retained by the considered body districts, iii) investigating the influence of GBCA administration timing during disease progression on the amount of retained Gd, and iv) using, in addition to healthy controls, a sham immunized control group to distinguish between simple inflammation and BBB breakdown caused by the immune response produced against antigens generating demyelination.

In this work, only one GBCA was studied because the emphasis was on the information gathered from comparing different injection procedures rather than comparing different GBCAs. Gadodiamide was chosen because it is well documented that, among clinically utilised drugs, it is the most prone to generate Gd deposition, allowing for the identification of potential variations between protocols even after just three GBCA administrations. Though the correlation analysis between the amounts of retained Gd against the pathological signs in CNS have not been evaluated, some considerations can be made. It is known that, in C57BL/6 EAE model, spinal cord is the favourite target area for plaques formation and multifocal, confluent areas of mononuclear inflammatory infiltration and demyelination in the peripheral white matter of the spinal cord are frequently observed.<sup>98-100</sup>

It was discovered that the spinal cord retains Gd six times more than the inflamed and healthy conditions. However, the cerebrum and cerebellum collect Gd at a lesser rate than the spinal cord, and there are no variations between EAE and SHAM animals. These findings suggest that, in areas characterised by minor demyelination, such as the brain, the lower but significant increased Gd retention (almost doubled for both EAE and SHAM mice) observed in comparison to h-CTRL mice could be related to the general inflammation state induced by IFA and Mycobacterium tuberculosis administration or by intravenous injection of Pertussis toxin, which characterises both EAE and SHAM mice. Conversely, where massive demyelination occurs, Gd retention increases dramatically. The hypothesis regarding the possible dual effect of neuroinflammation and demyelination on Gd retention is also supported by the fact that we have not reported an increase in the amount of Gd retention in the spinal cord of EAE injected with GBCA in the pre-symptomatic phase, when demyelination has not yet occurred. Interestingly, we found higher Gd retention in the cerebrum and cerebellum only when EAE and SHAM mice were treated with gadodiamide in the pre-symptomatic

phase and at the onset of the illness, i.e. a very short period after BBB rupture. Rather, when the GBCA injections are shifted to the chronic phase of illness, the quantity of Gd maintained is nearly identical to that retained by healthy animals. This finding lends credence to the idea that the temporal closeness of BBB rupture and GBCA injection might alter Gd retention in the CNS, with differing behaviour in the encephalon and spinal cord. The spinal cord's positive association between the quantity of retained Gd and the clinical score of each EAE mouse further confirms this idea. This finding appears to be particularly important for translation to human MS patients, since it draws attention to the possibility of greater Gd retention in the areas most affected by MS pathology. Importantly, this preferential accumulation of Gd in the spinal cord of EAE mice has been shown to be transient, with a reduction in Gd retention found when the sacrifice time is extended to 39 days following the previous injection, indicating an effective washout process.

An interesting result was obtained looking at the amount of retained Gd in the bones of EAE mice. Unlike in the other body districts, the extent of retained Gd is inversely related to disease progression (measured as the mean clinical score). This discovery is most likely related to the impairment caused by the model's sick circumstances, as well as the decreased mobility of ill mice. The TEM analysis allowed us to add spatial and qualitative information to the obtained results. Accordingly to<sup>101</sup> we observed Gd-containing deposits with typical sea-urchin shape in the basal lamina of blood vessels and as intracellular inclusions. Furthermore, for the first time, we identified the distinctive form of Gd-deposition not only in the cerebellum but also in the spinal cord of EAE animals. Hence, more TEM systemic research will be required to determine the precise location of retained Gd in the injured CNS of EAE mice.

The increased retention of Gd in the brain and spinal cord of EAE (and SHAM) mice, as determined by ICP-MS analysis, was not accompanied by an enhanced signal intensity in the corresponding MR  $T_{1w}$  images. This is not an unexpected result as, due to the limited number of injections, the administered dose (total dose 3.6 mmol/Kg) is likely not sufficient to give rise to a visible signal enhancement 21 days after the last administration. Moreover, images were acquired at 7T, and T1 relaxivity is expected to decrease a high B0.

## **Conclusion**

The presence of considerable levels of residual Gd is detected in the neurological system of mice due to disrupted BBB. A preferential but transient accumulation of Gd is detected in the spinal cord of EAE mice, which is the most injured area in this specific animal type. Gd retention in the cerebrum and cerebellum appears to be connected to the inflammation that occurs after immunization but not to demyelination.



## 2.2

### Inflammatory Bowel Disease (IBD-DSS)

## Introduction

Ulcerative colitis (UC) and Crohn's disease (CD) are lifelong, remitting diseases characterized by an inflammatory condition of the bowel, commonly called inflammatory bowel disease (IBD)<sup>102,103</sup>. It is a worldwide health-care issue with an ever-increasing prevalence. IBD is assumed to be caused by an abnormal and ongoing immune response to bacteria in the gut, which is triggered by the individual's genetic vulnerability. Although the origin of IBD is uncertain, it is certain that it includes a complex interaction of genetic, environmental, microbial, and immunological responses.

Intestinal inflammation is invariably accompanied by intestinal epithelial lesions, which enhance intestinal permeability<sup>104-106</sup>.

Recently, strong relationships between gastrointestinal tissue and nervous system have been reported. It is known<sup>107</sup> that the microbiota-gut-brain axis is a complex network that includes the enteric nervous system (ENS), autonomic nervous system (ANS), and neuroendocrine and neuroimmunity of the central nervous system (CNS). It has been demonstrated that IBD can be a strong risk factor for the development of severe brain dysfunctions. Colitis influences the composition of gut microbiota with an increase of gut microbiota endotoxins production,<sup>108</sup> able to trigger the onset and development of neuroinflammation. Endoscopy and biopsies, which are regarded the gold standard for the identification and quantification of ulcerative colitis and Crohn's disease, are used to make a clinical diagnosis of IBD. However, due to the invasiveness and patient discomfort associated with endoscopy, research has concentrated on noninvasive imaging techniques such as magnetic resonance imaging (MRI). This technique has the potential to provide useful insights into morphology and physiology of the whole gastrointestinal tract. Currently, about 40% of all MRI examinations<sup>109-111</sup> are carried out upon administration of exogenous Gadolinium-based contrast agents (GBCAs) to create contrast<sup>112</sup>. Although MRI is considered a safe technique, there are several concerns regarding gadolinium deposition in patients undergoing multiple administration of GBCAs<sup>113</sup>. Hence, the use of MRI for diagnosis and monitoring of IBD deserves caution regarding the employment of GBCAs. In the herein reported work, we investigated whether the occurrence of a strong gastrointestinal inflammation leads, upon administration of the linear GBCA gadodiamide (Gd-DTPA-BMA), to an enhanced Gd retention in CSN system, excretion organs and bones.

The study was carried out on a well-established murine model of colitis induced through the administration of dextran sulfate sodium (DSS) in the drinking water to C57/Bl6J mice<sup>114</sup>.

## Methods

### Animals

The in vivo experiments were performed on male C57/BL6 J mice of 10 weeks of age and a weight of  $21 \pm 2$  g (Envigo RMS srl Udine, Italy).

All experimental procedures were approved by the Ethical Committee of the University of Torino and authorized by the Italian Ministry of Health (authorization number: 808/2017-PR in 19/10/2017 and following integration in 18/03/2020). The experiments have been carried out in accordance with the European Community Parliament and Council Directives of 24 November 1986 (86/609/EEC) and 22 September 2010 (2010/63/EU). Mice were housed with a 12 hours (h) light/dark cycle and free access to food/water. Dextran sulfate sodium (DSS)-induced colitis model was carried out as reported in.<sup>115</sup> C57BL/6 J mice were administered with 3.0% DSS salt, (M.W 36-50kDa, 160110) in drinking water for one week. A Group of healthy mice administered with water was included in the study as a control.

Upon addition of DSS to drinking water, mice were monitored daily for body weight loss and presence of blood in the stool.

### Gadolinium Based Contrast Agent (GBCA) administration protocol

In this study, 2 intravenous injections of gadodiamide (Omniscan®, GE Healthcare, Gd(DTPA-BMA), a linear neutral GBCA, were administered to 4 groups (n=5, each group) of mice at a dose of 0.6 mmol/kg at 3 and 5 days during the DSS treatment week. Two groups (healthy vs treated) were sacrificed 10 days after the last injection (day 15 of the overall study); the other two groups (healthy vs treated) were sacrificed 30 days after the last injection (day 35 of the overall study). The day of the sacrifice, mice were deeply anesthetized (Zoletil 60 mg/kg and Rompun 5 mg/kg) and underwent cervical dislocation. After sacrifice, cerebrum, cerebellum, spleen, liver, kidneys and bone were collected. Each specimen was weighted, mineralized and underwent Gd determination by ICP-MS analysis.

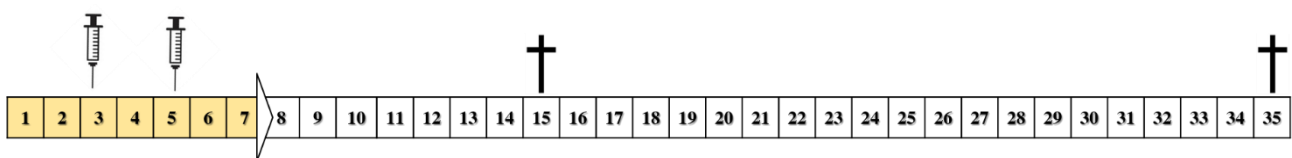


**Figure 1:** Scheme of the study. Yellow boxes indicates the period of DSS treatment. Syringes indicate the days when mice were injected with doses corresponding with 0.6 mmol/Kg of gadodiamide. Crosses indicate the sacrifice time at 15 days and 35 from the beginning of the DSS treatment.

### Morphological analysis of colon

The colon was isolated by all animals belonging to three groups, i.e. i) control untreated mice, ii) DSS-treated mice (at 15 day from treatment) and iii) DSS-treated mice (at 35 days from treatment). The colon and cecum were separated from the small intestine at the ileocecal junction, and the length was manually measured.

### *Inductively Coupled Plasma-Mass spectrometry (ICP-MS) quantification of Gd content*

The Gd content of the collected organs and tissues was measured by ICP-MS analysis (Element-2; Thermo-Finnigan, Rodano (MI), Italy) and the results expressed as nmol/g of wet tissue weight. The preparation of the samples and ICP-MS analysis were carried out as previously seen.

### *Histological analysis: Hematoxylin/eosin (H&E) staining*

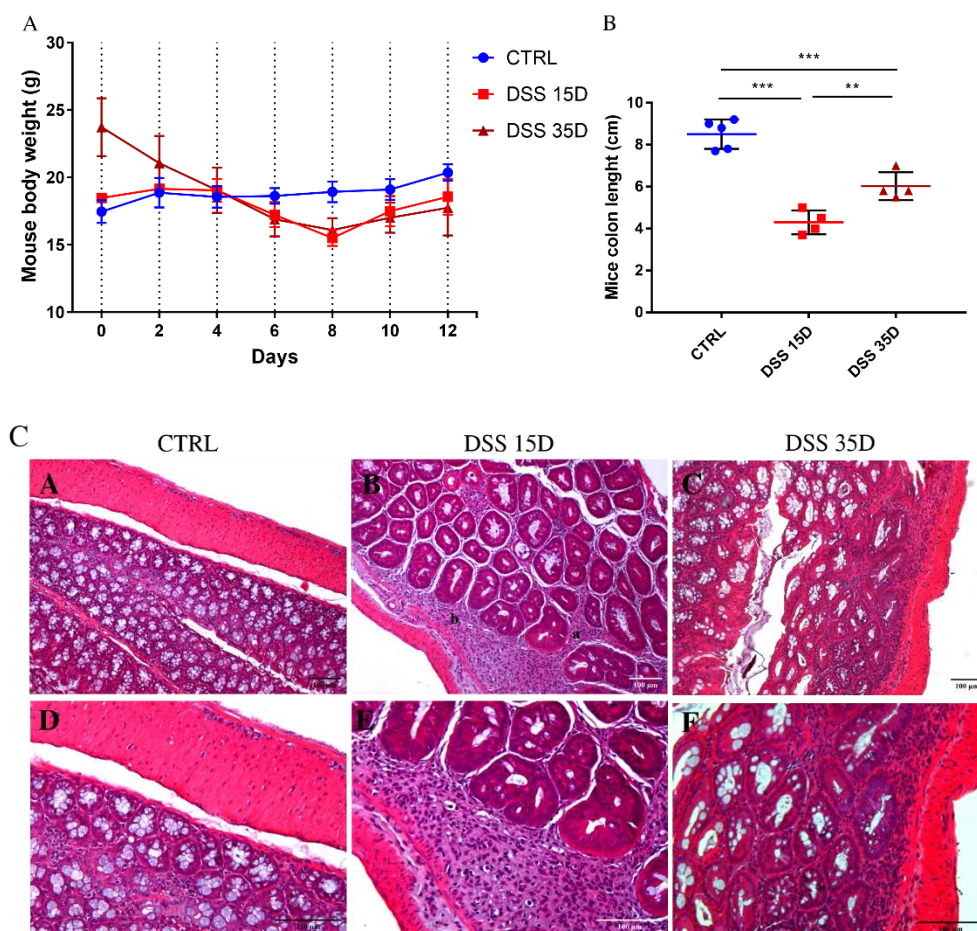
The colon was isolated by all animals belonging to three groups, i.e. i) control untreated mice, ii) DSS-treated mice (at 15 day from treatment) and iii) DSS-treated mice (at 35 days from treatment). Colon of mice from each group were fixed overnight in 4% buffered formaldehyde solution for paraffin inclusion and morphology evaluation. Colon morphology was evaluated by standard H&E staining on dewaxed 5- $\mu$ m sections.

### *Statistical Analysis*

All data are expressed as the mean values of at least three independent experiments  $\pm$  standard deviation (SD). Between group differences with respect to the mean Gd concentration were assessed using unpaired t test or two-way ANOVA followed by the Bonferroni's multiple comparison post-hoc test. Graph-Pad Prism 7.00 software was used for data analysis. Overall, statistical significance was defined as follows: \* $p < 0.05$ , \*\* $p < 0.01$ , \*\*\* $p < 0.001$ ; unless differently specified.

## Results

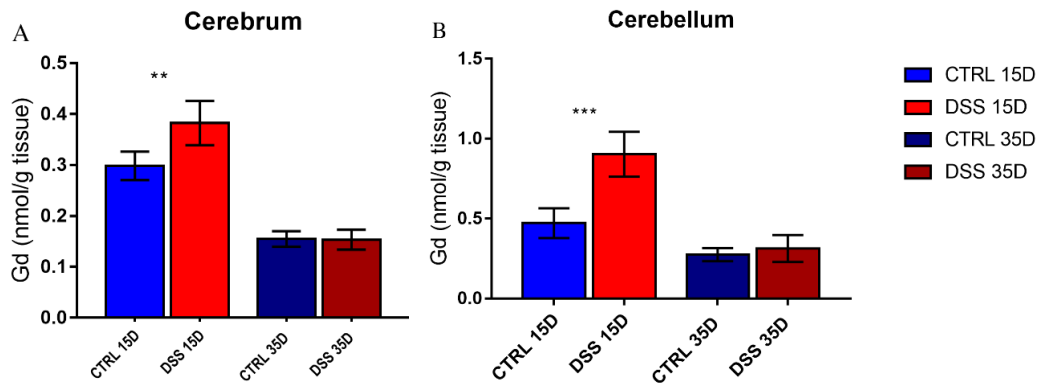
Figure 2A reports the weight of the mice during and immediately after the treatment. It shows a general weight loss in the group of DSS-treated mice, followed by a slow recovery after the finish of the treatment. On the contrary, the control group shows a slightly increase of the weight as normal condition. Figure 2B shows the difference in colon length measured after the sacrifice in three groups of mice. i.e. i) control healthy mice ( $8.5 \pm 0.7$  cm); ii) DSS-treated mice at day 15 ( $4.3 \pm 0.5715$  cm); iii) DSS-treated mice at day 35 ( $6.0.25 \pm 0.6625$  cm). A significant reduction of colon length is observed in DSS-treated mice at day 15 and at day 35, compared to the control group. Still, a small, recovery is present at longer times from the treatment. The histology examination of portions of colon through hematoxylin–eosin staining show the damage to colon mucosa in both the group of mice treated with DSS (Fig 2C). The pathophysiology of the colon was characterized by the presence infiltration of inflammatory cells into submucosa (a) and crypt loss (b); the group of mice sacrificed after 35 days showed a slight recovery of the crypt physiology and a reduction of the inflammatory cells infiltration.



**Figure 2:** (A) Mice body weight (g) and (B) mice colon length (cm) during DSS treatment compared to that of control group of mice drinking water. (C) The colons from each experimental group were processed for histological evaluation (hematoxylin–eosin staining, 10 $\times$  and 20 $\times$ ; scale bar, 100  $\mu$ m). \* $P$ <0.05, \*\* $P$ <0.01, \*\*\* $P$ <0.001.

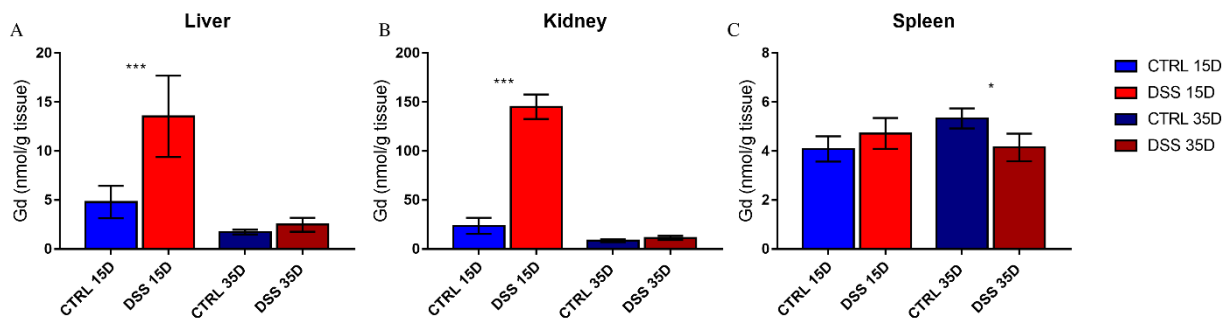
Mice belonging to the four study groups administered with two doses of gadodiamide (0.6 mmol/kg) were sacrificed at different time points as illustrated in the experimental part. Upon sacrifice, cerebrum, cerebellum, liver, kidneys, spleen and bones have been collected and digested for quantification of Gd by ICP-MS.

It was found that, compared to the control group, the amount of gadolinium retained in the cerebrum and cerebellum is significantly higher in the group of mice treated with DSS and sacrificed 10 days after the last GBCA injection (day 15 of the study) (Fig 3). On the other hand, when the sacrifice was performed 30 days after the injection (day 35 of the study), DSS-treated and control groups are no more different. Obviously, comparing the overall Gd retained 10 or 30 days after the injections, a significant reduction is observed due to the occurring Gd-elimination pathways.



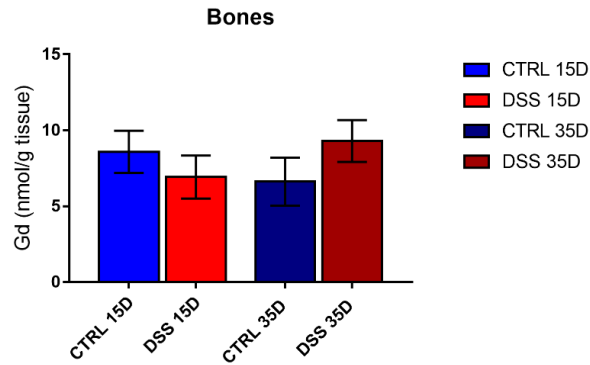
**Figure 3:** Amount of retained Gd in cerebrum (A) and cerebellum (B) of mice administered with two doses of gadodiamide at days 3 and 5 during the DSS-treatment. Two mice groups were sacrificed 15 days and two group of mice were sacrificed after 35 days. \*P<0.05, \*\*P<0.01, \*\*\*P<0.001

Figure 4 reports the metal concentration found in the excretion organs: liver, kidneys and spleen. The amount of Gd retained in liver and kidneys are extremely higher in the group of DSS-treated mice and sacrificed 10 days after the GBCA injection, analogously to what reported for CNS.



**Figure 4:** Amount of retained Gd in liver (A), kidney (B) and spleen (C) of mice administered with two doses of gadodiamide at days 3 and 5 during the DSS-treatment. Two mice groups were sacrificed 15 days and two group of mice were sacrificed after 35 days. \*P<0.05, \*\*P<0.01, \*\*\*P<0.001

On the other hand, in the spleen and bones (Fig 5), the amount of retained Gd is almost the same in the four investigated groups.



**Figure 5:** Amount of retained Gd in bone of mice administered with two doses of gadodiamide at days 3 and 5 during the DSS-treatment. Two groups of mice groups were sacrificed 15 days and two groups of mice were sacrificed after 35 days. \* $P < 0.05$ , \*\* $P < 0.01$ , \*\*\* $P < 0.001$

Figure 6 reports the correlation lines between Gd found in cerebrum and cerebellum with that retained in the bones of healthy and DSS-mice. An opposite trend is observed comparing the two groups of mice: while, in fact, for control mice the retention in CNS organ is directly proportional to the amount of Gd stored in the bones, in the case of colitis mice an inverse proportionality is observed.

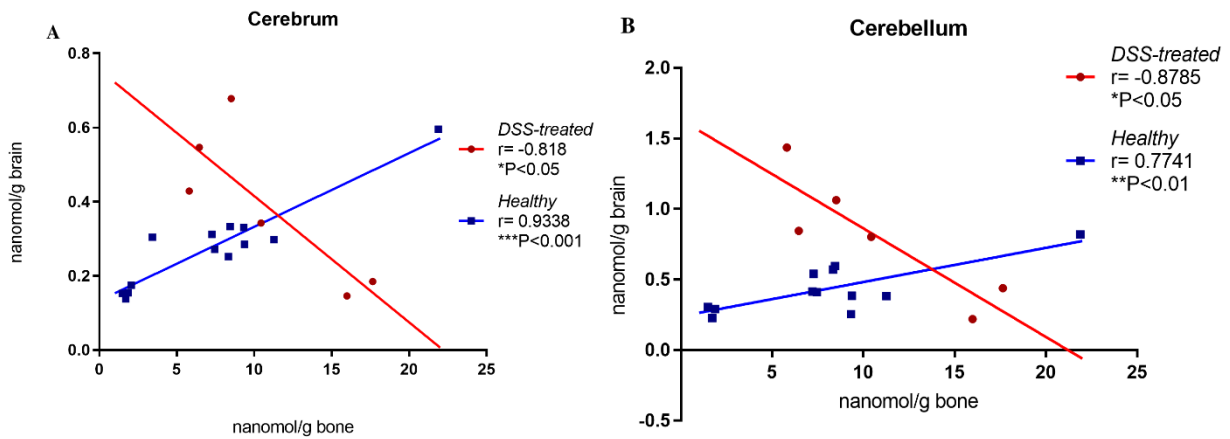


**Figure 6:** Amount of retained Gd in cerebrum (A) and cerebellum (B) with respect to the amount found in bones of mice belonging to the DSS-treated or to the healthy-control groups. days. \* $P < 0.05$ , \*\* $P < 0.01$ , \*\*\* $P < 0.001$

## Discussion

The gut-brain axis is a bidirectional information interaction system between the central nervous system (CNS) and the gastrointestinal (GI) tract, in which gut microbiota plays a key role. The system can communicate through several mechanisms affecting physiological functions at multiple levels.

Several studies<sup>116,117</sup> have shown that gut microbiota is associated with many diseases of CNS, such as depression, autism, anxiety, obesity, schizophrenia, diabetes, Parkinson's and Alzheimer's disease.<sup>107</sup> It has also been demonstrated a correlation between the developments of IBD and alteration in the Blood Brain Barrier (BBB) in the Central Nervous System (CNS).<sup>108,118</sup> The increase of BBB permeability can be surely considered important in explaining the deposition of Gd we reported in CNS upon administration of gadodiamide in DSS-treated mice.

Obtained results have shown a correlation between increased Gd retention upon administration of a linear GBCAs and the DSS induction of colon inflammation.

In DSS-treated mice a large gastrointestinal inflammation occurs, as reported by the shortening of colon length and by histological analysis.

This has a significant impact on the overall organism, as demonstrated by the weight loss in DSS-treated mice.

It is worth of note that a partial remission from the disease is present at longer times from the induction of the colitis. The effect is a recover from the IBD inflammation.

The quantification of Gd in tissues has shown an enhanced accumulation of Gd in DSS-mice both in CNS organs (cerebellum and cerebrum) and in extraction organs (liver and kidneys), at 10 days from gadodiamide injection (day 15 from induction of inflammation). No effect has been detected in spleen. These data suggest that systemic inflammation trigger a higher retention of Gd. Moreover, the increase in BBB permeability can be surely considered an important co-factor in explaining the deposition of Gd in CNS.

At longer times from the end of the treatment (30 days from gadodiamide injection and 35 days from induction of inflammation), when the physiological condition of mice almost completely returned to the initial condition, no significant differences between the control group and the treated one have been detected for CNS and extraction organs. This is likely a consequence of the remission of the pathology and reduction of inflammation.

A possible explanation regarding the higher amount of Gd found in the liver of DSS-treated mice in the acute phase of gut inflammation, is that this tissue is strictly connected with the gut-brain axis. Actually, recently it was decided to change the name of this system in microbiota-gut-liver-brain axis<sup>119</sup>. Gut and liver communicate in a bidirectional way, through portal vein, biliary tract and systemic circulation, the role of both the tissues in the microbiota homeostasis and consequently with the brain cannot be ignored.

Regarding kidneys, their size and weight were decreased after DSS administration to mice (*data not shown*); similar results were observed also in human patients affected by IBD<sup>120-122</sup>. The higher amount of retained gadolinium may be likely correlated with the macroscopic changes observed in this tissue. It was reported that DSS treatment induces a change in glomerular filtration fostered by an alteration of the glomerular barrier.<sup>123</sup> As a consequence, a greater reabsorption of salts and liquids in the renal tubule takes place to overcome the dehydration process. It can be speculated that, during this process, Gd-containing systems can be reabsorbed as well.

In the bones the mean value of retained Gd is similar in both healthy and DSS-mice and it doesn't significantly changes in time (Fig 5).

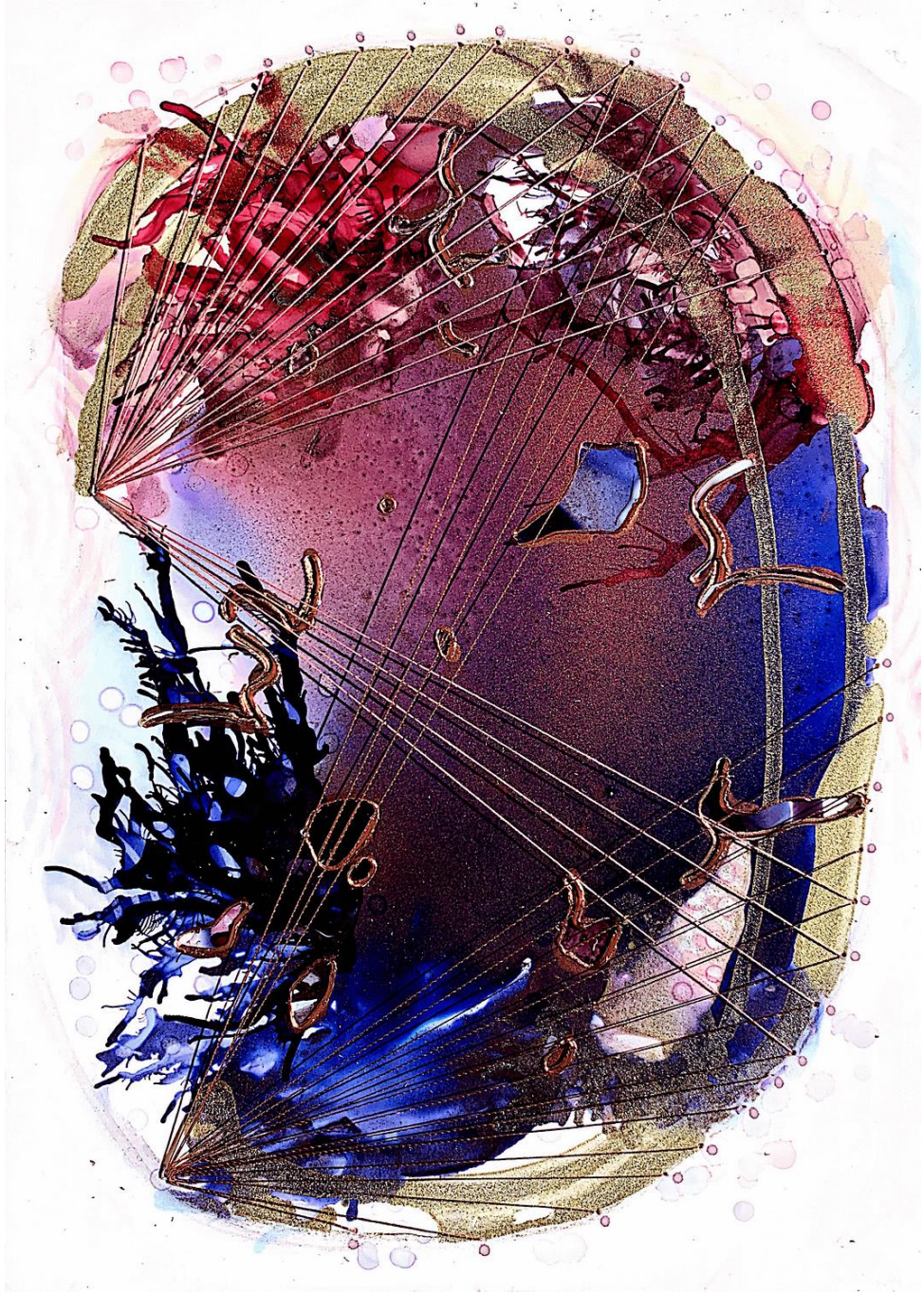
However, despite the mean values of retained Gd are not significantly different one to each other, an interesting behaviour came out from the analysis of the correlation between Gd found in cerebrum and cerebellum with that retained in the bones of healthy and DSS-mice (Fig 6). In healthy mice, in fact, the amount of Gd found in cerebrum and cerebellum is positively correlated with that deposited



in the bones, while in DSS-treated mice an opposite trend is observed. The behaviour associated to Gd retention in healthy mice is in line with what expected on the basis of the frequently recalled concept that bones are considered a sort of preferential accumulation site for metal ions<sup>165</sup> that, eventually, can come back in circulation in longer times, and be retained elsewhere (i.e. in the CNS). Concerning the DSS-treated mice, the observed inverse correlation between Gd retained in CNS and in bones is most likely due to intestine malabsorption caused by the gut inflammation model, which reduces the process that takes metals from absorption to storage in the bones. Certainly, other mechanisms should be considered such as the release of cytokines that might increase Gd retention in the brain, similar to what it was observed in the previous chapter inducing the neuronal inflammation.

## Conclusions

The obtained results showed that the alteration of the intestinal barrier permeability in a model of DSS-induced bowel inflammation can exert a temporary enhancing effect on Gd retention in CNS, bones and excretion organs. Yet, this effect is time dependent and is gradually fixed up to the point that the amount of retained Gd is no more distinguishable from that of control healthy mice. However, this is an important finding showing as inflammatory diseases can generally affect the deposition of Gd in the principal organs in the body, and this deserves caution in using multiple administrations of GBCAs in patients affected by inflammatory diseases, as colitis.



# CHAPTER 3

## Gadolinium retention in compartments other than Central Nervous System



# 3.1

## Gadolinium retention in Erythrocytes and Leukocytes from human and murine blood upon treatment with Gadolinium-Based Contrast Agents for Magnetic Resonance Imaging

*Based on Di Gregorio E, Furlan C, Atlante S, Stefania R, Gianolio E, Aime S. Gadolinium Retention in Erythrocytes and Leukocytes From Human and Murine Blood Upon Treatment With Gadolinium-Based Contrast Agents for Magnetic Resonance Imaging. Invest Radiol. 2020;55(1):30-37. doi:10.1097/RLI.0000000000000608*

## Introduction

To gain more insight into the occurring mechanisms that lead to Gd-retention, a number of studies have been undertaken at pre-clinical level by administering multiple doses of GBCAs to mice and rats<sup>29,40,42,44,101,124–127</sup>. These studies brought important insights about the way through which the GBCAs may access the CNS interstitium at the choroid plexus and, then, enter the glymphatic route in its slow excretion process<sup>44,52,128</sup>. During this process, the lower kinetic stability of linear GBCAs may yield chemical transformations that eventually result in the formation of insoluble Gd-containing deposits that remain unaltered over long periods of time<sup>40,42,101,126</sup>. Conversely, the higher stability of the macrocyclic GBCAs allows these systems to remain intact, thus allowing a relatively faster transit pathway. Although no clinical consequence associated to Gd-retention has yet been reported, the number of studies developed in the last few years provide new knowledge on how a metal containing xenobiotic may interact with complex biological matrices<sup>129</sup>. Still, a number of questions have to be tackled. Many research groups,<sup>130–133</sup> have been interested to know to what extent Gd may be retained in tissues other than the brain. By analysing the Gd content in organs and tissues of mice administered with multiple doses of GBCA, it is evident that in several organs Gd is present at concentrations much higher than those found in the CNS. In particular, an enhanced retention was observed in the excretion organs such as the spleen, kidneys, and liver, and was maintained at relatively long time after the last administration<sup>134</sup>. One may surmise that GBCAs (or structures derived from the association between dechelated Gd and biomolecules) could be found in all tissues they enter into contact with. Being administered intravenously, the tissue that GBCAs first (and mostly) encounter is blood. The concentrations of GBCAs in blood are routinely measured, most often after the separation of plasma from blood cells (Red Blood Cells, RBCs, and White Blood Cells, WBCs). The changes in total Gd concentration in plasma allows the lifetime of a given GBCA in the patient/animal body to be established. However, one may surmise that the contiguity of GBCAs (high concentrations) and blood cells may yield internalization processes, thus removing part of the GBCA from the filtration process that occurs at the glomerular level. Moreover, Gd entrapped inside cells may contribute in supplying organs such as the spleen and liver. Herein we report results that show that indeed very tiny quantities of GBCAs enter RBCs and WBCs, thus introducing new insights for the description of the complex excretion and retention pathways of administered GBCAs.

# Materials and Methods

## Materials, chemicals and animals

The following clinical Gadolinium based contrast agents were employed in this study: i) gadoteridol (Prohance®, Bracco Imaging, Gd(HP-DO3A)), ii) gadobenate dimeglumine (Multihance®, Bracco Imaging, Gd-BOPTA), iii) gadodiamide (Omniscan®, GE Healthcare, Gd(DTPA-BMA)) and iv) gadopentetate dimeglumine (Magnevist®, Bayer, Gd-DTPA). Ficoll Hystopaque-1039 (d=1.039 g/mL), heparin and all other chemicals were purchased from Sigma-Aldrich Co. LLC. In vitro experiments were performed using buffy coat derived from a total amount of 11 healthy donors. In vivo experiments were carried out by using a total amount of 60 healthy male CD-1 IGS mice (Charles River Laboratories, Calco, Italy) bred at the Molecular Biotechnology Center of the University of Torino (It). Mice were kept in standard housing (12 h light/dark cycle) with rodent chow and water available ad libitum). Experiments were performed according to national rules and policies on animal handling.

## In-vitro incubation of human blood with GBCAs and separation of the blood components

Buffy coat, obtained from healthy donors, was incubated with GBCAs (gadoteridol, gadobenate dimeglumine, gadodiamide or gadopentetate dimeglumine). 5 mL of buffy coat blood was diluted with PBS 1X (1:1 v:v) and added of 100 µL of commercial solutions of each of the four contrast agents. The final Gd concentration was 5 mM (overall osmolarity  $292 \pm 12$  mOsm/L, pH=7.2). Incubation time was 30 minutes, 1, 2 and 3 hours in a thermostatic mixer at 37°C.

In the case of gadoteridol, blood was also incubated with increasing concentrations (1, 5, 10 and 20 mM) of GBCA at the fixed time of 1 hour. Blood cell components: plasma fraction, WBCs and RBCs, were isolated by using the well-known Ficoll Histopaque method. Then, WBCs and RBCs were washed three times with PBS 1X to eliminate the unloaded GBCAs.

WBCs were suspended in 200 µL of double distilled water and sonicated to induce cell lysis; the protein content was assessed by Bradford Quantification Assay. Then the corresponding number of cells ( $n^{\circ}$ WBCs) was calculated through the following calibration curve:

$$n^{\circ}WBCs = 1.74 \times 10^7 \times \text{mg}_{\text{prot}}$$

Red blood cells (RBCs) were lysed with bidistilled water and the concentration of Hemoglobin ( $[Hb]_{\text{sample}}$ ), as reporter of the number of RBCs, was evaluated by measuring the absorbance in the SORET band region ( $\lambda=413$  nm,  $\epsilon=145000$ ) by using a 6715 UV-Vis Spectrophotometer Jenway (Bibby Scientific Limited, Beacon Road, Stone, Staffordshire, ST15 OSA, UK). The exact number of RBCs (cells/µL) in the sample was calculated using the average values for number of RBCs ( $N_{\text{cell}}=5$  million cells per microliter) and mean haemoglobin concentration ( $[Hb]_{\text{mean}}=15$  g/dL), in human blood with the following formula:

$$n^{\circ}RBCs = \frac{[Hb]_{\text{sample}} \times N_{\text{Cell}}}{[Hb]_{\text{mean}}}$$

The Gd content inside WBCs, RBCs and plasma was determined by ICP-MS, after being mineralized according to the protocol described below.

### Gd-retention in blood ex vivo and separation of the blood components

A single dose of gadodiamide or gadoteridol (1.2 mmol/kg) was *i.v.* administered to healthy male CD-1 IGS mice (mean body weight  $35 \pm 5$ g). Untreated healthy male mice were used as controls. Mice were sacrificed by cervical dislocation, in agreement with ethical European guidelines, at different time points: 24 h, 48 h, 96 h and 10 days after the administration.

After sacrifice, selected organs were recovered (blood, liver, spleen, kidney, cerebrum and cerebellum). Blood components (WBCs, RBCs and plasma) were isolated and quantified as above reported. Calculation of the number of RBCs in the sample was performed, analogously to what done in human blood, using the average values for number of RBCs (9.5 million cells per microliter)<sup>135</sup> and haemoglobin concentration (14 g/dL)<sup>136</sup> in mouse blood. The Gd content was determined by ICP-MS, after being mineralized according to the protocol described below.

### Mineralization of the blood components and ICP-MS analysis

RBCs were destroyed by applying an osmotic shock through the addition of distilled water. Then lysed RBCs were added (1:3) to concentrated HNO<sub>3</sub> (67 %) and each acidic suspension was mineralized with a microwave apparatus at 160 °C for 40 min (Milestone MicroSYNTH Microwave lab station equipped with an optical fiber temperature control and HPR-1000/6M6-position high-pressure reactor, Bergamo, Italy).

In order to ensure that Gd in RBC samples from mice administered with the GBCAs were above the limit of quantification (LOQ) of the ICP-MS technique, three aliquots (500 µL each) of RBCs from the same mice were mineralized and recovered all together in 3 mL of bidistilled water for the subsequent ICP-MS analysis.

The WBCs pellet was collected by using 200 µL of PBS and cells were lysed by sonication using a Badelin Sonoplus Sonicator working at 20 KHz (30s at 30% of power), then the samples were added (1:3) to concentrated HNO<sub>3</sub> (67 %) and mineralized as above reported.

Plasma samples from human blood were diluted (1:500) with double distilled water, then added (1:10) to concentrated HNO<sub>3</sub> (67 %) and each acidic suspension was mineralized according to the procedure described above. Plasma samples from mice blood were added (1:3) to concentrated HNO<sub>3</sub> (67 %) and each acidic suspension was mineralized according to the procedure described above.

The Gd content of the blood components was measured by ICP-MS analysis (Element-2; Thermo-Finnigan, Rodano (MI), Italy), and the results were expressed as µmol/mL in the case of plasma and µmol/cell in the case of RBCs and WBCs. The calibration curve was obtained using 8 absorption standard solutions (Sigma-Aldrich) containing concentrations of Gd in the range of 0.001 to 0.1 µg/mL. The LOQ in our ICP-MS analyses was determined to be 0.0005 µg/mL (100 times higher than blank solution). Considering the mean volumes of the different blood components recovered from mice and the dilutions made in the preparation of the samples for ICP-MS, the LOQ of the method were  $8 \times 10^{-16}$  µmol/cell for RBCs and  $7.4 \times 10^{-15}$  µmol/cell for WBCs.

### Mineralization of murine organs and ICP-MS analysis

After collection, organs and tissues were weighed and concentrated HNO<sub>3</sub> (67 %) was added to the samples. The dissolved organ-containing solutions were mineralized with a microwave apparatus at 160 °C for 40 min. After mineralization, the samples were recovered in double distilled water and analysed for Gd content through ICP-MS analysis as reported above and the results were expressed as nmol/g of wet tissue weight. Considering the mean weights of the organs/tissues recovered from mice and the dilutions made in the preparation of the samples for ICP-MS, the LOQ of the method with respect to the respective tissues/organs were as follows: liver, 0.012 nmol/g; spleen, 0.071 nmol/g; kidney, 0.022 nmol/g; cerebrum, 0.025 nmol/g; cerebellum, 0.065 nmol/g.



### Determination of the amount of intact GBCAs in RBCs and WBCs derived from human blood through UPLC-MS analysis

Specimens obtained from human blood incubated with gadodiamide or gadoteridol (5mM, 3 hours) underwent ultra performance liquid chromatography–mass spectrometry (UPLC-MS) analysis for the determination of the amount of intact Gd-DTPA-BMA and Gd-HPDO3A, respectively. RBCs and WBCs were isolated using Ficoll Histopaque solution, as previously described.

The collected WBCs were suspended in 200 µL of double distilled water, sonicated to induce cell lysis, added with the internal standard and centrifuged to remove cell membranes. Samples were then treated with Methanol/formic acid 0.1% (H<sub>2</sub>O/MeOH, 1:4), filtered using SPE cartridges (Oasis Waters, USA) to remove matrix interferences and lyophilized. RBCs samples were lysed by osmotic shock using double distilled water (1:10), added with the internal standard, centrifuged to remove cell membranes, filtered through Vivaspin 6 MWCO PSE (10000 kDa; Sartorius stedim, UK) to remove proteins and lyophilized.

Then samples have been resuspended in 0.1 mL Milli-Q water and analysed by UPLC-MS using an Acquity Hclass UPLC system coupled to an Acquity QDa detector (Waters, Vimodrone, Italy). Briefly, an Acquity UPLC ethylene bridged hybrid hydrophilic interaction liquid chromatography (BEH HILIC) column (2.1 x 100 mm; 1.7 mm particle size), set at 40 °C, with a VanGuard precolumn, was used in isocratic elution. Mobile phase A: 24 % (ammonium formate, 12.5 mM; formic acid, 12.5 mM; 3.75 pH); mobile phase B: 76 % (acetonitrile); flow rate: 0.6 mL/min; injection volume: 4 µL. The chromatographic conditions were chosen on the basis of a previously reported high-performance liquid chromatography method, either in the full scan mode (range, 250–800 m/z) or in the selected ion monitoring (SIM) mode, used to separate GBCAs<sup>34,137,138</sup>.

The set-up of this method involved acquisition of calibration curves obtained by adding aliquots of an appropriate internal standard (Tm-HPDO3A or Tm-DTPA-BMA) to RBCs samples at a final concentration of 5-50 µM and aliquots of the gadolinium complexes to be analysed in the same concentration range. To quantify the amount of intact gadolinium complexes in the blood cells, 2.5 nmol of the internal standard (*i.e.*, the selected thulium complex) were added to each sample before the extraction protocol. Selected ion monitoring (SIM) chromatographic peaks of the intact gadolinium complexes were integrated with respect to the corresponding peaks of the internal standard. Samples were analysed in triplicate. The amount of gadolinium complexes was obtained by using the following formula:

$$[\text{Gd} - \text{complex}] = \frac{K \times A(\text{Gd}) \times [\text{Tm} - \text{complex}]}{A(\text{Tm})}$$

where A(Gd) and A(Tm) are the areas of the peaks that correspond to gadolinium and thulium complexes, respectively, and K is the experimentally derived conversion factor.

Both for WBCs and RBCs samples, the total Gd content was determined by ICP-MS, after mineralization according to the protocol described before. Beside Gadolinium, the amount of thulium was determined through ICP-MS, in order to calculate the recovery percentage upon the extraction protocol. The mean recovery ratio was  $0.607 \pm 0.07$ . The recovery correction factor was applied to each sample in order to take into account the amount of gadolinium lost during the extraction process.

### Determination of the amount of intact GBCAs in RBCs derived from murine blood through UPLC-MS analysis

RBCs derived from murine blood of male CD-1 IGS mice administered with a single dose of gadodiamide or gadoteridol (1.2 mmol/kg), and sacrificed at 24 h, 48 h, 96 h and 10 days, were isolated from plasma by centrifugation. Samples were then lysed by osmotic shock using bidistilled water (1:10), added of the internal standard, filtered through Vivaspın 6 MWCO PSE (10000 kDa; Sartorius stedim, UK) and lyophilized. Each sample was resuspended in 0.1 mL milliQ water and analysed by UPLC-MS for the determination of the amount of intact Gd-DTPA-BMA and Gd-HPDO3A, respectively, as described before. The total Gd content was determined by ICP-MS, after mineralization following the protocol described before.

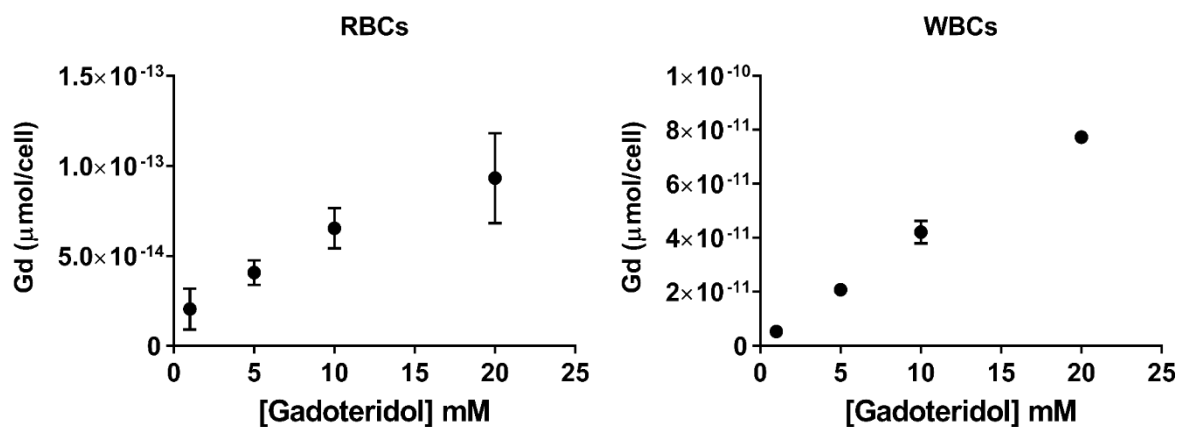
### Statistical Analysis

All data are expressed as the mean values of at least three independent experiments  $\pm$  standard deviation (SD). Between group differences with respect to the mean Gd concentration were assessed using unpaired t test or two-way ANOVA followed by the Bonferroni's multiple comparison *post-hoc* test. Graph-Pad Prism 7.00 software was used for data analysis. Overall, statistical significance was defined as follows: \* $p < 0.05$ , \*\* $p < 0.01$ , \*\*\* $p < 0.001$ ; unless differently specified.

## Results

### *In vitro experiments with human blood*

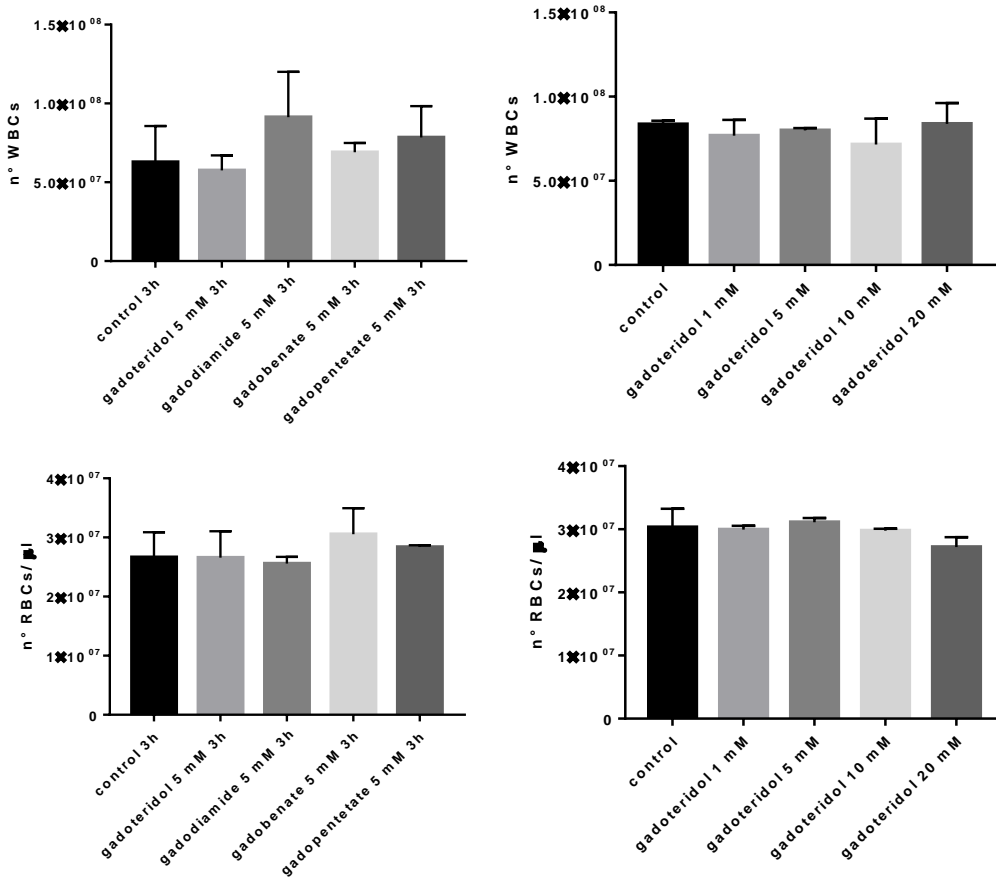
Blood samples from healthy donors were incubated with gadoteridol in the concentration range 1-20 mM for 1 hour (Fig 1).



**Figure 1:** Amount of Gd recovered in RBCs and WBCs upon incubation of whole human blood with Gadoteridol (1, 5, 10 and 20 mM) for 1 hour at 37°C.

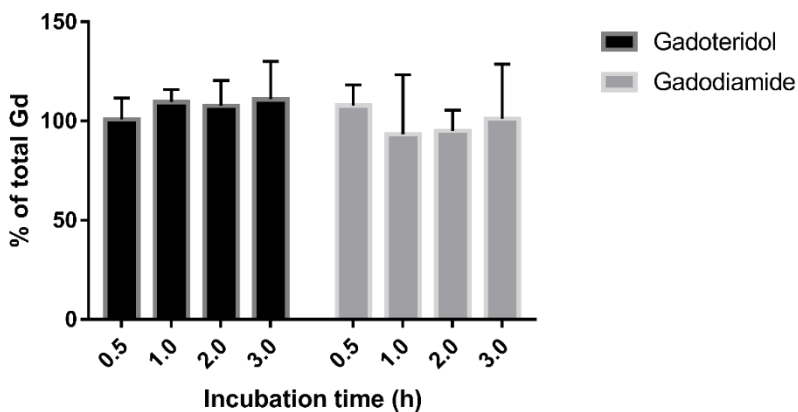
A direct proportionality between GBCA concentration and the amount of internalized Gd was observed both in leukocytes (White Blood Cells, WBCs) and erythrocytes (Red Blood Cells, RBCs). The explored concentration range reaches higher concentrations than those ones GBCAs can reach in blood once administered to human patients at 0.1 mmol/kg (ca. 2 mM). In this *in vitro* incubation study, our purpose was to establish whether GBCAs could enter RBCs and WBCs and to determine the Gd chemical form once internalized. Thus, we chose to investigate a relatively high concentration range in order to force the internalization process and to obtain a sufficient amount of internalized Gd. We found that 5 mM was a good compromise to have enough analytical sensitivity. Next, to compare different GBCAs, blood samples from healthy donors were incubated with gadoteridol (Prohance®, Gd(HP-DO3A)), gadobenate dimeglumine (Multihance®, Gd-BOPTA), gadodiamide (Omniscan®, Gd(DTPA-BMA)) and gadopentetate dimeglumine (Magnevist®, Gd-DTPA) at the concentration of 5mM for 30 minutes, 1, 2 and 3 hours, respectively.

Figure 2 reports the number of RBCs and WBCs in blood upon incubation with the four GBCAs with respect to control blood. No difference was evidenced comparing blood treated with gadoteridol, gadodiamide, gadobenate or gadopentetate in 5mM concentration for 3 h to control blood treated with saline for the same timeframe. Analogously, the number of RBCs and WBCs did not change significantly increasing the concentration (1-20 mM) of gadoteridol in the incubation medium with respect to control blood.



**Figure 2:** Number of WBCs and RBCs in blood incubated with the four GBCAs at 5mM concentration for 3 h or with gadoteridol at variable concentration for 1 h. Any significant difference was evidenced between groups.

Although, around 100% of the GBCAs was recovered in plasma (Fig 3), for all the tested contrast agents at any time point, a detectable amount of Gd was found in leukocytes and erythrocytes (Fig 4). The amount of Gd taken up by both types of cells increased upon increasing the incubation time.



**Figure 3:** Amount of Gd recovered in plasma upon incubation of whole human blood with Gadoteridol and Gadodiamide (5mM) as a function time expressed as percentage of total recovered Gd.

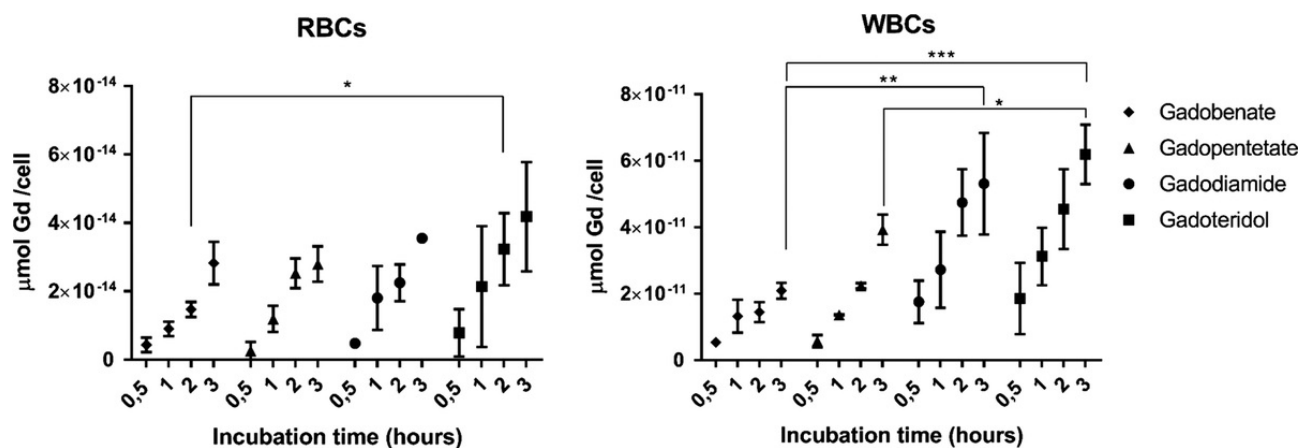


**Figure 4:** Amount of Gd recovered in RBCs and WBCs upon the incubation of GBCAs at 5 mM concentration in human whole blood samples as a function of the incubation time (n = 3 each group). Data resulted to be significantly different for: WBCs, gadobenate vs gadodiamide 2 hours ( $P < 0.01$ ); WBCs, gadobenate vs gadoteridol 2 hours ( $P < 0.01$ ); WBCs, gadopentetate vs gadodiamide 2 hours ( $P < 0.05$ ); WBC, gadopentetate vs gadoteridol 2 hours ( $P < 0.05$ ); WBCs, gadobenate vs gadodiamide 3 hours ( $P < 0.01$ ); WBCs, gadobenate vs gadoteridol 3 hours ( $P < 0.001$ ); WBCs, gadopentetate vs gadoteridol 3 hours ( $P < 0.05$ ).

While the different GBCAs were entrapped into RBCs in similar amounts, in the case of WBCs, the neutral Gd-complexes, gadodiamide and gadoteridol, showed to be internalized in larger quantity in respect to the negatively charged gadopentetate and gadobenate.

The ability to capture the exogenous GBCAs appears much more pronounced in the case of WBCs as the amount of internalized Gd per cell is two orders of magnitude higher than that found in RBCs. Next, the quantification of the amount of intact Gd-complexes (determined by UPLC-MS analysis) over the total amount of Gd (determined by ICP-MS), which were recovered from WBCs and RBCs in human blood incubated with gadoteridol and gadodiamide (5 mM for 3 hours), was assessed (Fig 5).

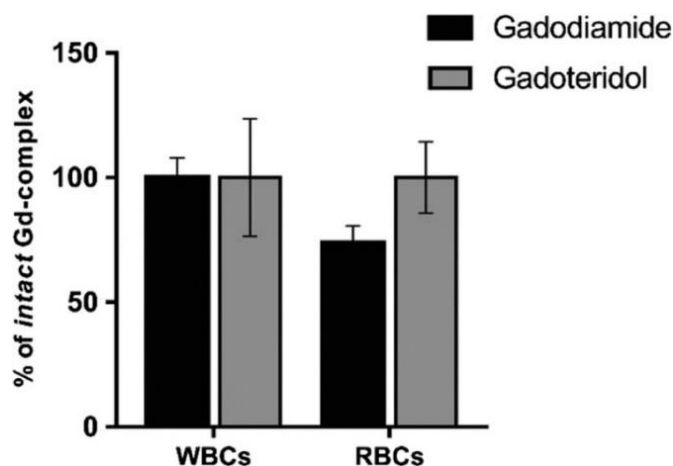
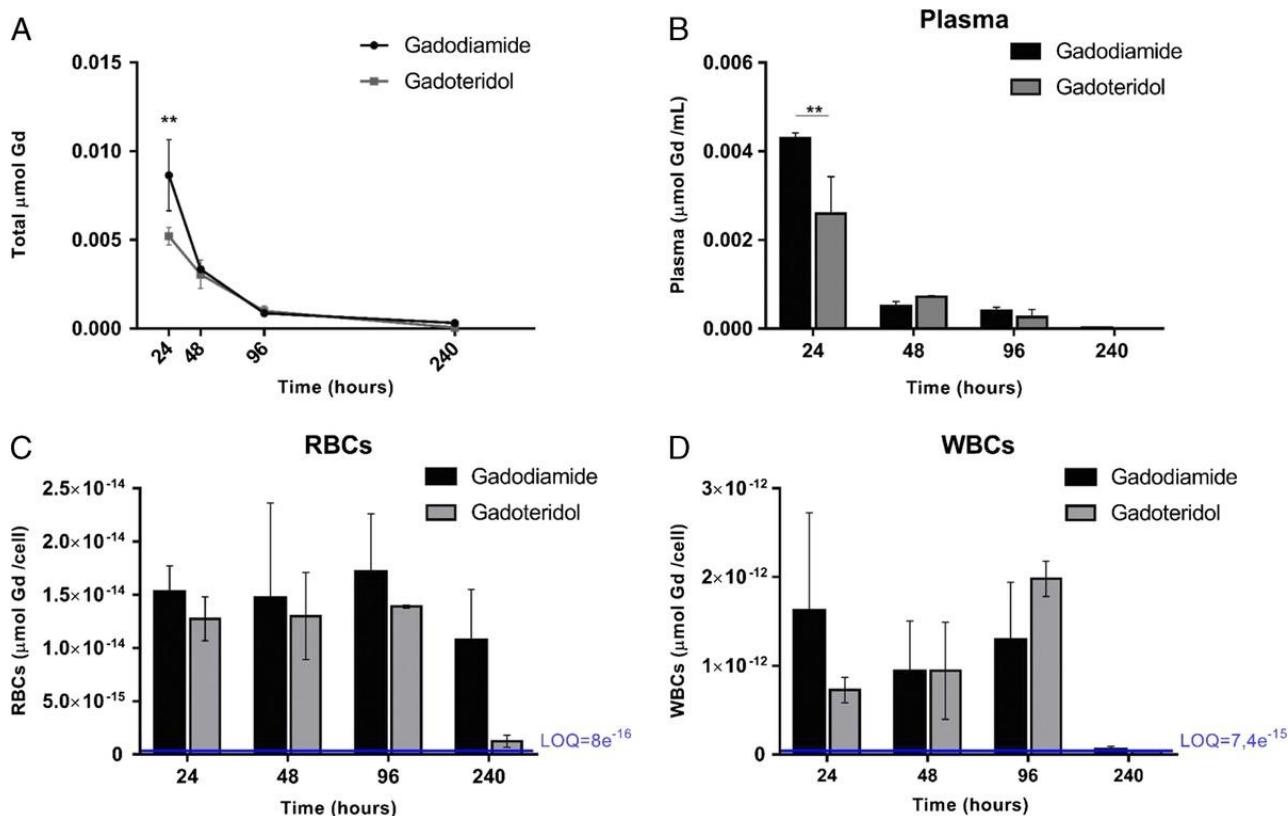


**Figure 5:** Results of UPLC-MS analysis in percentage of intact Gd complexes in human RBCs and WBCs from blood incubated for 3 hours with gadoteridol or gadodiamide (5 mM, 37°C, n = 6 each group).

The total amount of Gd determined in WBCs upon 3 hours of incubation with gadoteridol and gadodiamide corresponded to intact Gd-HPDO3A and Gd-DTPABMA respectively. In RBCs a difference between the two GBCAs was evidenced as gadoteridol was entirely found as intact Gd-HPDO3A ( $104\% \pm 15$ ), while the amount of intact Gd-DTPA-BMA decreased to  $74\% (\pm 6.8)$ .

## Gd-retention in RBCs and WBCs from blood of mice administered with GBCAs

CD1 mice were administered with a single dose (1.2 mmol/kg) of gadoteridol or gadodiamide and sacrificed at different time points: 24, 48, 96 hours and 10 days. The dose of 1.2 mmol/kg in mice is consistent with the FDA guidelines<sup>33</sup> about conversion of animal doses to human equivalent doses based on body surface area, and equivalent to the clinical dose of 0.1 mmol/kg.



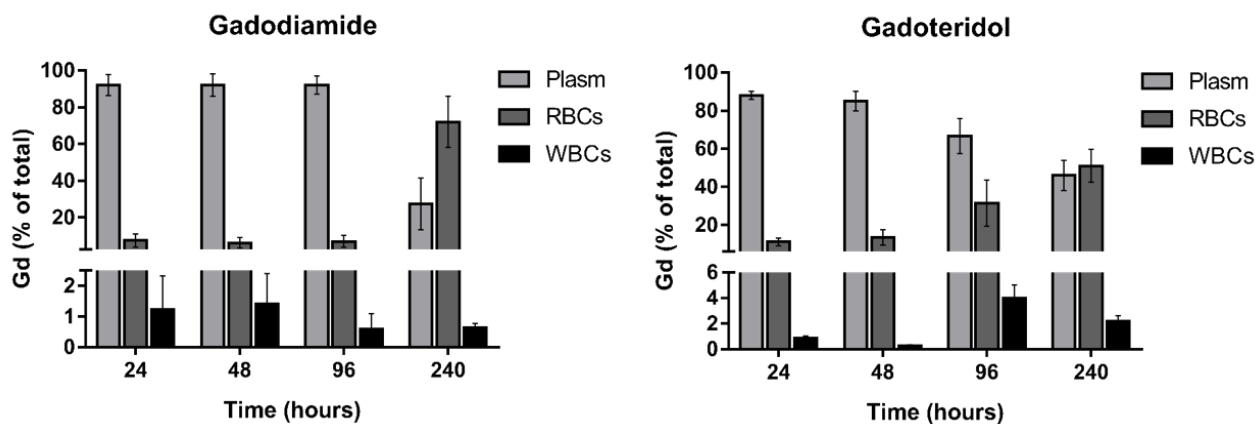
**Figure 6:** A, Total amount of Gd found in the blood of healthy mice 24, 48, 96, and 240 hours after the administration of GBCAs (1.2 mmol/kg of GBCA; n = 6 each group). Amount of Gd found in plasma (B), RBCs (C), and WBCs (D) 24, 48, 96, and 240 hours after the administration of a single dose of GBCAs (1.2 mmol/kg).

Figure 6A reports the pharmacokinetic profile of the two contrast agents in blood. As expected, the amount of total Gd found in blood decreased as the sacrifice time increased, due to the progressive elimination of the GBCA from the body. As the elimination half-time of GBCAs in healthy mice is normally around 5-20 minutes,<sup>23</sup> 24 hours after the administration (first time point investigated) the amount of retained Gd was less than 1/5000 of the total dose administered (ca. 36 micromoles), over time it further decreased.

The amounts of Gd retained in plasma, RBCs and WBCs are reported as a function of the sacrifice time (Fig 6 B, C and D). The behaviour observed in plasma reflected what was observed in whole blood (Fig 6A), as most of the GBCAs were dissolved in the plasma. On the contrary, in RBCs and WBCs, the overall amount of entrapped Gd appeared rather constant over the first 96 h, both for gadodiamide and gadoteridol (although showing more scattered values for the former in WBCs). When the amount of retained Gd was determined 10 days after administration, the residual Gd in WBCs - both for mice administered with gadodiamide and gadoteridol - was very low (even if slightly higher than the limit of quantification, LOQ), whereas, for RBCs, the amount of Gd found in mice

administered with gadodiamide remained relatively high, and it was very low for mice administered with gadoteridol.

Looking at the amount of retained Gd normalized to the number of cells it is worth noting that, as observed in the previous section with human blood, each WBC appears to internalize an amount of Gd that is two orders of magnitude higher than the one internalized by RBCs.



**Figure 7:** Amounts of retained Gd in murine plasma, RBCs, and WBCs expressed as percentage of total recovered Gd as a function of the kill time (n = 6 each group).

Figure 7 reports the relative amounts of Gd retained in the different blood fractions, expressed as the percentage of total recovered Gd as a function of sacrifice time. It can be noted that, while the percentage of Gd retained in plasma decreased, the percentage of Gd found in RBCs increased with time, especially in the case when the less stable gadodiamide was administered. The percentage of Gd found in WBCs is always very low because of the low number of WBCs with respect to the other blood cellular components (1% in volume).

In analogy to what was done for human RBCs and WBCs, the quantification of the amount of intact Gd-complexes was addressed in murine RBCs. Figure 8 shows the percentage of intact Gd-complexes in RBCs from mice administered with gadodiamide or gadoteridol 24 hours and 10 days after the administration. The very low amount of Gd recovered in WBCs prevented the quantification of intact Gd-complexes in WBCs.

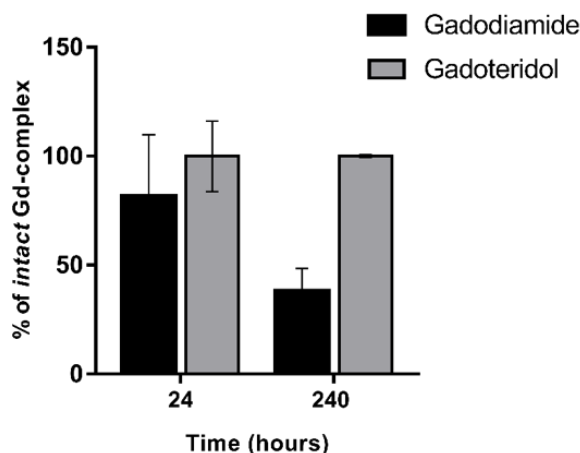


**Figure 8:** Percentage of intact Gd complexes in human RBCs of mice administered with gadoteridol or gadodiamide 24 hours and 10 days after the administration (n = 3 each group).

The biodistribution analysis of the two contrast agents was completed by collecting and analysing the Gd content in the spleen, liver, kidneys, cerebrum and cerebellum (Fig 9). In the cerebrum and

cerebellum, at relatively short times (up to 96 h), the amount of retained Gd increased slightly and generally did not appear significantly different for either the linear or the macrocyclic agent. The difference became significant when the sacrifice time was brought to ten days, showing a greater retention of Gd in the case of gadodiamide. In the liver and spleen, which are the organs devoted to RBC elimination, gadodiamide yielded constant or even increased values of retained Gd at the 10 days time point. Conversely, organs from mice treated with gadoteridol showed a steady decrease of retained Gd. In the kidneys, gadodiamide and gadoteridol seemed to behave in a very similar way.

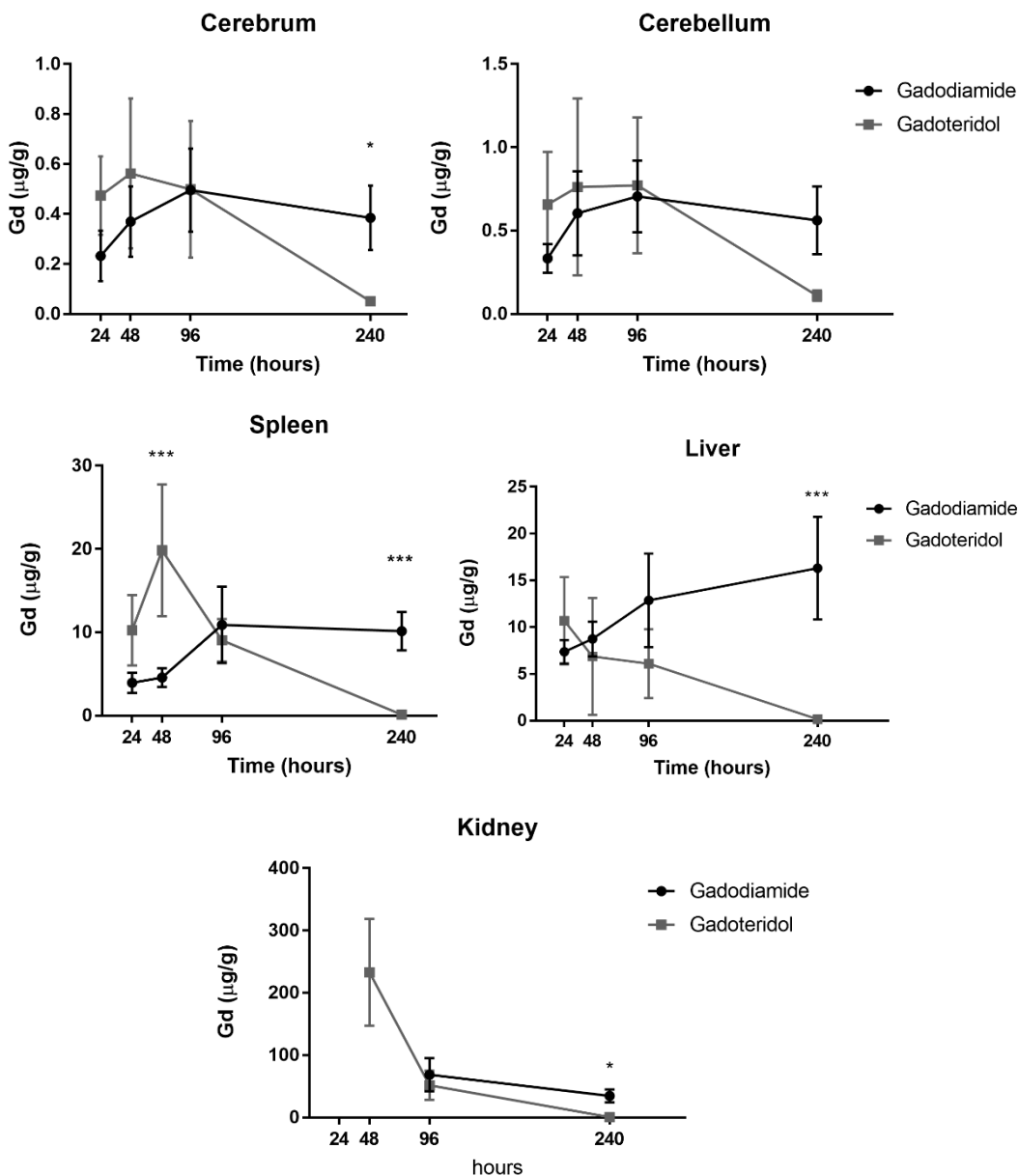


**Figure 9:** Amount of Gd retained in cerebrum, cerebellum, spleen, liver, and kidneys of mice administered with a single intravenous dose of 1.2 mmol/ 2 mmol/kg of gadodiamide or gadoteridol as a function of the kill time (n = 6 each group). Data of Gd retention in the kidneys at 24 hours and 48 hours (for gadodiamide) are not available due to technical problems encountered in the storage of specimens. ns indicates not significant, \* $P < 0.05$ , \*\* $P < 0.01$ , \*\*\* $P < 0.001$ .



## Discussion

The aim of this study was to assess the uptake of GBCAs from RBCs and WBCs.

First, we investigated the ability of four commercial GBCAs (Prohance®, Omniscan®, Multihance® and Magnevist®) endowed with different stabilities and structural features to distribute among the blood components (plasma, RBCs and WBCs) upon *in vitro* incubation in human blood.

These experiments showed that all the investigated GBCAs were able to enter RBCs and WBCs, even if the very large majority of GBCAs remained in the plasma. WBCs are lower in number, but with a more complex cellular structure, while RBCs are rather simple systems without a nucleus and with a limited enzymatic armoury, but much higher in number. The total amount of Gd retained in the RBCs pool is much larger than that found for WBCs.

Assuming a normal mean corpuscular volume (MCV) of 90 fL<sup>139</sup>, after 3 hours of incubation with GBCA at 5 mM concentration, the maximum concentration of Gd in one RBC is around 0.45 µM. This value appears definitively low when compared to the concentration of most abundant metal ions in red blood cells (i.e. ca. 150 µM Zn, 300 µM Ca, 13 µM Cu, 3 mM Mg) but of the same order of magnitude of other less abundant metal ions (i.e. ca. 0.4 µM Cr, 0.9 µM Ni, 0.3 µM Mn)<sup>140,141</sup>.

We are aware of the fact that the concentration used in human blood incubation experiments is higher than what can be reached when GBCAs are injected in 0.1 mmol/kg dose. (ca. 2 mM); anyway, the concentration was pushed to higher values in order to reach enough analytical sensitivity.

Moreover, the incubation with GBCAs at the concentration of 5 mM is not expected to affect neither blood parameters (viscosity and osmolarity) nor RBCs' and platelets' morphology and functionality (i.e. MCV, MCHC, Hb content, Hct, oxygen saturation, RBCs' deformability and fragility, platelet aggregation time). Previously<sup>142</sup>, dealing with a work aimed at generating labeled RBCs, we carried out an extensive evaluation of erythrocytes' morphology and physiology, upon loading high amounts of Gd-HPDO3A complex into RBCs ( $3 \times 10^8$  Gd-complexes per cell that corresponds to an intracellular concentration of ca. 4 mM) and no difference in cells viability and functionality was evidenced between native RBCs and labeled RBCs.

Furthermore, Reinhart et coworkers<sup>143</sup> extensively investigated the consequence of the use of gadoterate and some commercial iodinate contrast agents on blood parameters (viscosity, platelet function, RBCs' morphology). They too did not observe any significant effect associated to the presence of gadoterate although used at a concentration that is much higher than those ones applied in the present work. If the total amounts are normalized to the number of cells, it appears that the ability to uptake the exogenous Gd-containing species is much more pronounced in the case of WBCs as the amount of internalized Gd per cell is two orders of magnitude higher than that found in RBCs (Fig 4). Tentatively, this finding may be ascribed to the phagocytic activity associated to leukocytes, which is not present in erythrocytes.

All four considered GBCAs enter RBCs to a very similar extent, as expected in the case that the operating mechanism is a simple diffusion process guided by the concentration gradient. In the case of WBCs, it appears that the charge of the GBCA is more important in determining the uptake than the overall structure. In fact, the non-ionic gadodiamide and gadoteridol enter the cells in greater quantities than in respect to the ionic (negatively charged) contrast agents gadopentetate and gadobenate. Most likely this behaviour can be ascribed to the repulsive effect of the negative GBCAs with the negatively charged cell surfaces.<sup>144</sup>

In the case of gadoteridol, the role of the concentration on the amount of retained Gd in RBCs and WBCs was also investigated (Fig 1). Increasing the concentration of the complex in the incubation suspension, the amount of internalized Gd increases in a directly proportional way. Next, in order to assess whether internalized Gd corresponds to the administered GBCA, the amount of intact Gd-complexes inside white and red blood cells was determined by UPLC-MS analysis and reported as a percentage of the total Gd - determined by ICP-MS (Fig 5). For this experiment, only gadoteridol and gadodiamide were used as representatives of the most and the least stable commercial GBCAs respectively. Upon three hours of incubation in human blood, both the Gd-complexes were recovered

intact in WBCs. However, in the case of RBCs after 3 h of incubation, while all Gadoteridol is still intact, only 74% of gadodiamide was found as intact Gd-DTPA-BMA. This result indicates that gadodiamide and gadoteridol enter the blood cells as intact complexes and that - in the investigated time frame (3 hours) - Gadoteridol is stable in the intracellular microenvironment, while a partial dissociation of Gadodiamide occurs in RBCs. This behaviour can likely be associated to the very high concentration of zinc inside RBCs (ten times higher than in plasma) which may promote transmetallation reactions<sup>145</sup>.

The next step was to collect blood from mice, to which a single dose (1.2 mmol/kg) of GBCA was administrated by *i.v.* injection. Also for this experiment, only gadoteridol and gadodiamide were used. The sacrifice time was set at 24 h, 48 h, 96 h and 10 days and the recovered blood was separated into the three components (plasma, RBCs and WBCs) (Fig 6).

The blood specimens acquired at 24, 48 and 96 hours, yielded results similar to those achieved in the *in vitro* incubation, where by far the largest percentage of Gd is found in plasma. At the time point of 10 days, the Gd retained in plasma resulted markedly decreased as a consequence of the progressive elimination of the GBCAs from the body. The amounts of Gd found in plasma 4 and 10 days after the administration are consistent with the value reported by Rasschaert et al. 6 days after the last administration in a study where a total dose of 12 mmol/kg of gadodiamide was administered to healthy rats.<sup>146</sup> In RBCs and WBCs, the amount of retained Gd is almost constant for both gadodiamide and gadoteridol, up to 96 hours after the administration. Most interesting are the results obtained when the amount of retained Gd was analysed 10 days after the administration: in WBCs the amount of residual Gd - both in the case of gadoteridol and gadodiamide - is very low (even if higher than the limit of quantification, LOQ); in the case of RBCs gadoteridol is almost completely eliminated, while the amount of Gd in gadodiamide treated animals remains close to the value determined at 96h. Most likely the explanation of this result has to attributed to the different thermodynamic and kinetic stability of the two GBCAs, as found in several studies of Gd retention in brain and other tissues/organs<sup>29,40,42,44,124,125</sup>. Support for this hypothesis was found through the UPLC-MS analysis on RBCs of mice administered with gadoteridol and gadodiamide in order to determine the chemical form of Gd retained in the cells. While 24 h after the administration of both CAs the recovered Gd is mainly under the form of intact Gd-complex, ten days after the administration Gadoteridol is still recovered as intact Gd-HPDO3A, but only ca. 40% of the total Gd is intact Gd-DTPA-BMA.

The *in vivo* stability of GBCAs depends i) on the equilibrium stability constants of all the complexes that may form in biofluids through competition reactions in the presence of GBCAs, and ii) on the kinetic stability (inertness) of Gd<sup>3+</sup>-chelates, which determine the amount of Gd<sup>3+</sup> ion released from the GBCAs during their retention in the living system.<sup>11</sup> To predict the possibility of transmetallation reactions we should know the equilibrium, kinetic and pharmacokinetic properties of the GBCA of interest at physiological conditions<sup>29</sup>. The macrocyclic gadoteridol tolerates longer excretion times because its dissociation rate is negligibly low (about 7 orders of magnitude slower than the excretion rate) at physiological pH. On the other hand, the excretion rate of gadodiamide is only about 7 times faster than that of the dissociation rate, and this might be responsible for the release of Gd<sup>3+</sup> ion from Gd(DTPA-BMA) in the living system and, eventually, to its transformation into other Gd-containing species.

During the ten days between the IV injection and blood collection, gadoteridol remains intact and can be excreted by the cells, while the less robust (kinetically and thermodynamically) gadodiamide partially transforms into other Gd-containing species that remain in RBCs. This finding parallels the behaviour observed for the two agents in their transit in the brain.<sup>34,40</sup>

Contrary to RBCs, which have a very long life (ca. 120 days), leukocytes have much shorter lifetime, from 6 hours to few days, thus their elimination cycle is much faster and 10 days after the administration a very small amount of residual Gd is detected in the leukocytes fraction. Although in our study the percentages of intact GBCAs were not determined in the plasma fraction, we rely on the study from Rasschaert et al,<sup>146</sup> where LC-ICP-MS measurements indicated that, after repeated

gadodiamide administration, plasma Gd was predominantly in a dissociated and soluble form (around 90% of total Gd).

The Gd-biodistribution analysis was completed by collecting and analysing the organs involved in the excretion from the body (the spleen, liver and kidneys) and in cerebrum and cerebellum (Fig 9). In the cerebrum and cerebellum, the obtained results reflect those reported in previous studies.<sup>44</sup> In fact at relatively short times, the amount of retained Gd is generally not significantly different whether the linear (less stable) or macrocyclic (more stable) agent is used. The difference becomes significant when the sacrifice time is brought to ten days, with higher retention when the less stable gadodiamide is used.

Unfortunately, data of Gd retention in the kidneys at 24h and 48h (for gadodiamide) are not available due to technical problems encountered in the storage of specimens. The available data, i.e. those relative to 4 and 10 days after the administration, indicate an analogous renal Gd retention in both gadoteridol and gadodiamide administered mice.

In the liver and spleen (organs devoted to RBCs elimination) of mice treated with gadodiamide, we observed an overall increase in the amount of retained Gd. The amount of Gd retained in the spleen and liver increases in the first 96h upon gadodiamide administration, then it remains almost constant in the 96h-240h range in spleen and slightly increases in liver.

On the contrary, the amount of Gd retained in the liver and spleen upon gadoteridol administration decreases during time. This finding supports the view that, for the less kinetically stable Gd-complex, a process that occurs on a slower time scale may be operative to contribute to gadolinium retention. However, it has to be pointed out that, ten days after the administration, the amount of Gd retained in RBCs is a very low fraction (ca. 1%) of the total Gd retained in spleen and liver, thus it seems that the Gd found in these organs does not receive a significant contribution from the blood cells.

In summary, the detection of quantifiable amounts of Gd in RBCs and WBCs indicates that GBCAs can cross also cellular membranes most likely by simple diffusion, or eventually by micropinocytosis (in the case of WBCs). Before this observation, GBCAs were scrutinized only for their ability to escape from the vascular bed, through dysfunction of the junctions responsible for maintaining the integrity of the vascular compartment. The finding that the hydrophilic GBCA molecules may cross membranes by simple diffusion against the concentration gradient opens new questions on the possible role of cellular uptake in the complex process that leads to Gd retention. In this context, we plan to investigate the uptake/transport of GBCAs in endothelial cell culture.



## 3.2

In vivo study of a macrocyclic Gadolinium Based Contrast Agent and the retention in spleen, bones and bladder.

## Introduction

Despite nearly all gadolinium is cleared from the circulation by renal excretion over the first several hours in patients with normal renal function, it was observed that some gadolinium can accumulate in brains of patients who received multiple doses of GBCAs. Apart from the brain, it has been shown that even higher amounts of Gd can accumulate in other organs such as liver, spleen, kidneys and bone<sup>36</sup>.

The study herein presented aims at elucidating the washout kinetics of a macrocyclic GBCA and the Gd retention in several tissues of healthy preclinical animal models. A particular attention has been paid to organs which have been poorly investigated by the scientific community up to now, notably the bladder, spleen and bones, but potentially able to accumulate high amounts of metal. Concerning the bones, it has been proposed that they may be a “deep compartment” for the long storage of gadolinium<sup>147,148</sup>. Based on this hypothesis, some authors assume gadolinium storage in the cortical bone<sup>149</sup>, others in the bone marrow<sup>148</sup>. From the bone, dissociated Gd might even be gradually released in other body districts.

First, it was decided to include the bladder among the investigated organs for the determination of their Gd content since the main function of this organ is to act as a short-term storage site for urine, while maintaining the composition of the urine similar to that generated by the kidneys. It is already well known in literature that some xenobiotics and toxic substances contained in the urine could possibly be retained in the bladder and lead to some consequences<sup>150–152</sup>. Therefore, we hypothesized that also Gd, free or chelated, could accumulate in this district, and decided to investigate it deeper through the quantification of the total amount of retained Gd, the determination of its chemical form and the assessment of eventual morphological changes through histology.

Concerning the spleen, we aimed at elucidating if the Gd<sup>3+</sup> mainly accumulates in the fibrous or cellular district.<sup>35,44</sup> Finally, by investigating the bone, we strived for understanding whether Gd<sup>3+</sup> accumulates to higher extent in the matrix or in the bone marrow.<sup>32,153</sup>

The GBCA, which has been employed in this study, is gadoteridol. This choice was made since it can be considered one of the safest GBCAs, as demonstrated in a study by Cho et al.<sup>154</sup>, which was considering 6163 subjects in a wide range of ages and covering a broad spectrum of imaging applications.

## Methods

### Chemicals

Gadoteridol (Gd-HPDO3A, ProHance 0.5 mol/L; Bracco Imaging, Milan, Italy) was kindly provided by Bracco Imaging. The Tm-HPDO3A standard for UPLC-MS analysis, was synthesized by mixing 1:1 molar ratio of TmCl<sub>3</sub> and the aqueous solution of the HPDO3A ligand, at neutral pH, at 50°C, overnight. The amount of residual free Tm<sup>3+</sup> ions was precipitated at basic pH (pH=11) and removed by filtration. The Tm<sup>3+</sup> concentration in the standard solution was determined by ICP-MS analysis.

### Animals

All in vivo experiments involving animals were conducted in accordance with national laws on experimental animals (L.D. no. 26/2014, Directive 2010/63/EU). Healthy six/eight-week-old male Balb/c mice were used, with a mean weight of 24 ± 1 g.

### GBCAs administration and collection of tissues

20 intravenous injections of Gadoteridol were administered to mice at the dose of 0.6 mmol/kg intravenously over a period of 4 weeks. The mice were divided in 4 groups (n=10 each) on the base of the sacrifice, since it was performed at different time points from the last injection: 4 days, 15 days, 30 days and 90 days. After sacrifice, the following organs/tissues were harvested and weighted: cerebrum, cerebellum, liver, spleen, kidneys, both the tibia bones and bladder. Urine was also collected. One tibia was weighted, mineralized and total Gd quantified through ICP-MS. The other tibia was handled in order to separate bone matrix and bone marrow and Gd quantified separately (see below). Splens from 5 mice were analysed for the quantification of the total amount of retained Gd while splens from the other 5 mice were processed to measure the amount of Gd in the splenocytes and in its fibrous part (see below). In bladder, beside ICP-MS total Gd quantification, UPLC-MS was performed to study the chemical form of the retained metal (see below). An additional group of mice (n=5) not administered with any GBCA was added as a control group.

### Separation of splenocytes and fibrous part from the spleen

The capsule was separated from the cellular pulp. In order to do so, the spleen has been filtered with a 40 µm filter to cut off the capsule and let the red and white pulp cells go through. The fibrous part was collected from the cell strainer and stored for the subsequent determination of Gd content.<sup>155,156</sup> The cells were pelleted and resuspended with 1 ml of lysis buffer per spleen. Erythrocytes were lysed in order to collect just splenocytes. To this purpose, eBioscience™ 1X RBC Lysis Buffer by ThermoFisher was used. Indeed, the ammonium chloride contained in the buffer lyses red cells with very little effect on lymphocytes. The reaction was stopped after 7 minutes by adding 40-50 mL of 1X PBS. The cells were again pelleted and counted. The purpose of the counting was to build a line correlating the number of cells with the number of proteins, following the same procedure described in the bone marrow section below.

### Separation of bone marrow from the tibia

For one of the two tibiae, after having exported the junction, the matrix was separated from the bone marrow which was washed out with 200 µL of PBS<sup>157,158</sup>. Cells of the bone marrow were then counted

and proteins were quantified using the Bradford assay. These last steps were performed to build a line correlating the number of cells with the quantity of proteins. The collected bone marrow samples were analyzed through ICP-MS for Gd quantification and data reported as Gd per cell. Bone matrix (compact bone and periosteum) was also analyzed through ICP-MS for Gd quantification.

### Induced Coupled Plasm-Mass Spectrometry (ICP-MS)

The Gd content of the collected organs and tissues was measured by ICP-MS analysis after the mineralization process. The procedure and the analysis were performed as showed in the previous chapter.

### UPLC for bladder samples

Concerning the bladder, quantification of the intact Gd-HPDO3A (Gadoteridol, ProHance) was performed by using UPLC (Ultra Performance Liquid Chromatography)/ESI-MS with an Acquity H-class UPLC system coupled to an Acquity QDa detector (Waters, Vimodrone, Italy). This step was performed to study the chemical form of the retained metal.

The schematic representation of the used protocol is reported in Scheme 1. As first step, the bladder has been homogenized with 300  $\mu\text{L}$  of purified water. 100  $\mu\text{L}$  of homogenate were stored at  $-18^\circ\text{C}$  for subsequent ICP-MS analysis for the determination of total Gd content. 200  $\mu\text{L}$  of the homogenate were collected and acidified with formic acid 0.2%. Then, a Tm-HPDO3A standard was added to the solution with a final concentration of 5 or 10  $\mu\text{M}$ . The sample was centrifuged at 9000 rpm for 15/20 minutes. The supernatant was extracted, quantified and placed on a XAD resin column, previously prepared, in order to desalt the solution. The salts were eluted with water acidified with formic acid 0.2% (Fractions 1-7 in Fig.1, volume 1 mL each fraction), while the desalted sample was collected in acetonitrile fractions (fractions 9-18 in Fig 1, volume 1 mL each fraction). The obtained solution has been dry-evaporated using a rotavapor. Once ready, the sample was resuspended in a volume of milliQ water equal to the one of the sample placed on the XAD column (50-200  $\mu\text{L}$ ). The sample was ready for UPLC analysis.

A Phenomenex Kinetex UPLC hybrid hydrophilic interaction liquid chromatography (HILIC) column (2.1 $\times$ 100 mm; 1.7-mm particle size) with a Phenomenex precolumn was used in isocratic elution with mobile phase 50%  $\text{CH}_3\text{CN}$  – 50% ammonium formate ( $\text{HCOONH}_4$ ), 100 mM, pH 3.3. The flow rate was set at 0.3 mL/min for a total high-performance liquid chromatography MS analysis time of 5 minutes (for each sample). The temperature of the column was kept at  $40^\circ\text{C}$ . The injection volume was 10  $\mu\text{L}$ . The chromatographic conditions were set on the basis of a previously reported high-performance liquid chromatography method used to separate GBCAs.<sup>34,35</sup>

Electrospray ionization (ESI+)-MS was performed either in the full scan mode (range, 250–800 m/z) or in the selected ion monitoring (SIM) mode. Instrumental MS conditions were as follows: capillary voltage, 0.8 kV; cone voltage, 20 V; source temperature,  $120^\circ\text{C}$ ; and probe temperature,  $600^\circ\text{C}$ .

The signal of gadoteridol (Gd-HPDO3A) was acquired in the SIM mode at  $[\text{MH}]^+$  equal to 557–558–559–560–562 and in its adduct with  $\text{K}^+$  at  $[\text{MK}]^+$  equal to 595–596–597–598–600. The selected reference standard was Tm-HPDO3A with  $[\text{MH}]^+$  equal to 571–572 and  $[\text{MK}]^+$  equal to 609–610, respectively.

The set-up of this method involved acquisition of calibration curves obtained by adding aliquots of Gd-HPDO3A and of the appropriate internal standard (Tm-HPDO3A) to bladder homogenates at a final concentration in the range 0.5–20  $\mu\text{M}$  (in triplicate). The analysis of these calibration lines allowed to calculate an experimentally derived conversion factor (K) defined as the ratio between the areas of the peaks that correspond to thulium and gadolinium complexes respectively, at the same concentration value. In bladder homogenates, this value was calculated to be  $1.13 \pm 0.06$ .



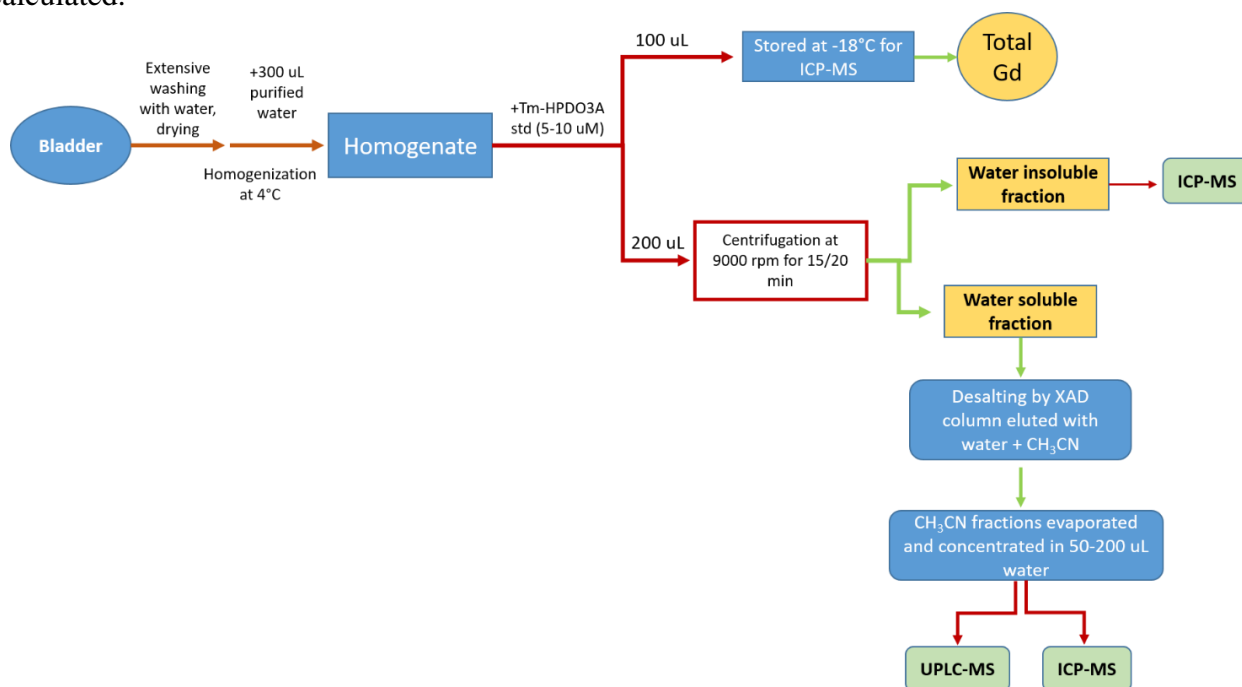
To quantify the amount of intact gadolinium complexes in the bladder samples, the internal standard was added to homogenates in concentration of 5 or 10  $\mu\text{M}$ . SIM chromatographic peaks of the intact gadolinium complexes were integrated with respect to the corresponding peaks of the internal standard.

The amount of intact Gd-HPDO3A was calculated by using the following formula:

$$[\text{Gd} - \text{complex}] = \frac{K \times A(\text{Gd}) \times [\text{Tm} - \text{complex}]}{A(\text{Tm})}$$

where  $A(\text{Gd})$  and  $A(\text{Tm})$  are the areas of the peaks that correspond to gadolinium and thulium complexes respectively, and  $K$  is the experimentally derived conversion factor.

Then the relative percentage of intact complex over total Gd, determined by ICP-MS analysis, was calculated.



**Scheme 1:** Sample preparation procedures for ICP-MS and UPLC-MS analytical methods.

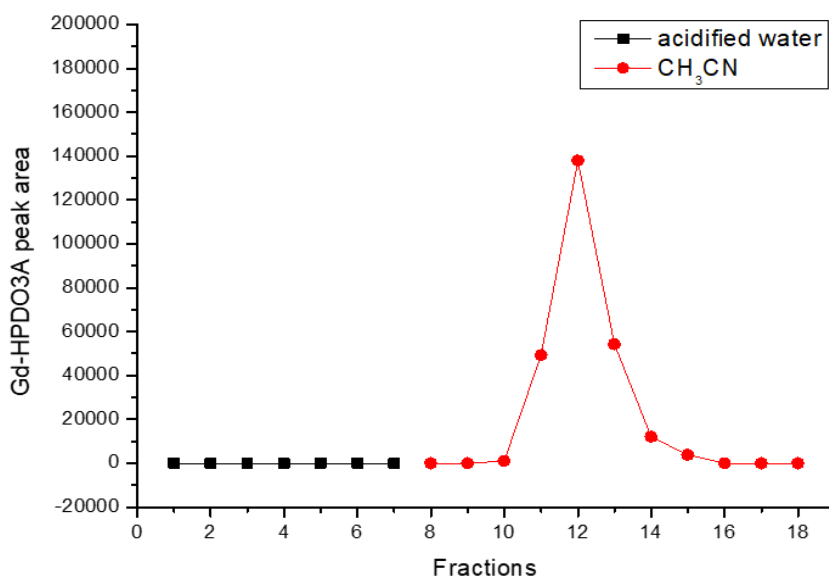


**Figure 1:** Desalting of bladder homogenates on a XAD column by elution with acidified water and acetonitrile (1 mL each fraction) followed by UPLC-MS analysis.

### Trichrome staining

The trichrome staining is intended for use in the histological visualization of collagenous connective tissue fibers in tissue sections. Bladder, kidney, liver and spleen were collected (n=2) from each group of mice. Then, the tissues were formalin fixed, paraffin embedded, sectioned and trichrome staining was performed using a Trichrome Staining Kit (Abcam, ab150686) according to the manufacturers' directions.

### Statistical analysis

All data were expressed as the mean values of at least three independent experiments  $\pm$  standard deviation (SD). The statistical analysis were performed using one-way ANOVA followed by the Bonferroni's multiple comparison post-hoc test. The mean of each data set was compared to the control group. The statistical significance was defined as follows: \*p<0.05, \*\*p<0.01, \*\*\*p< 0.001; unless differently specified.

# Results

## *Gadolinium retention: general overview*

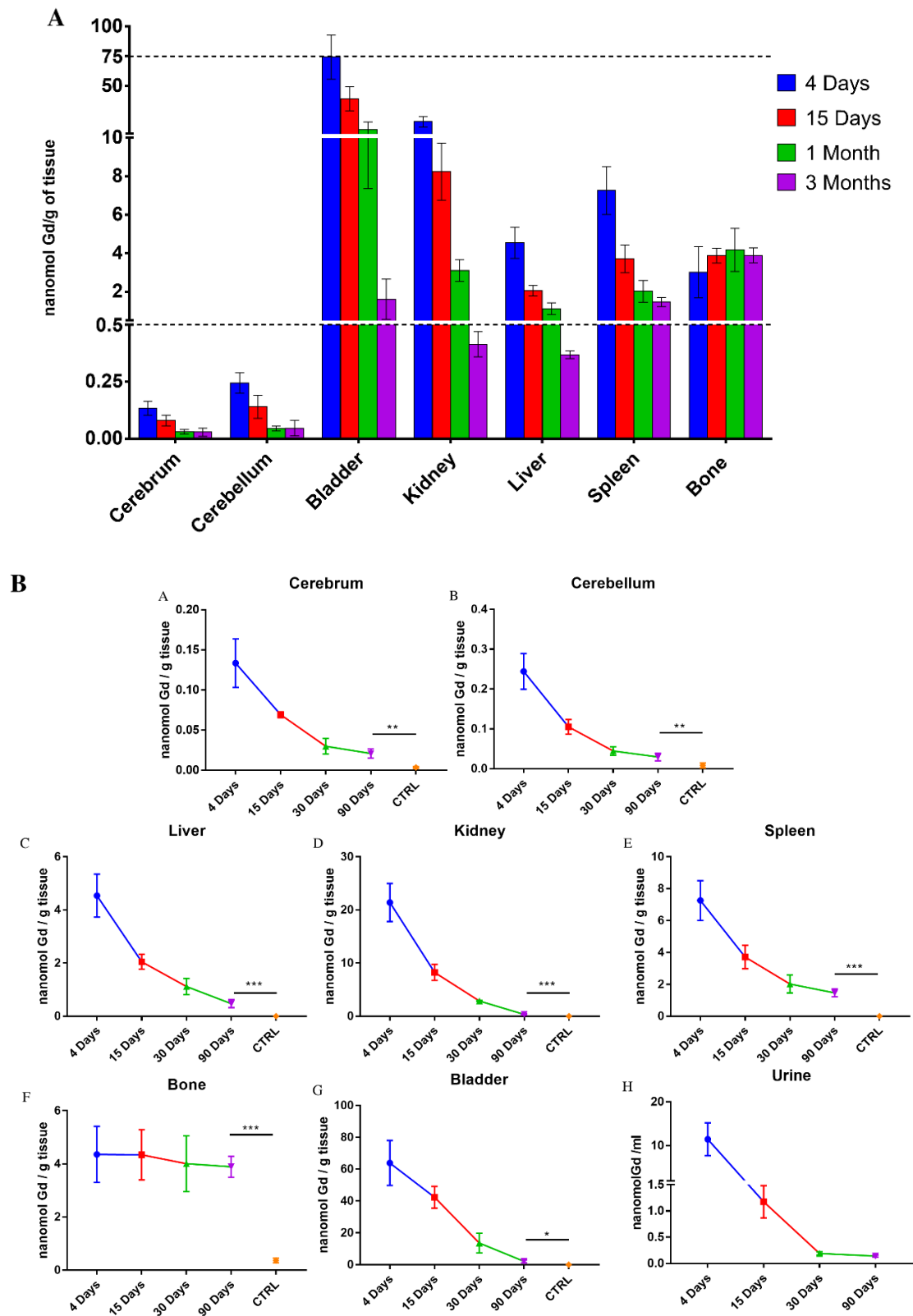


**Figure 2:** Gadoteridol excretion curve in all the harvested organs: in (B) are showed separately (A) cerebrum, (B) cerebellum, (C) liver, (D) kidney, (E) spleen, (F) bone, (G) bladder and (H) urine. The orange point correspond to the baseline values determined in control mice, which never received GBCA administration.

Figure 2 reports the amount of Gd retained in all the investigated organs/tissues 4, 15, 30 and 90 days after the last GBCA injection. At the shortest times, the quantification of Gd in the bladder showed the highest amount of metal retained among all the investigated organs. Then the amount of retained Gd gradually decreased to reach values similar to those found in spleen and bones. The obtained washout curves indicate a general decrease of the content of Gd upon increasing the sacrifice time in almost all the organs investigated. However, the amounts of residual Gd at 3 months, in general, are significantly higher than the baseline values determined in the organs of control mice, which never received GBCA injection. The mean total Gd concentrations retained in cerebrum, cerebellum, liver and kidneys at 30 and 90 days after the last administration are in line with previously reported results<sup>41,124,159</sup>.

Liver and kidneys tissues were histologically examined with trichrome staining for the visualization of collagenous connective tissue fibers (Fig 3). For both organs, no differences with respect to control tissues were observed. The only blue sections (highlighting collagen) are those around blood vessels in liver and the glomeruli in kidneys.

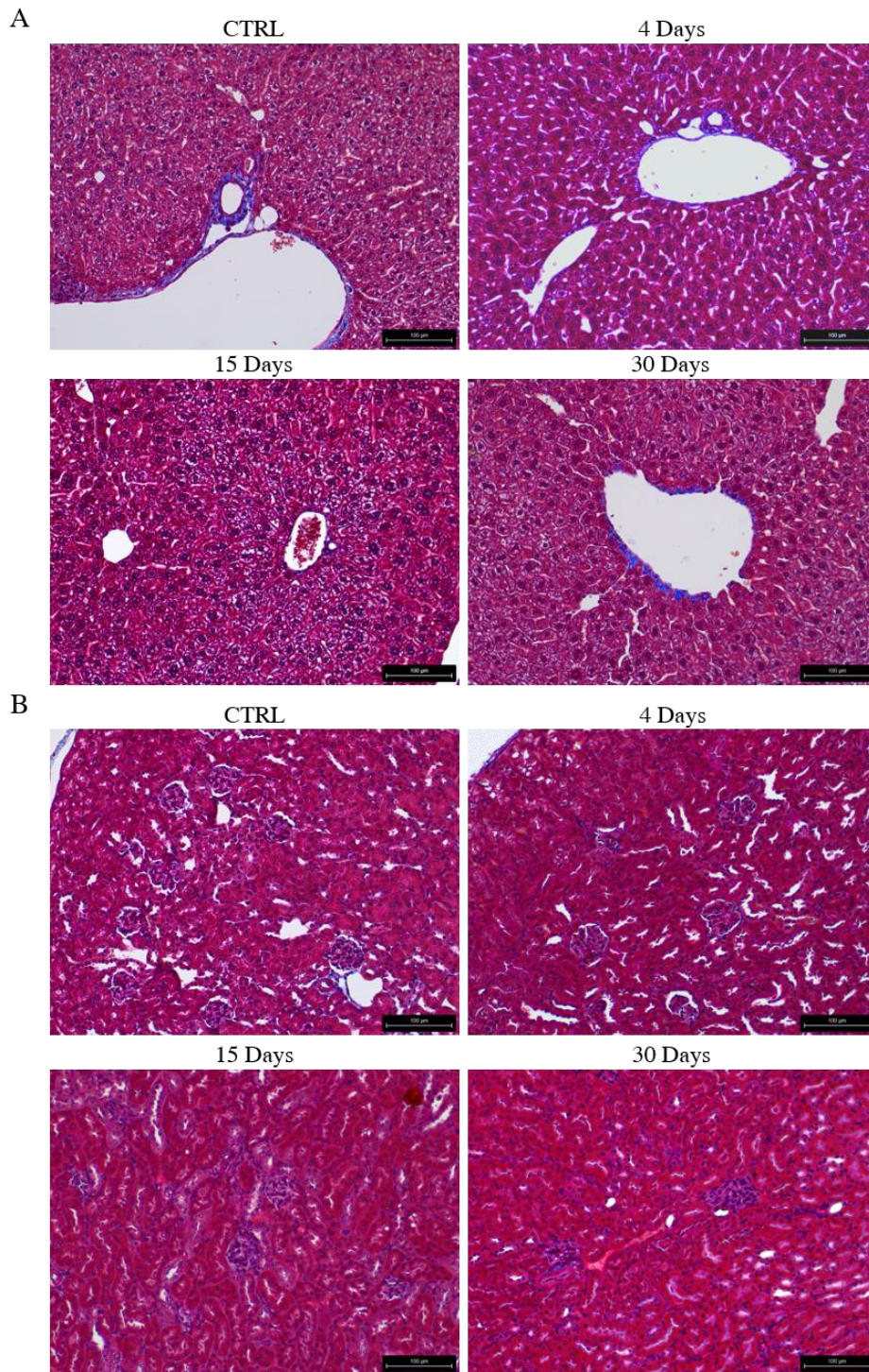


**Figure 3:** Trichrome staining on liver (a) and kidneys (b) samples with 20x enlargement. Blue: collagen; Red: muscle fibers; Black/Blue: nuclei

### Bladder and urine

The concentration of Gd decreases rapidly in urines confirming that the administered gadoteridol is almost completely cleared from the body through the renal route.

In parallel, in the bladder, very high concentrations of Gd were determined. Four and fifteen days after the last administration, bladder tissue retains the highest amount of Gd among all the

investigated organs and 90 days after the last administration the Gd concentration is still 83 times higher than the baseline value.

In figure 4, the time dependent decrease of Gd concentration found in the bladder is compared to that relative to urines. The two decreasing profiles are rather similar (beyond the different units), suggesting that the high amount of Gd found in the bladder is likely related to passage and stasis of urines, which contain a very large amount of GBCA starting from the hours immediately after the administration. 90 days after the last gadoteridol administration, the concentration of  $Gd^{3+}$  is still around 200 times higher than the established reference interval for  $Gd^{3+}$  concentration in urine in individuals not previously exposed to GBCAs<sup>160</sup>.

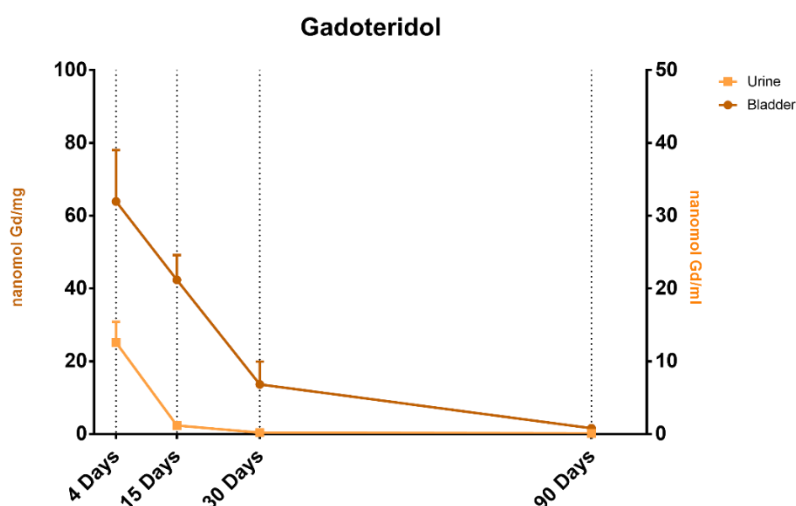


**Figure 4:** Gadoteridol excretion curve in bladder and in urine at 4, 15, 30 and 90 days after the last administration.

The bladder was also analysed to determine the amount of water insoluble or intact gadoteridol with respect to the total Gd concentration measured by ICP-MS (Scheme 1). In figure 5, the amount of Gd found in the water-soluble and insoluble fractions recovered from the bladders are reported, and compared to the total Gd amount, both as absolute micromoles values (Fig 5A) or relative percentages (Fig 5B).

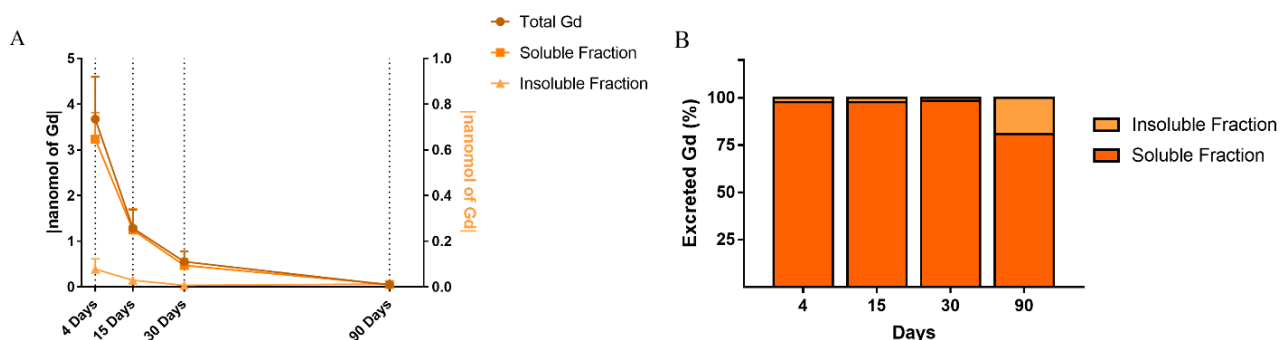


**Figure 5:** Amount of Gd (nanomoles in A and percentage in B) extracted from the water soluble and insoluble fractions of the bladder compared to total.

It can be noticed that almost all (94.5-99.1 %) gadolinium is recovered in the water soluble fraction extracted from bladder homogenates up to 1 month after the last gadoteridol administration. Interestingly, 3 months after injections, the percentage of Gd present in the insoluble fraction increases to 27%. Accordingly, the water soluble Gd decreased to 77%. The bladder was further investigated for the quantification of the amount of intact gadoteridol in the water soluble fraction extracted from homogenized tissue. As reported in figure 6, the amount of intact Gd-complex corresponds to ca. 100% up to 1 month after the injections, whereas it decreases to  $64 \pm 13\%$  when the analysis is moved to 3 months.

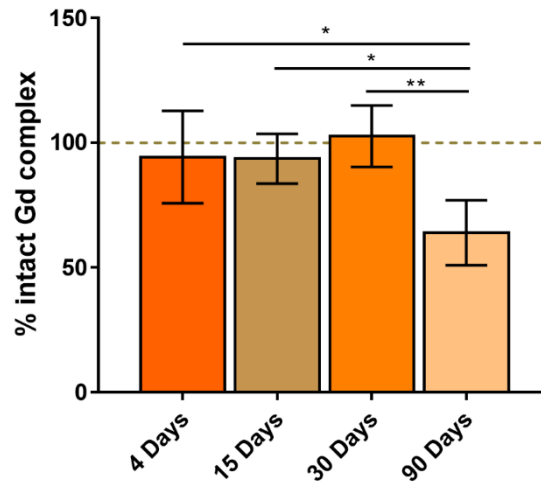


**Figure 6:** Percentage of intact gadoteridol with respect to total Gd found in the bladder.

Trichrome staining histological images on bladder tissues from mice administered with gadoteridol are reported in figure 7A. Two groups of control mice were included in the examinations, namely “control young” and “control old”, corresponding to mice, not treated with gadoteridol, 7 weeks or 18 weeks old, respectively. The group of “control old” mice was included in the study to rule out morphological changes due to physiological ageing of the mice.

The quantitative analysis of collagen (blue colored) content in the different specimens is reported in figure 7B. As can be noticed, either by observing the images and their quantitative analysis, the content of collagen significantly increases in bladders of mice administered with gadoteridol with respect to control mice. Moreover, the amount of collagen increases with increasing sacrifice time after the last injection. A thickening of the epithelium can be observed as well.

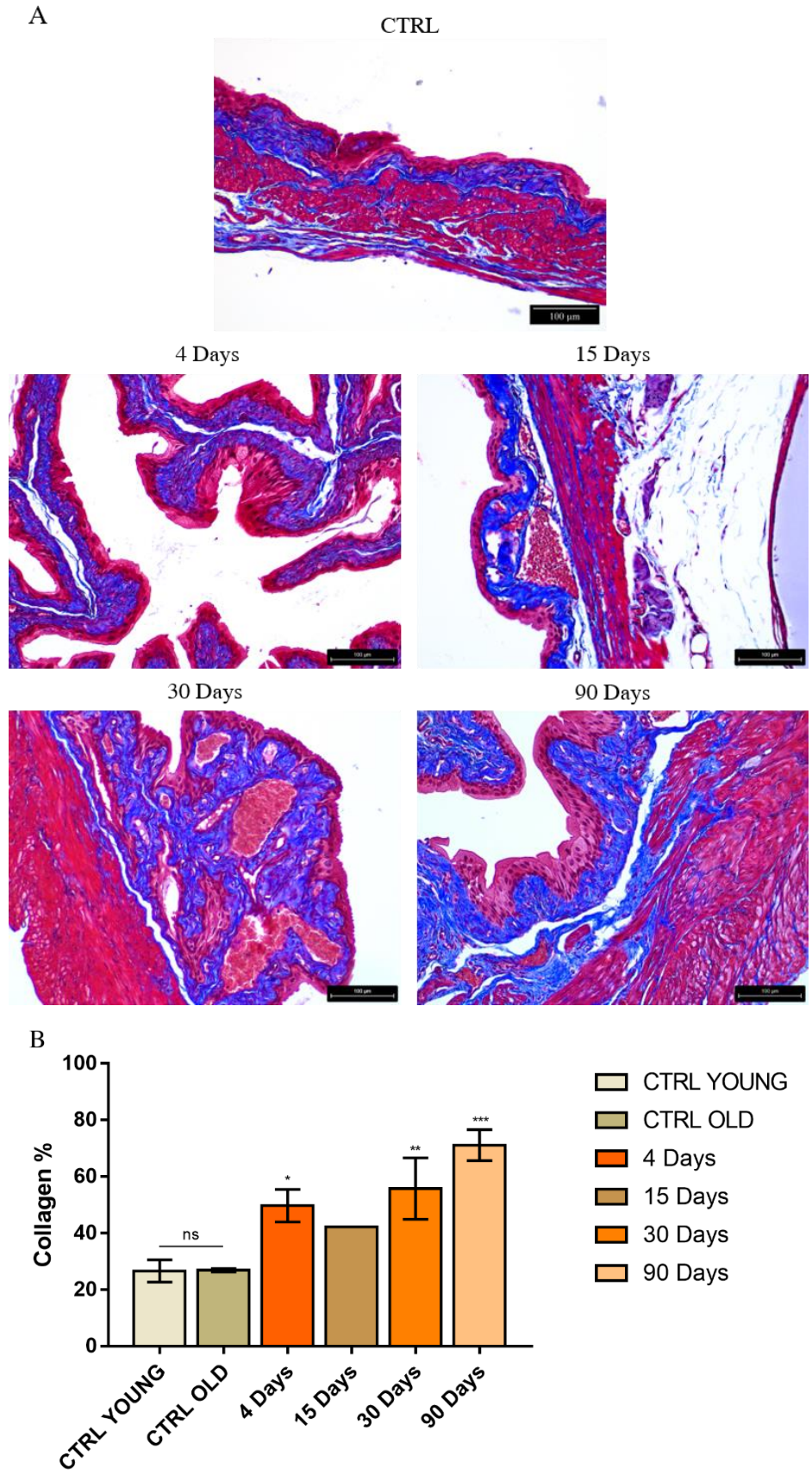


**Figure 7:** A. Trichrome staining on bladder samples with 20X enlargement at different timepoints after the last gadoteridol administration. Blue: collagen; Red: muscle fibers; Black/Blue: nuclei. B) Quantitative analysis of blue colored pixels indicative of collagen content.



## Spleen

The spleen, together with bones and bladder, is one of the organs where Gd is retained at high concentration for longer times. The Gd concentration found 90 days after the administrations is 621 times higher than baseline value.

In this study, we aimed at distinguishing the amount of Gd retained in the spleen capsule and in the spleen pulp splenocytes. To be able to calculate the amount of Gd per cell, a correlation line between the mg of proteins and the number of splenocytes has been built (Fig 8). The R squared of the line is 0.892 and the p-value is <0.0001. Indeed, having lysed the erythrocytes, the splenocytes population was composed by T and B cells, monocytes, granulocytes, dendritic cells, natural killer cells and macrophages<sup>161</sup>.

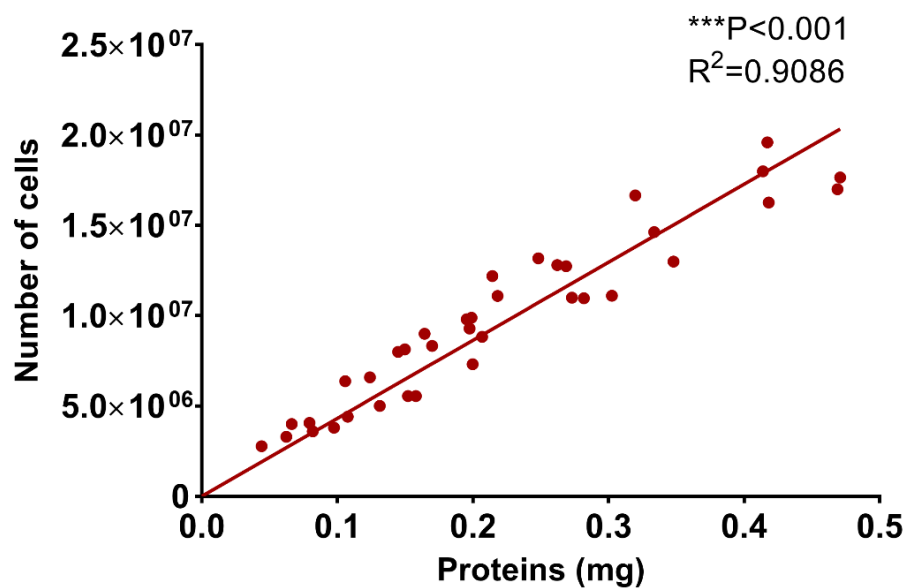


Figure 8: Correlation line between the mg of proteins and number of splenocytes.

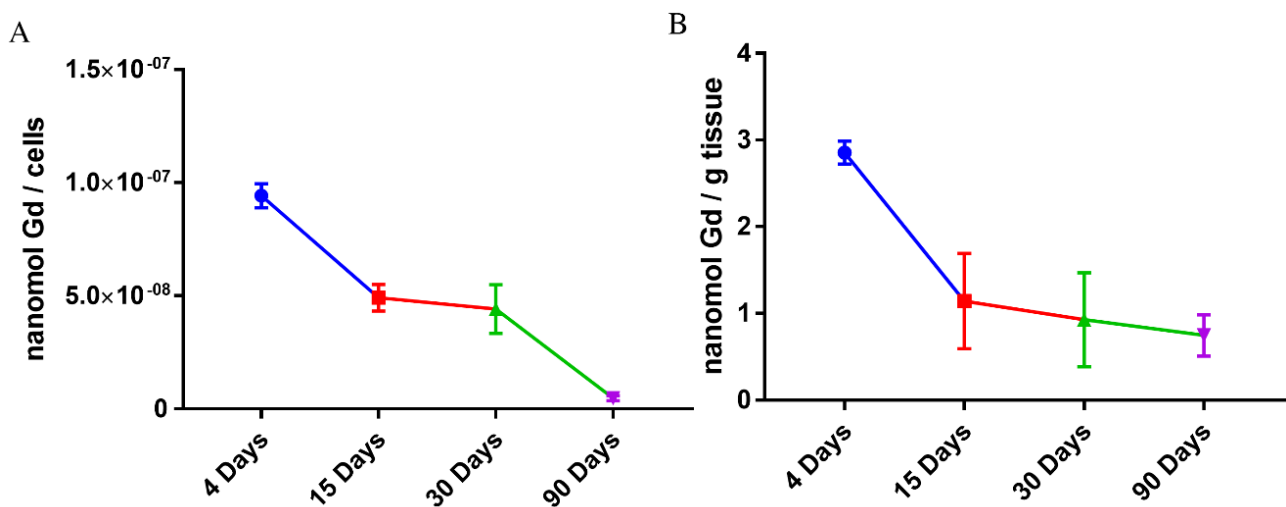
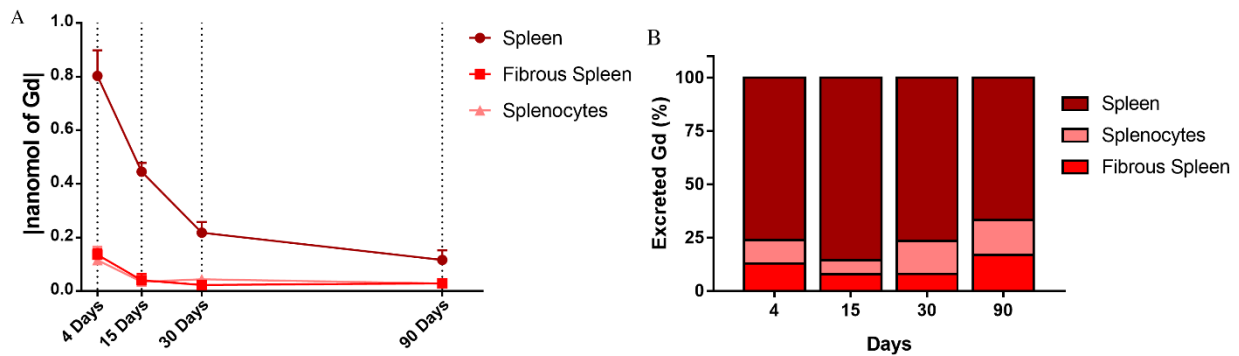


Figure 9: Gadoteridol excretion curve in A) splenocytes and B) spleen capsulae.

Interestingly, when the number of moles of Gd found in the pulp (splenocytes only) and the capsulae (fibrous tissue) are compared to the total number of Gd moles retained in the entire spleen (Fig 10), it can be noticed that only 20-40% of total Gd is recovered. This means that most of Gd<sup>3+</sup> retained in

the spleen (60-80%) belongs to splenic regions which were not investigated in the experimental protocol used in this study, such as red blood cells, extracellular matrix etc.



**Figure 10:** A) total amount of Gd (in nanomoles) found in the entire spleen, into splenocytes and in the capsulae. B) percentage of Gd found in splenocytes and capsulae with respect to total Gd found in the entire spleen (100%).

On this organ, trichrome staining was performed at the different time points, but no differences with respect to the control were observed. The blue parts, as previously described, are the ones highlighting collagen. As we can observe from figure 11, there is no blue-colored tissue, except the nuclei of the lymphocytes in the white pulp.

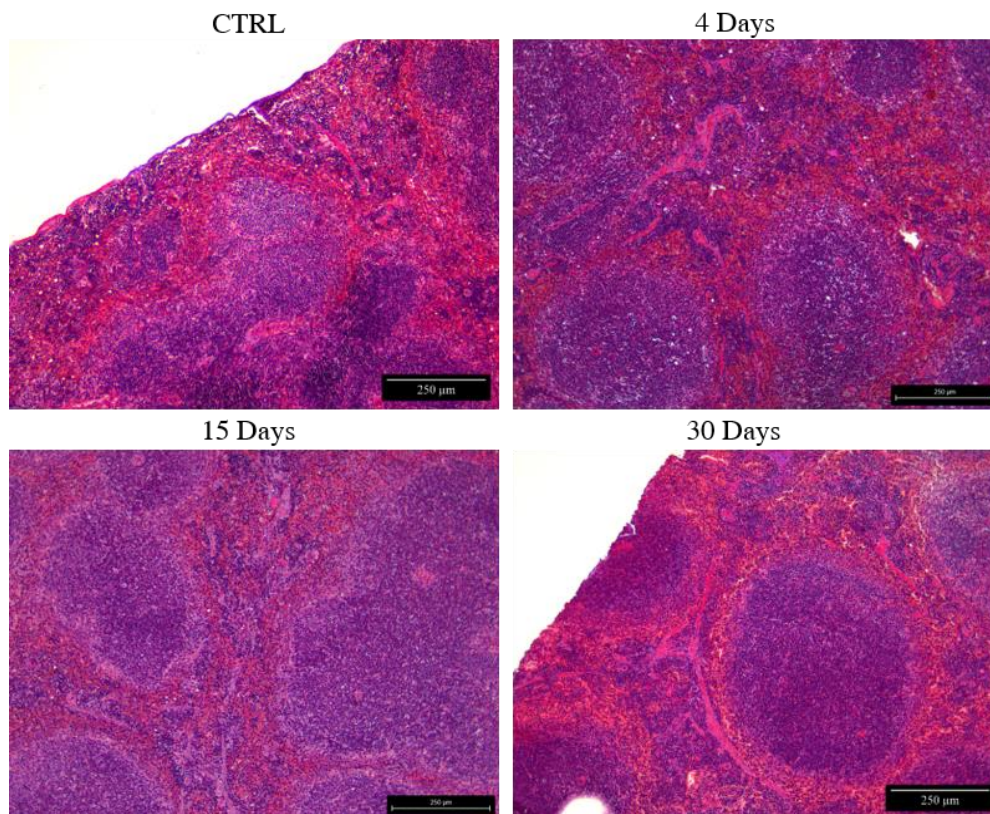


**Figure 11:** Trichrome staining on spleen samples. 10x enlargement. Blue: collagen; Red: muscle fibers; Black/Blue: nuclei

## Bone

The mean total Gd concentrations retained in the bone reported in figure 2 showed that the Gd retained in this organ remains almost constant over time. The aim of this investigation was to distinguish the amount of Gd retained in bone matrix and in bone marrow.

In order to do so, and in particular to be able to calculate the amount of Gd per cell of the bone marrow, a correlation line between the mg of proteins and the number of cells has been built (Fig 12). Despite the R squared of the line is only 0.6108, the p-value is <0.001.

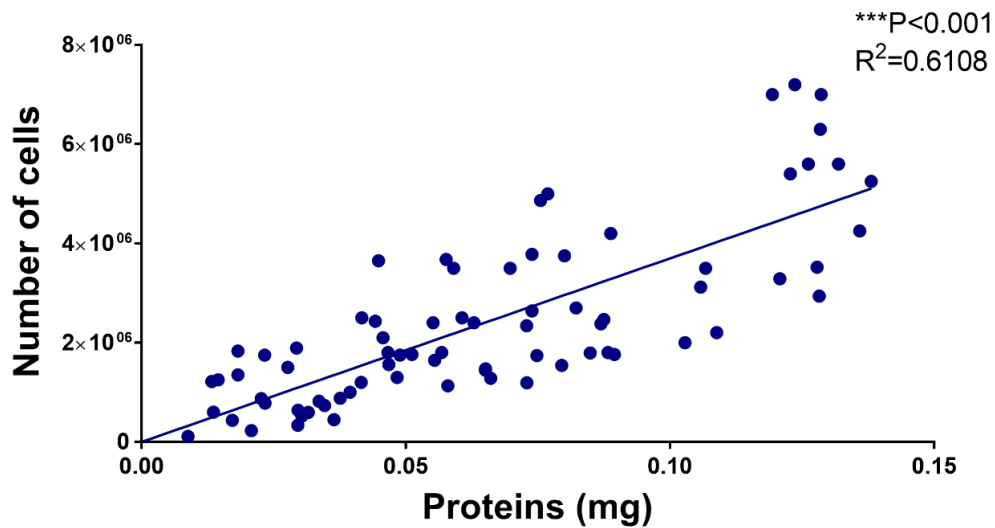


**Figure 12:** Correlation line between the mg of proteins and number of bone cells.

The mean total Gd concentrations retained in the bone marrow and in the bone matrix are reported in figure 13 A and B, respectively.

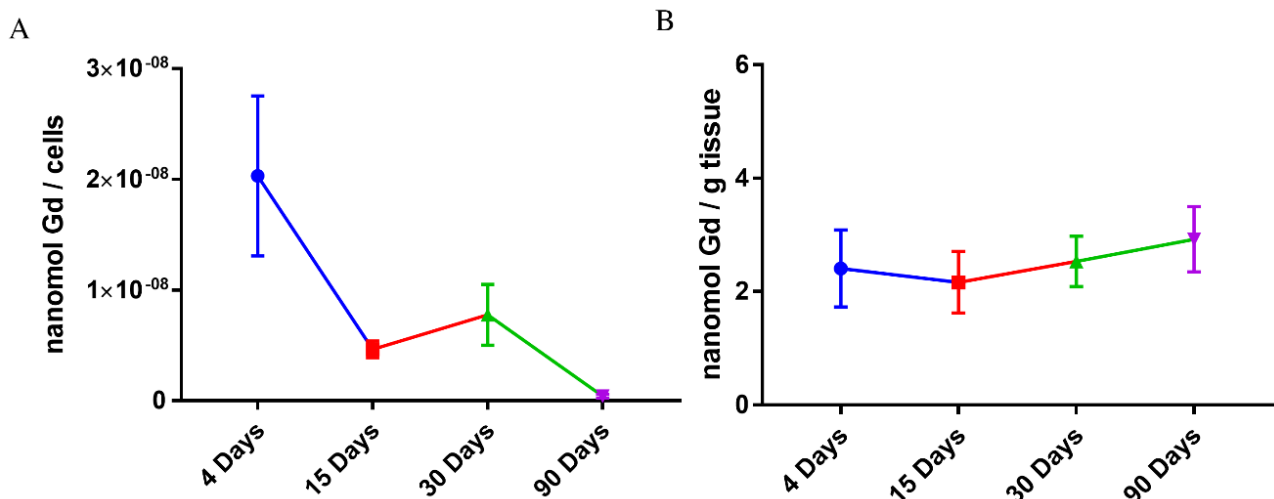


**Figure 13:** Gadoteridol excretion curve in bone marrow cells (A) and in bone matrix (B).

As done for the spleen, we deemed interesting to compare the amounts of total moles of Gd found in the matrix or in the bone marrow cells with the number of moles found in the whole tibia (Fig 14). As expected, most of Gd retained in the organ remained in the bone matrix, while a very low and time-decreasing amount was found in the bone marrow cells.

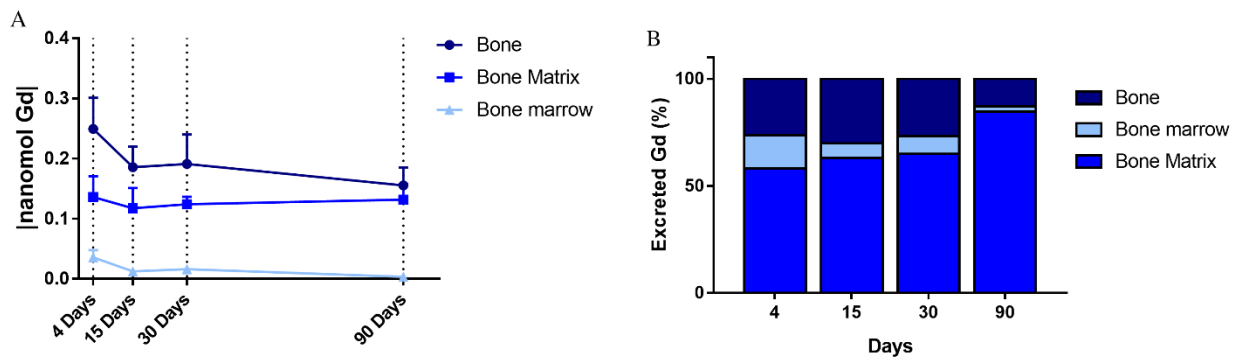


**Figure 14:** A): The total amount of Gd (in nanomoles) found in the entire tibia, into bone marrow cells and in the bone matrix.

## Discussion

The research herein presented aims to clarify the washout kinetics of gadoteridol in different organs of healthy preclinical animal models and to elucidate the possible morphological alterations and effects of the gadolinium retention on these organs, both over short and long terms. The organs, which have been analysed, are cerebrum, cerebellum, liver, spleen, bones, bladder and kidneys. Particular attention has been dedicated to bladder, since it is the organ devoted to the short-term storage of urines, through which GBCAs are eliminated, and it was reported that toxicants metabolized and excreted in the urine may have oncogenic implications for bladder urothelium<sup>162</sup>. This is the first study analysing this organ in the field of Gadolinium retention.

Moreover, the herein presented study also focuses on discerning the amount of  $Gd^{3+}$  retained in bone matrix and in bone marrow, and in the fibrous part of the spleen over the spleen pulp splenocytes.

As it can be noticed from figure 2, at the shortest times, the amount of  $Gd^{3+}$  retained in the bladder was the highest over all the other investigated organs. Nevertheless, at later time points, the amount of metal retained gradually decreases reaching similar values with respect to other organs, such as spleen and bones.

Overall, in all the investigated organs, a general time dependent decrease of the amount of retained  $Gd^{3+}$  can be observed. However, it must be pointed out that the residual amount of metal retained at 90 days after the injections is significantly higher than controls in all the investigated organs. For what concerns cerebrum and cerebellum, our results are in line with previous studies<sup>41,124,125</sup>. Indeed, it is well documented in literature that small amounts of  $Gd^{3+}$  can be retained in these organs, even in cases of normal renal function. As a support for this claim, *Frenzel et al.*<sup>125</sup> established the ability of GBCAs to cross BBB, even though the mechanism for this passage is still not clear. It seems that the Dentate Nucleus and the Globus Pallidus could be the most involved regions in this mechanism, as they are rich in receptors and transporters for metal ions<sup>29</sup>.

Concerning liver and kidneys, our results are consistent with previous studies<sup>124,159</sup>. On these organs, the trichrome staining did not highlight any differences with respect to the control as reported in figure 3, consistent with previous studies in which it was reported that tiny amounts of metal retained in the various organs is not combined to any histopathological change<sup>29</sup>.

We have also decided to analyse the urinary bladder. The main function of this organ is to act as a short-term storage for the urine, maintaining the composition of this fluid similar to the one generated by the kidneys<sup>163</sup>. Excluding the actively transported substances, the urothelium should be impermeable to all substances present in both the urine and the blood<sup>163</sup>. Nevertheless, the scientific community is increasingly aware of the fact that the bladder, if exposed to certain substances present in the urine, could retain some of them. Indeed, a study from *Bjurlin et al.*<sup>162</sup> points out that biomarkers of carcinogens present in electronic cigarettes, and therefore in the urine, are linked to bladder cancer. They declare that long-term implications of urothelial exposure to these toxicants are not well understood at the moment, but could be concerning. As a matter of fact, our results point out that the findings of the above mentioned study<sup>162</sup> could be transferred also to  $Gd^{3+}$  retention issue.

Our data prove a rapid excretion of the metal in the urine, confirming that the administered GBCA is almost completely excreted through the renal route. Nonetheless, in bladder very high amount of retained  $Gd^{3+}$  are found, especially at the shortest sacrifice times. The decreasing Gd content profiles in bladder and in urine (Fig 4) are rather similar, to suggest that the high amount of Gd found in the bladder is likely related to the passage and stasis of urines<sup>160</sup>. Unfortunately, there are no available results in the literature to be compared with our findings: further analysis considering other GBCAs and their retention in this organ is a current research ongoing in our laboratory.

The amount of water insoluble or intact soluble gadoteridol with respect to the total  $Gd^{3+}$  concentration in the bladder were also determined. The rationale for this experimental set-up relies on the fact that it is expected that eventual dechelated Gd could form water insoluble deposits while intact gadoteridol maintains its high solubility in aqueous solutions. In a recent paper<sup>164</sup> where the speciation of gadolinium in the water-insoluble rat brain fraction after administration of GBCAs was

carried out, it was found that, for the linear GBCAs, the insoluble brain fraction contain more than 50% of Gd in unidentified forms while the macrocyclic gadoterate was found to be accumulated exclusively as intact complex in the water soluble part of the brain. Our results confirm that most of the gadolinium retained after gadoteridol injection is in the water soluble fraction, even though this percentage decreases with increasing time, especially at 90 days post administration. The fact that gadoteridol administration led mainly to the retention of intact soluble GBCA are consistent with a previous study by *Gianolio et al.*<sup>34</sup>, where the speciation of gadoteridol in rat's brain was investigated. Very interestingly, the increase of the amount of Gd retained in the insoluble fraction 90 days after the injections is accompanied by a decrease of the amount of intact Gd-HPDO3A. This observation, besides being the first ever reported where a macrocyclic Gd-complex is not recovered completely as intact GBCA, leads to hypothesize, at very long times after administration, a partial dechelation of the Gd ion which can be recovered in the insoluble part of the bladder homogenate.

Another important outcome, which can be retrieved from the herein presented study about the bladder, is the fact that the retention of the metal could cause same morphological changes on the histology of the organ. Indeed, trichrome staining showed an increase in the amount of matrix (in particular HA, other glycosaminoglycans and collagen) at increasing time points. Moreover, a hyperplasia of the urothelium could also be assessed, as reported in figure 7.

This last finding is consistent with a recent study by *Tang et al*<sup>165</sup>, in which they found out that mice exposed to electronic cigarette smoke can develop bladder urothelial hyperplasia, whereas this type of lesion is extremely rare in control mice. This is in line with our first hypothesis, which lead us to analyse the bladder: some xenobiotics and toxic substances contained in the urine could possibly be retained in the bladder and lead to some consequences, which can be more or less harmful. In our case, mice did not show any type of disorder or bad consequence from gadoteridol administration.

Concerning the spleen, the total amount of retained Gd<sup>3+</sup> is consistent with previous results from *Di Gregorio et al.*<sup>124</sup>. Nevertheless, herein the main aim of our research on the spleen was to distinguish the amount of metal retained in the spleen fibrous capsule and in the spleen pulp splenocytes.

The spleen is made of red pulp and white pulp, separated by the marginal zone; 76-79% of a normal spleen is red pulp (Fig 15)<sup>166</sup>. Unlike white pulp, which mainly contains lymphocytes such as T cells, red pulp is made up of several different types of blood cells, including platelets, granulocytes, red blood cells, and plasma. The red pulp of the spleen is composed of connective tissue known also as the cords of Billroth (consisting of fibrils and connective tissue cells with a large population of monocytes and macrophages) and many splenic sinusoids that are filled with blood, giving it a red color.

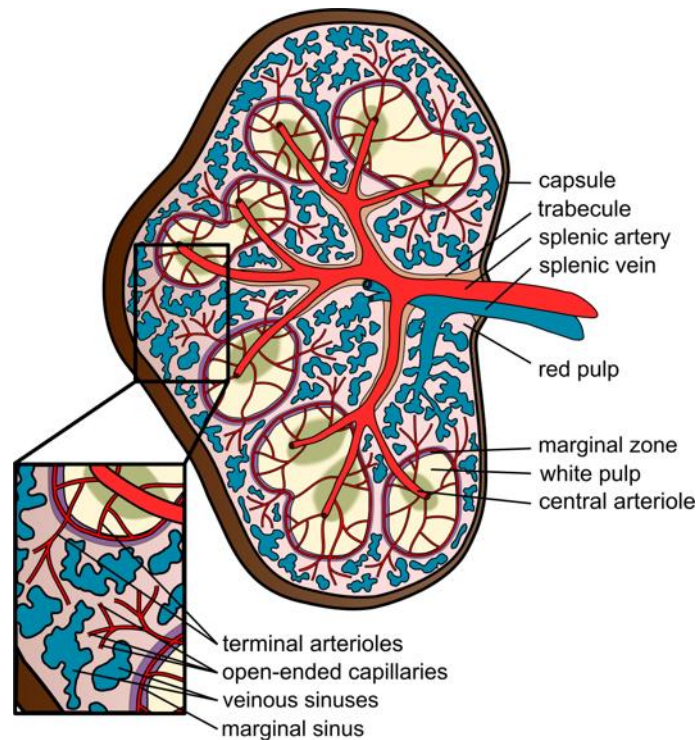


**Figure 15:** Anatomy of the rodent spleen. The spleen is compartmentalized into distinct zones organized according to their vascularization. The splenic artery branches into central arterioles sheathed by lymphoid tissue called the white pulp (WP). The central arterioles further divide into terminal arterioles which either end in the sinus of the marginal zone (MZ) that surrounds the WP or become open-ended capillaries in the cords of the red pulp (RP). In the RP, blood discharged by these capillaries runs into venous sinuses, which collect into the splenic vein. Large splenic arteries and veins are supported by trabeculae stemming from the contractile capsule of the spleen<sup>167</sup>.

As explained in the experimental section, we used a protocol for the isolation of splenic cells consisting in their separation from the fibrous parts. Subsequent lysis of red blood cells with a proper buffer allowed for the isolation of leukocytes.

We found out that most of the metal retained in the spleen was not recovered by summing the quantity retrieved in the fibrous parts and in the leukocytes. Therefore, the majority of  $Gd^{3+}$  in the spleen must be retained in parts of the organ which have not been investigated in this study, such as red blood cells and part of the extra cellular matrix (ECM).

This hypothesis seems to be plausible as the spleen is characterized by a peculiar ECM structure and a molecular composition diversified for the different compartments (WP, RP and MZ)<sup>168</sup>.

Particularly prominent reticular fibers occur in secondary lymphoid organs, such as the spleen, where, because of their fluid draining function, they have also been termed “conduits”. Conduits in this context are, therefore, reticular fibers with an unusually large diameter (1–2 $\mu$ m), characterized by an outer basement membrane layer, and a central fibrillar collagen core as a defined substructure. It is likely that Gadolinium eventually retained within these structures could be washed away and loosed during the extraction procedure.

The histological study performed on this organ showed no alterations in collagen content, nor histopathological changes, as reported in figure 11, which is consistent with the observations of a previous study by *Gianolio et al.*<sup>44</sup> change of the spleen.

Finally, our  $Gd^{3+}$  quantifications in the bones are in line with previous studies, such as the ones by *Di Gregorio et al.*<sup>29,159</sup> and from *Bussi et al.*<sup>24</sup> As can be deduced by figure 2, the amount of metal retained is almost constant over time.

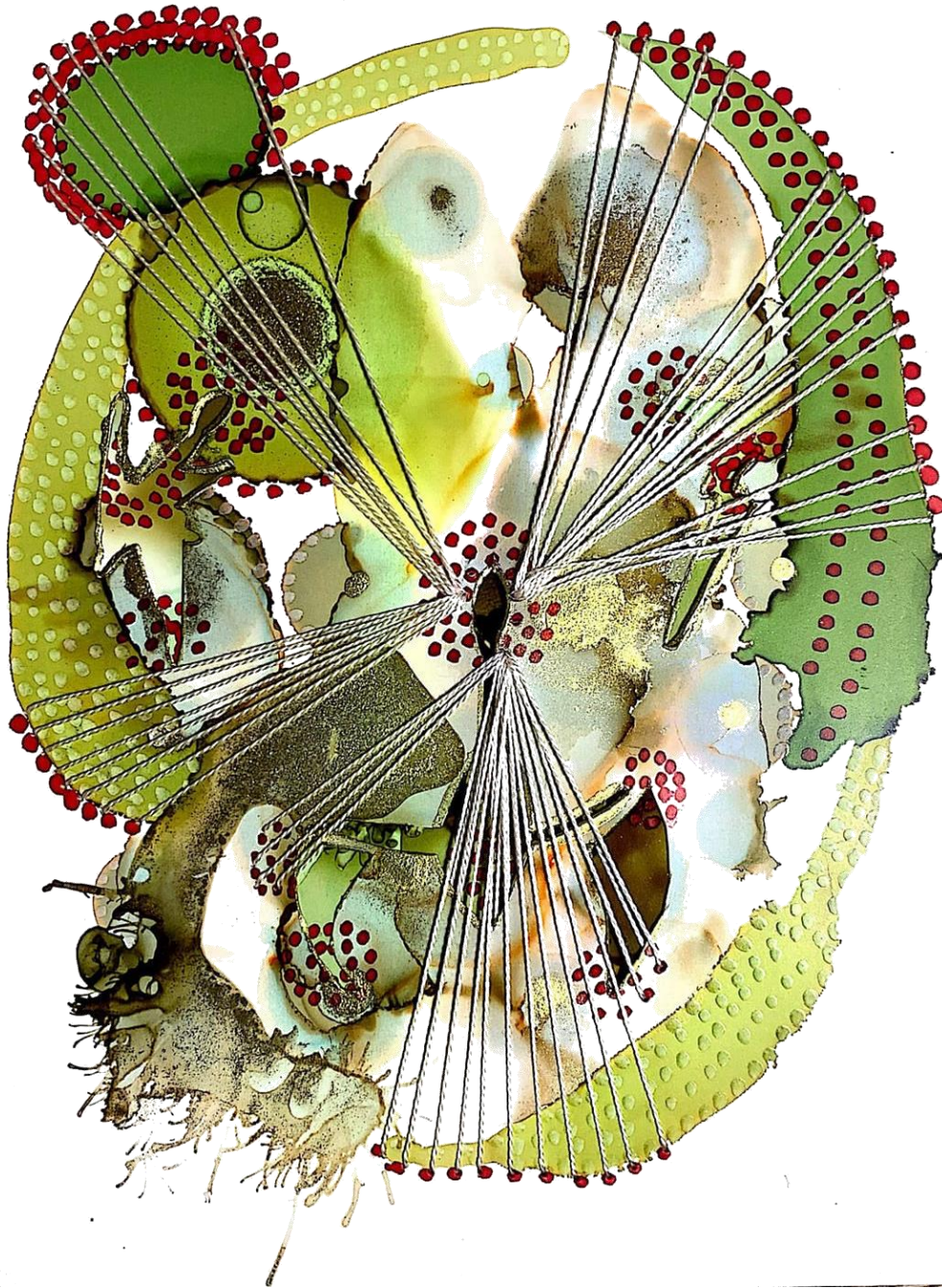
Here, our purpose was to distinguish the amount of  $Gd^{3+}$  retained in the bone matrix from the one in the bone marrow. The results allow to conclude that  $Gd^{3+}$  accumulates to a higher extent in the matrix

with respect to the bone marrow. This finding is sound as the bone matrix is composed by 67% of inorganic matter, in particular calcium phosphate<sup>169</sup>.

The extreme stability of the macrocyclic chelate Gd-HPDO3A should avoid migration and fixation of the metallic cation into the tissues. It was, however, recently established that a residual fraction of gadolinium remains in the skeleton, either of patients dosed with Gd DTPA-BMA and Gd-HPDO3A, even after several years<sup>170</sup>. A possible substitution of the Gd<sup>3+</sup> cation within the chelates was proposed to account for this observation, although the speciation of the gadolinium embedded in the bone was not established in that study. The thermodynamic possibility for gadolinium to enter the apatite lattice, and its long life within bone, assumes its incorporation as “free” rather than chelated Gd<sup>3+</sup><sup>171</sup>.

This hypothesis was recently confirmed in a study from Schlatt et al<sup>149</sup> where the speciation analysis of gadolinium from GBCAs in bones was carried out. The authors concluded that, both in the case of linear and macrocyclic contrast agents, the gadolinium found in the bones samples was mostly present as dechelated metal or otherwise bound to endogenous components, but not complexed to initial ligand.





# GENERAL CONCLUSIONS

The overall goal of the work presented here was to gain a better understanding of the mechanisms involved in the Gd retention and long-term consequences that may occur in human patients through investigations carried out at the preclinical level in mice animal models. As previously stated in the other chapters, one of the major concerns about Gd deposition in the body is the stability of GBCAs in an *in vivo* system. Since 2017, the linear compounds, characterized by lower stability constants, are no longer used in clinical practice;<sup>10</sup> nevertheless, deposition of Gd has been associated also to use of the macrocyclic Gd-based contrast agents. The free ion Gd<sup>3+</sup> is extremely toxic, because its characteristic to be a competitor for many ions required for proper functioning of the body, in particular Ca<sup>2+</sup>.<sup>172</sup> As aforementioned, one of the main goal of Gd retention studies is to understand the mechanisms behind the metal deposition in the CNS.

The influence of GBCAs structural variations and different formulation on Gadolinium retention has been the focus of attention in **Chapter 1**. The goal of the first part was to see if minor structural changes can affect the biodistribution and retention of macrocyclic Ln(III)-complexes (Ln(III)= Gd, Eu or Tb) in the main body districts when several closely related systems were given with simultaneous *i.v.* administration. The data presented indicate how, using complexes of different Lanthanide ions, it is possible to directly compare the biodistribution of different complexes, removing the uncertainties associated with animal model's variability. The behavior of the macrocyclic complexes here studied suggests that slight structural variations are sufficient to cause major changes in molecular interactions with macromolecules present in the extracellular and extravascular environment during the washout process. Indeed, it is well known that the paravascular space in the brain, through which glymphatic excretion is thought to occur, contains Glycosaminoglycans (GAGs)-based fibers that operate as a sort of sieve system for xenobiotics and wastes as they travel down the excretion pathway.<sup>48</sup> It was proposed that GAG structures might provide reversible anchoring sites for the formation of H-bonds to the GBCAs. Even though our research focused on macrocyclic compounds, analogous processes are likely to occur in linear systems as well. However, because simple generalisations do not hold true, the behaviour of any GBCA in its transit through the extracellular matrix must be studied separately.

In the second section of Chapter 1, the purpose was to explore if the Gd-retention phenomenon could be affected by a different elimination pathway, i.e. renal and/or hepatobiliary. The different interactions with the molecules of the microenvironment in which an exogenous molecule is distributed, i.e. the blood, which is the first district GBCAs experience once they are intravenously injected in the patients, are related to the different pathways that an exogenous molecule goes through *in vivo*. This study provided information on Gd retention in various organs/tissues in relation to the GBCA's ability to bind serum proteins, specifically albumin, the protein most present in blood.<sup>173,174</sup> While increasing the size of the paramagnetic complex through non covalent albumin binding results in less Gd retained in the CNS organs (cerebrum and cerebellum), the amount of metal retained in the other studied organs (liver, kidneys, muscle and bones) increases dramatically. These findings are especially important for assessing the Gd-retention issue when using blood-pool GBCAs for angiographic applications. The prolonged circulation period associated with these type of contrast agents, in theory, could raise concerns about increased Gd retention in the main organs of the body. The research presented in the last part of chapter 1 is a continuation of the study presented before, and it aimed at determining the extent of Gd-retention when a GBCA is encapsulated in the aqueous cavity of a nanosized liposome. The outcomes found out clearly indicated that the size of the administered Gd-based compound had an enhancing effect on the extent of Gd retention, in particular in the organs deputed to the contrast agent excretion (kidney, liver and spleen). The CNS (cerebrum and cerebellum) was the only districts where the amount of retained Gd was not increased when using a nanosized Gd-based system, most likely due to a higher hindrance in BBB crossing. The encapsulation of Gd-DTPABMA in the liposomal cavity, was thought with the aim to protect the GBCA from eventual interactions with the molecules of the microenvironment, thus increasing its

stability and decreasing Gd release and retention; in addition, the increased size of the system would disadvantage the GBCA's BBB crossing. Unfortunately, this approach did not result to be successful as the extent of Gd retention resulted to be increased with respect to the administration of the free GBCA.

Patients afflicted by a range of diseases are frequently subjected to several contrast enhanced Magnetic Resonance scans during their life. Thus, models of pathologies where GBCAs are commonly used in clinics were addressed in **Chapter 2**. In the first section, Multiple Sclerosis (MS) was taken into consideration because MRI is a crucial technique in the diagnosis, as well as in disease monitoring and therapy efficacy evaluation, of this pathology. In addition, alterations in blood-brain barrier permeability are commonly detected in MS by parenchymal leakage of GBCAs. This may raise concern in patients as tiny amounts of Gd can be retained in the brain of patients upon the administration of GBCAs.

The study of the amount of Gd retention in the CNS and peripheral organs of a MS preclinical animal model was carried out on an immune-mediated mouse model (Experimental Autoimmune Encephalomyelitis -EAE). The presence of significant levels of retained Gd was detected when the BBB in the neurological system of mice was disrupted. A preferential but transitory deposit of Gd had been reported in the spinal cord of EAE mice, which contains the most sclerotic plaques, in this MS model. Notably, this preferential deposit of Gd in the EAE tissue has been shown to be temporary, since increasing the sacrifice time, resulted in a reduction in Gd retention, indicating a successful washout process. Gd retention in the cerebrum and cerebellum appeared to be linked to immunization-induced inflammation rather than demyelination.

The second part of the chapter looked at a model of Inflammatory Bowel Disease (IBD) and its link with CNS via the microbiota-gut-brain axis. It was studied if inducing a substantial gastrointestinal inflammation in a well-established mouse model of colitis with dextran sulphate sodium (DSS) leads to increased Gd retention in the CNS system, excretion organs, and bones after injection of GBCA. The findings revealed that altering the permeability of the intestinal barrier in a model of DSS-induced colon inflammation might temporarily increase Gd retention in some body districts. However, this impact was time-dependent and eventually stabilised until the quantity of retained Gd was no longer distinct from that of healthy control mice. Since, inflammation is the link between both the models used in the chapter 2, the results obtained in these two preclinical studies may urge care when employing several GBCA doses in individuals with inflammatory diseases like colitis or MS.

Through the years, much attention has been paid to Gd retention in the CNS and the possible long-term consequence. Recently, two relatively new topics have been raised curiosity: the behavior of Gd in other districts than CNS, and the speciation of retained Gadolinium.<sup>34,137,149,175</sup>

Therefore, Gadolinium retention in compartments other than the CNS was the subject of **Chapter 3**. The work's initial goal was to investigate Gd behavior in the blood, because this is the tissue which GBCAs meet the most when injected intravenously. The presence of detectable levels of Gd in Red Blood Cells and White Blood Cells suggests that GBCAs can pass cellular membranes by simple diffusion or, more likely, micropinocytosis (in the case of WBCs). Previously, GBCAs were solely examined for their capacity to escape from the vessel by causing the junctions that keep the vascular compartment intact to malfunction. The discovery that hydrophilic GBCA molecules can penetrate membranes by simple diffusion against a concentration gradient raises fresh issues about the role of cellular absorption in the complex Gd retention mechanism. In this chapter, also UPLC-MS was performed to assess whether internalized Gd corresponds to the intact administered GBCA or to the free ion. The obtained data demonstrated that gadodiamide and gadoteridol entered blood cells as intact complexes, and that only Gadoteridol was stable in the intracellular milieu over the examined time frame, whereas Gadodiamide underwent partial dissociation in RBCs. Same results were showed by the *in vivo* study: while the recovered Gd is mostly intact Gd-complex 24 hours after administration

of both CAs, only Gadoteridol is still recovered intact 10 days after the administration. Indeed, as previously stated, the equilibrium stability constants of all the complexes that may form in biofluids through competition reactions in the presence of GBCAs, as well as the kinetic stability (inertness) of  $Gd^{3+}$ , determine the in vivo stability of Gd-chelates.<sup>11</sup>

In the second section of the chapter the targets of the research were bladder, spleen and bones.

Because the majority of GBCAs are almost entirely excreted through urine, it was decided to examine the bladder. Certainly, some xenobiotics and toxic substances found in the urine have been shown in the literature to be retained in the bladder and cause problems<sup>162</sup>. Next, spleen and bones were analysed because they are recognized as among the organs with highest capacity of gadolinium accumulation<sup>176,177</sup>. We found that the bladder is a highly specialised organ for metal retention. This finding is most likely due to the passage and stasis of urines containing a substantial quantity of GBCA beginning from the hours immediately after the treatment. The repeated administration of gadoteridol results in a massive Gd retention in the bladder tissue with a decreasing profile while time passing after the administrations. The GBCA is recovered entirely in its intact Gd-complex form up to one month after injections, whereas it is partially dechelated increasing the sacrifice time at 3 months. The gadolinium accumulation in the bladder tissue is accompanied by an increase in collagen content and hyperplasia of the urothelium.

From the analysis of the spleen, it was found that most of Gd is retained in its fibrous extracellular matrix component; this finding is likely related to the spleen's peculiar and unique extracellular matrix<sup>168</sup>, which allows Gd to stick after an initial washout.

The study of the bones revealed a rapid deposition of Gd with a quite low the excretion rate, especially in the bone matrix, where the majority of Gd was kept.

# REFERENCES

1. Vijayalaxmi, Fatahi M, Speck O. Magnetic resonance imaging (MRI): A review of genetic damage investigations. *Mutat. Res. Mutat. Res.* 2015;764:51–63.
2. Hashemi, Ray Hashman, William G. Bradley and CJL. *MRI: the basics: The Basics*. Lippincott Williams & Wilkins; 2012.
3. McRobbie DW, Moore EA, Graves MJ. *MRI from picture to proton.*; 2017.
4. Andr Jung B, Weigel M. Review: MR Physics for Clinicians Spin Echo Magnetic Resonance Imaging. Available at: [www.wileyhealthlearning.com](http://www.wileyhealthlearning.com).
5. Joseph P Hornak. *The basics of MRI*. (<http://www.cis.rit.edu/htbooks/mri>, ed.). Technology, Rochester Institute of; 2006.
6. Lohrke J, Frenzel T, Endrikat J, et al. 25 Years of Contrast-Enhanced MRI: Developments, Current Challenges and Future Perspectives. *Adv. Ther.* 2016;33(1):1–28.
7. Van Zijl PCM, Yadav NN. Chemical exchange saturation transfer (CEST): What is in a name and what isn't? *Magn. Reson. Med.* 2011;65(4):927–948.
8. Xiao YD, Paudel R, Liu J, Ma C, Zhang ZS ZS. MRI contrast agents: Classification and application (Review). *Int. J. Mol. Med.* 2016;38:1319–1326.
9. Bellin MF, Van Der Molen AJ. Extracellular gadolinium-based contrast media: An overview. *Eur. J. Radiol.* 2008;66(2):160–167.
10. European Medicines Agency. Gadolinium-containing contrast agents. 2017.
11. Baranyai Z, Brücher E, Uggeri F, et al. The role of equilibrium and kinetic properties in the dissociation of Gd[DTPA-bis(methylamide)] (Omniscan) at near to physiological conditions. *Chem. - A Eur. J.* 2015;21(12):4789–4799.
12. Baranyai Z, Pálkás Z, Uggeri F, et al. Dissociation kinetics of open-chain and macrocyclic gadolinium(III)-aminopolycarboxylate complexes related to magnetic resonance imaging: Catalytic effect of endogenous ligands. *Chem. - A Eur. J.* 2012;18(51):16426–16435.
13. Weinmann HJ, Laniado M MW. Pharmacokinetics of GdDTPA/dimeglumine after intravenous injection into healthy volunteers. *Physiol. Chem. Phys. Med. NMR.* 1984;16:167–172.
14. Baranyai Z, Pálkás Z, Uggeri F, et al. Equilibrium studies on the Gd<sup>3+</sup>, Cu<sup>2+</sup> and Zn<sup>2+</sup> complexes of BOPTA, DTPA and DTPA-BMA ligands: Kinetics of metal-exchange reactions of [Gd(BOPTA)]<sup>2-</sup>. *Eur. J. Inorg. Chem.* 2010;(13):1948–1956.
15. Burai L, Brücher E, Király R, et al. [Complexation properties of the ligand EOB-DTPA and the kinetic stability of Gd(EOB-DTPA)]. *Acta Pharm. Hung.* 2000;70(3–6):89–96.
16. Caravan P, Comuzzi C, Crooks W, et al. Thermodynamic stability and kinetic inertness of MS-325, a new blood pool agent for magnetic resonance imaging. *Inorg. Chem.* 2001;40(9):2170–2176.
17. Imura H, Choppin GR, Cacheris WP, et al. Thermodynamics and NMR studies of DTPA-bis(methoxyethylamide) and its derivatives. Protonation and complexation with Ln(III). *Inorganica Chim. Acta.* 1997;258(2):227–236.
18. Clarke ET, Martell AE. Stabilities of trivalent metal ion complexes of the tetraacetate derivatives

- of 12-, 13- and 14-membered tetraazamacrocycles. *Inorganica Chim. Acta.* 1991;190(1):37–46.
19. Kumar K, Tweedle MF, Malley MF, et al. Synthesis, Stability, and Crystal Structure Studies of Some Ca<sup>2+</sup>, Cu<sup>2+</sup>, and Zn<sup>2+</sup> Complexes of Macrocyclic Polyamino Carboxylates. *Inorg. Chem.* 1995;34(26):6472–6480. Available at: <https://pubs.acs.org/sharingguidelines>.
20. Sarka L, Burai L, Brücher E. The rates of the exchange reactions between [Gd(DTPA)]<sup>2-</sup> and the endogenous ions Cu<sup>2+</sup> and Zn<sup>2+</sup>: a kinetic model for the prediction of the in vivo stability of [Gd(DTPA)]<sup>2-</sup>, used as a contrast agent in magnetic resonance imaging. *Chemistry.* 2000;6(4):719–724.
21. Spinazzi A, Lorusso V, Pirovano G, et al. Safety, tolerance, biodistribution, and MR imaging enhancement of the liver with gadobenate dimeglumine: results of clinical pharmacologic and pilot imaging studies in nonpatient and patient volunteers. *Acad. Radiol.* 1999;6(5):282–291.
22. Hamm B, Staks T, Mühler A, et al. Phase I clinical evaluation of Gd-EOB-DTPA as a hepatobiliary MR contrast agent: safety, pharmacokinetics, and MR imaging. *Radiology.* 1995;195(3):785–792.
23. Tweedle MF, Wedeking P, Kumar K. Biodistribution of radiolabeled, formulated gadopentetate, gadoteridol, gadoterate, and gadodiamide in mice and rats. *Invest. Radiol.* 1995;30(6):372–380. Available at: <http://europepmc.org/abstract/MED/7490190>.
24. Sarka L, Burai L, Király R, et al. Studies on the kinetic stabilities of the Gd<sup>(3+)</sup> complexes formed with the N-mono(methylamide), N'-mono(methylamide) and N,N"-bis(methylamide) derivatives of diethylenetriamine-N,N,N',N",N"-pentaacetic acid. *J. Inorg. Biochem.* 2002;91(1):320–326.
25. Tóth É, Király R, Platzek J, et al. Equilibrium and kinetic studies on complexes of 10-[2,3-dihydroxy-(1-hydroxymethyl)-propyl]-1,4,7,10-tetraazacyclododecane-1,4,7-triacetate. *Inorganica Chim. Acta.* 1996;249(2):191–199. Available at: <https://linkinghub.elsevier.com/retrieve/pii/0020169396050943>.
26. Davies J, Siebenhandl-Wolff P, Tranquart F, et al. Gadolinium: pharmacokinetics and toxicity in humans and laboratory animals following contrast agent administration. *Arch. Toxicol.* 2022;96(2):403–429. Available at: <https://doi.org/10.1007/s00204-021-03189-8>.
27. Attari H, Cao Y, Elmholt TR, et al. A Systematic Review of 639 Patients with Biopsy-confirmed Nephrogenic Systemic Fibrosis. *Radiology.* 2019;292(2):376–386. Available at: <https://doi.org/10.1148/radiol.2019182916>.
28. Grobner T. Gadolinium—a specific trigger for the development of nephrogenic fibrosing dermopathy and nephrogenic systemic fibrosis? *Nephrol Dial Transpl.* 2006;21:1104–1108. Available at: <https://academic.oup.com/ndt/article/21/4/1104/1932577>.
29. Gianolio E, Gregorio E Di, Aime S. Chemical Insights into the Issues of Gd Retention in the Brain and Other Tissues Upon the Administration of Gd-Containing MRI Contrast Agents. *Eur. J. Inorg. Chem.* 2019;2019(2):137–151.
30. Kanda T, Ishii K, Kawaguchi H, et al. High signal intensity in the dentate nucleus and globus pallidus on unenhanced T1-weighted MR images: Relationship with increasing cumulative dose of a gadoliniumbased contrast material. *Radiology.* 2014;270(3):834–841.
31. McDonald RJ, Levine D, Weinreb J, et al. Gadolinium retention: A research roadmap from the 2018 NIH/ACR/RSNA workshop on gadolinium chelates. *Radiology.* 2018;289(2):517–534.
32. McDonald R, McDonald JS, Kallmes DF, et al. Intracranial gadolinium deposition after contrast-enhanced MR imaging. *Radiology.* 2015;275:772–782.

33. Food and Drug Administration center for Drug Evaluation and Research (CDER). Guidance for industry Estimating the maximum safe starting dose in initial clinical trials for therapeutics in adult healthy volunteers. *Pharmacol. Toxicol.* 2005;(July).
34. Gianolio E, Bardini P, Arena F, et al. Gadolinium Retention in the Rat Brain: Assessment of the Amounts of Insoluble Gadolinium-containing Species and Intact Gadolinium Complexes after Repeated Administration of Gadolinium-based Contrast Agents. *Radiology.* 2017;285(3):839–849.
35. Di Gregorio E, Furlan C, Atlante S, et al. Gadolinium retention in erythrocytes and leukocytes from human and murine blood upon treatment with gadolinium-based contrast agents for magnetic resonance imaging. *Invest. Radiol.* 2020;55(1):30–37.
36. Tedeschi E, Caranci F, Giordano F, et al. Gadolinium retention in the body: what we know and what we can do. *Radiol. Medica.* 2017;122(8):589–600.
37. Harvey HB, Gowda V, Cheng G. Gadolinium Deposition Disease: A New Risk Management Threat. *J. Am. Coll. Radiol.* 2020;17(4):546–550. Available at: <https://doi.org/10.1016/j.jacr.2019.11.009>.
38. Ramalho M, Ramalho J, Burke LM, et al. Gadolinium Retention and Toxicity—An Update. *Adv. Chronic Kidney Dis.* 2017;24(3):138–146.
39. Lancelot E, Desché P. Gadolinium retention as a safety signal: Experience of a manufacturer. *Invest. Radiol.* 2020;55(1):20–24. Available at: [www.investigativeradiology.com](http://www.investigativeradiology.com).
40. Robert P, Fingerhut S, Factor C, et al. One-year Retention of Gadolinium in the Brain: Comparison of Gadodiamide and Gadoterate Meglumine in a Rodent Model. *Radiology.* 2018;288(2):424–433.
41. Strzeminska I, Factor C, Robert P, et al. Long-Term Evaluation of Gadolinium Retention in Rat Brain After Single Injection of a Clinically Relevant Dose of Gadolinium-Based Contrast Agents. 2020. Available at: [www.investigativeradiology.com](http://www.investigativeradiology.com).
42. Jost G, Frenzel T, Boyken J, et al. Long-term Excretion of Gadolinium-based Contrast Agents: Linear versus Macrocyclic Agents in an Experimental Rat Model. *Radiology.* 2019;290(2):340–348. Available at: <http://pubs.rsna.org/doi/10.1148/radiol.2018180135>.
43. Aime S, Jost G, Frenzel T, et al. *Letters to the Editor Differences in Molecular Structure Markedly Affect GBCA Elimination Behavior Response From.*; 2013.
44. Di Gregorio E, Ferrauto G, Furlan C, et al. The Issue of Gadolinium Retained in Tissues: Insights on the Role of Metal Complex Stability by Comparing Metal Uptake in Murine Tissues Upon the Concomitant Administration of Lanthanum- and Gadolinium-Diethylenetriaminopentaacetate. *Invest. Radiol.* 2018;53(3):167–172.
45. Le Fur M, Ratile NJ, Correcher C, et al. Yttrium-86 Is a Positron Emitting Surrogate of Gadolinium for Noninvasive Quantification of Whole-Body Distribution of Gadolinium-Based Contrast Agents. *Angew. Chemie - Int. Ed.* 2020;59(4):1474–1478.
46. Scott JE. Supramolecular organization of extracellular matrix glycosaminoglycans, in vitro and in the tissues. *FASEB J. Off. Publ. Fed. Am. Soc. Exp. Biol.* 1992;6(9):2639–2645.
47. Bussi S, Coppo A, Botteron C, et al. Differences in gadolinium retention after repeated injections of macrocyclic MR contrast agents to rats. *J. Magn. Reson. Imaging.* 2018;47(3):746–752.
48. Lei Y, Han H, Yuan F, et al. The brain interstitial system: Anatomy, modeling, in vivo measurement, and applications. *Prog. Neurobiol.* 2017;157:230–246. Available at:

<http://dx.doi.org/10.1016/j.pneurobio.2015.12.007>.

49. Gillis A, Gray M, Burstein D. Relaxivity and diffusion of gadolinium agents in cartilage. *Magn. Reson. Med.* 2002;48(6):1068–1071.
50. Castelli DD, Caligara MC, Botta M, et al. Combined High Resolution NMR and <sup>1</sup>H and <sup>17</sup>O Relaxometric Study Sheds Light on the Solution Structure and Dynamics of the Lanthanide(III) Complexes of HPDO3A. 2013. Available at: <https://pubs.acs.org/sharingguidelines>.
51. Bobot M, Thomas L, Moyon A, et al. Uremic toxic blood-brain barrier disruption mediated by AhR activation leads to cognitive impairment during experimental renal dysfunction. *J. Am. Soc. Nephrol.* 2020;31(7):1509–1521. Available at: <https://doi.org/10.1681/ASN.2019070728>.
52. Jost G, Frenzel T, Lohrke J, et al. Penetration and distribution of gadolinium-based contrast agents into the cerebrospinal fluid in healthy rats: a potential pathway of entry into the brain tissue. *Eur. Radiol.* 2017;27(7):2877–2885.
53. Shamam YM, De Jesus O. Nephrogenic Systemic Fibrosis. In: Treasure Island (FL); 2022.
54. Giesel FL, Von Tengg-Kobligh H, Wilkinson ID, et al. Influence of human serum albumin on longitudinal and transverse relaxation rates (R1 and R2) of magnetic resonance contrast agents. *Invest. Radiol.* 2006;41(3):222–228.
55. Pappa T, Refetoff S. Thyroid Hormone Transport Proteins: Thyroxine-Binding Globulin, Transthyretin, and Albumin. *Curated Ref. Collect. Neurosci. Biobehav. Psychol.* 2017:483–490.
56. Haginaka J. 8.9 Chromatographic Separations and Analysis: Protein and Glycoprotein Stationary Phases. *Compr. Chirality.* 2012;8:153–176.
57. Ibrahim MA, Hazhirkarzar B, Dublin AB. Gadolinium Magnetic Resonance Imaging. In: Treasure Island (FL); 2022.
58. Bremerich J, Bilecen D, Reimer P. MR angiography with blood pool contrast agents. *Eur. Radiol.* 2007;17(12):3017–3024.
59. Gianolio E, Cabella C, Colombo Serra S, et al. B25716/1: A novel albumin-binding Gd-AAZTA MRI contrast agent with improved properties in tumor imaging Topical Issue in honor of Ivano Bertini. Guest editors: Lucia Banci, Claudio Luchinat. *J. Biol. Inorg. Chem.* 2014;19(4–5):715–726.
60. Laurent S, Elst L Vander, Muller RN. Comparative study of the physicochemical properties of six clinical low molecular weight gadolinium contrast agents. *Contrast Media Mol. Imaging.* 2006;1(3):128–137. Available at: [www.interscience.wiley.com](http://www.interscience.wiley.com).
61. Henrotte V, Muller RN, Bartholet A, et al. The presence of halide salts influences the non-covalent interaction of MRI contrast agents and human serum albumin. *Contrast Media Mol. Imaging.* 2007;2(5):258–261.
62. Noce A La, Stoelben S, Scheffler K, et al. B22956/1, a New Intravascular Contrast Agent for MRI. *Acad. Radiol.* 2002;9(2):S404–S406.
63. Cavagna FM, Lorusso V, Anelli PL, et al. Preclinical profile and clinical potential of gadocoletic acid trisodium salt (B22956/1), a new intravascular contrast medium for MRI. *Acad. Radiol.* 2002;9 Suppl 2:S491-4.
64. de Haen C, Anelli PL, Lorusso V, et al. Gadocoletic acid trisodium salt (b22956/1): a new blood pool magnetic resonance contrast agent with application in coronary angiography. *Invest. Radiol.* 2006;41(3):279–291. Available at: <http://journals.lww.com/00004424-200603000-00011>.



65. Lorusso V, Pascolo L, Ferneti C, et al. In vitro and in vivo hepatic transport of the magnetic resonance imaging contrast agent B22956/1: role of MRP proteins. *Biochem. Biophys. Res. Commun.* 2002;293(1):100–105.
66. Cavagna FM, Anelli PL, Lorusso V, et al. B-22956, a new intravascular contrast agent for MR coronary angiography. *Proc Intern Soc Magn Reson Med.* 2001;1(December 2014):519.
67. Pascolo L, Cupelli F, Anelli PL, et al. Molecular mechanisms for the hepatic uptake of magnetic resonance imaging contrast agents. *Biochem. Biophys. Res. Commun.* 1999;257(3):746–752.
68. Heffern MC, Matosziuk LM, Meade TJ. Lanthanide Probes for Bioresponsive Imaging. 2013. Available at: <https://pubs.acs.org/sharingguidelines>.
69. Jezzard P, Buxton RB. The Clinical Potential of Functional Magnetic Resonance Imaging. *J. Magn. Reson. Imaging.* 2006;23:787–793. Available at: [www.interscience](http://www.interscience).
70. Zhang H, Maki JH, Prince MR. 3D Contrast-Enhanced MR Angiography. *J. Magn. Reson. Imaging.* 2007;25:13–25.
71. Mulder WJM, Strijkers GJ, Van Tilborg GAF, et al. Lipid-based nanoparticles for contrast-enhanced MRI and molecular imaging. *NMR Biomed.* 2006;19:142–164. Available at: [www.interscience.wiley.com](http://www.interscience.wiley.com).
72. Wahsner J, Gale EM, Rodríguez-Rodríguez A, et al. Chemistry of MRI Contrast Agents: Current Challenges and New Frontiers. *Chem. Rev.* 2019;119(2):957–1057.
73. Marasini R, Thanh Nguyen TD, Aryal S. Integration of gadolinium in nanostructure for contrast enhanced-magnetic resonance imaging. *Wiley Interdiscip. Rev. Nanomedicine Nanobiotechnology.* 2020;12(1):1–17.
74. Gizzatov A, Key J, Aryal S, et al. Hierarchically structured magnetic nanoconstructs with enhanced relaxivity and cooperative tumor accumulation. *Adv. Funct. Mater.* 2014;24(29):4584–4594. Available at: [www.MaterialsViews.com](http://www.MaterialsViews.com).
75. McDonald WI, Compston A, Edan G, et al. Recommended diagnostic criteria for multiple sclerosis: Guidelines from the International Panel on the Diagnosis of Multiple Sclerosis. *Ann. Neurol.* 2001;50(1):121–127.
76. Polman CH, Reingold SC, Banwell B, et al. Diagnostic criteria for multiple sclerosis: 2010 Revisions to the McDonald criteria. *Ann. Neurol.* 2011;69(2):292–302.
77. Yang L, Krefting I, Gorovets A, et al. Nephrogenic systemic fibrosis and class labeling of gadolinium-based contrast agents by the Food and Drug Administration. *Radiology.* 2012;265(1):248–253.
78. Errante Y, Cirimele V, Mallio CA, et al. Progressive increase of T1 signal intensity of the dentate nucleus on unenhanced magnetic resonance images is associated with cumulative doses of intravenously administered gadodiamide in patients with normal renal function, suggesting dechelation. *Invest. Radiol.* 2014;49(10):685–690.
79. Kanal E, Tweedle MF. Residual or retained gadolinium: Practical implications for radiologists and our patients. *Radiology.* 2015;275(3):630–634.
80. Cocozza S, Pontillo G, Lanzillo R, et al. MRI features suggestive of gadolinium retention do not correlate with Expanded Disability Status Scale worsening in Multiple Sclerosis. *Neuroradiology.* 2019;61(2):155–162.
81. Tanaka M, Nakahara K, Kinoshita M. Increased signal intensity in the dentate nucleus of patients

with multiple sclerosis in comparison with neuromyelitis optica spectrum disorder after multiple doses of gadolinium contrast. *Eur. Neurol.* 2016;75(3–4):195–198.

82. Schlemm L, Chien C, Bellmann-Strobl J, et al. Gadopentetate but not gadobutrol accumulates in the dentate nucleus of multiple sclerosis patients. *Mult. Scler.* 2017;23(7):963–972.

83. Forslin Y, Shams S, Hashim F, et al. Retention of gadolinium-based contrast agents in multiple sclerosis: Retrospective analysis of an 18-year longitudinal study. *Am. J. Neuroradiol.* 2017;38(7):1311–1316.

84. Stojanov DA, Aracki-Trenkic A, Vojinovic S, et al. Increasing signal intensity within the dentate nucleus and globus pallidus on unenhanced T1W magnetic resonance images in patients with relapsing-remitting multiple sclerosis: correlation with cumulative dose of a macrocyclic gadolinium-based contrast agent, gadobutrol. *Abbreviations MRI Magnetic resonance imaging Gd Gadolinium SI Signal intensity RRMS Relapsing-remitting multiple sclerosis SPMS Secondary progressive multiple sclerosis. Z. Djindjica.* 2016;48:807–815.

85. Splendiani A, Perri M, Marsecano C, et al. Effects of serial macrocyclic-based contrast materials gadoterate meglumine and gadobutrol administrations on gadolinium-related dentate nuclei signal increases in unenhanced T1-weighted brain: a retrospective study in 158 multiple sclerosis (MS) patients. *Radiol. Medica.* 2018;123(2):125–134.

86. Kelemen P, Alaoui J, Sieron D, et al. T1-weighted Grey Matter Signal Intensity Alterations After Multiple Administrations of Gadobutrol in Patients with Multiple Sclerosis, Referenced to White Matter. *Sci. Rep.* 2018;8(1):1–8. Available at: <http://dx.doi.org/10.1038/s41598-018-35186-w>.

87. Langner S, Kromrey ML, Kuehn JP, et al. Repeated intravenous administration of gadobutrol does not lead to increased signal intensity on unenhanced T1-weighted images—a voxel-based whole brain analysis. *Eur. Radiol.* 2017;27(9):3687–3693.

88. Tedeschi E, Cocozza S, Borrelli P, et al. Longitudinal assessment of dentate nuclei relaxometry during massive gadobutrol exposure. *Magn. Reson. Med. Sci.* 2018;17(1):100–104.

89. Wang S, Hesse B, Roman M, et al. Increased Retention of Gadolinium in the Inflamed Brain after Repeated Administration of Gadopentetate Dimeglumine: A Proof-of-Concept Study in Mice Combining ICP-MS and Micro- A nd Nano-SR-XRF. *Invest. Radiol.* 2019;54(10):617–626.

90. Bittner S, Afzali AM, Wiendl H, et al. Myelin Oligodendrocyte glycoprotein (MOG35-55) induced experimental autoimmune encephalomyelitis (EAE) in C57BL/6 mice. *J. Vis. Exp.* 2014;(86):3–7.

91. Hasselmann JPC, Karim H, Khalaj AJ, et al. Consistent induction of chronic experimental autoimmune encephalomyelitis in C57BL/6 mice for the longitudinal study of pathology and repair. *J Neurosci Methods.* 2018:71–84.

92. Montarolo F, Raffaele C, Perga S, et al. Effects of Isoxazolo-Pyridinone 7e, a Potent Activator of the Nurr1 Signaling Pathway, on Experimental Autoimmune Encephalomyelitis in Mice. *PLoS One.* 2014;9(9):e108791. Available at: <https://doi.org/10.1371/journal.pone.0108791>.

93. Montarolo F, Perga S, Martire S, et al. Nurr1 reduction influences the onset of chronic EAE in mice. *Inflamm. Res.* 2015;64(11):841–844.

94. Center for Drug Evaluation and Research. Guidance for Industry: Estimating the Maximum Safe Starting Dose in Initial Clinical Trials for Therapeutics in Adult Healthy Volunteers. *US Dep. Heal. Hum. Serv.* 2005;(July):1–27. Available at: <http://www.fda.gov/downloads/Drugs/Guidance/UCM078932.pdf>.

95. Lombardi M, Parolisi R, Scaroni F, et al. Detrimental and protective action of microglial extracellular vesicles on myelin lesions: astrocyte involvement in remyelination failure. *Acta Neuropathol.* 2019;138(6):987–1012. Available at: <https://doi.org/10.1007/s00401-019-02049-1>.
96. Lassmann H. The changing concepts in the neuropathology of acquired demyelinating central nervous system disorders. *Curr. Opin. Neurol.* 2019;32(3):313–319.
97. Manu Rangachari and Vijay K. Kuchroo. Using EAE to better understand principles of immune function and autoimmune pathology. *J Autoimmun.* 2013;23(1):1–7. Available at: <https://www.ncbi.nlm.nih.gov/pmc/articles/PMC3624763/pdf/nihms412728.pdf>.
98. Melanie D. Sweeney, Abhay P. Sagare and BVZ. Blood–brain barrier breakdown in Alzheimer’s disease and other neurodegenerative disorders. *Physiol. Behav.* 2018;176(1):1570–1573.
99. Nishihara H, Engelhardt B. Brain Barriers and Multiple Sclerosis: Novel Treatment Approaches from a Brain Barriers Perspective. In: *Handbook of Experimental Pharmacology.*; 2020.
100. Constantinescu CS, Farooqi N, O’Brien K, et al. Experimental autoimmune encephalomyelitis (EAE) as a model for multiple sclerosis (MS). *Br. J. Pharmacol.* 2011;164(4):1079–1106.
101. Rasschaert M, Schroeder JA, Wu T Di, et al. Multimodal Imaging Study of Gadolinium Presence in Rat Cerebellum: Differences between Gd Chelates, Presence in the Virchow-Robin Space, Association with Lipofuscin, and Hypothesis about Distribution Pathway. *Invest. Radiol.* 2018;53(9):518–528.
102. Gary PH. JBM. SCT et al. Inflammatory bowel disease (first part). *New English J. Med.* 1990;323(16):1120–1123.
103. Langholz E, Munkholm P, Davidsen M, et al. Course of ulcerative colitis: Analysis of changes in disease activity over years. *Gastroenterology.* 1994;107(1):3–11. Available at: <https://www.sciencedirect.com/science/article/pii/001650859490054X>.
104. Miki K, Moore DJ, Butler RN, et al. The sugar permeability test reflects disease activity in children and adolescents with inflammatory bowel disease. *J. Pediatr.* 1998;133(6):750–754.
105. Valle-pinero AY Del, Deventer HE Van, Fourie NH, et al. Gastrointestinal permeability in patients with irritable bowel syndrome assessed using a four probe permeability solution. *Clin. Chim. Acta.* 2014:97–101.
106. Greenwood-Van Meerveld B. Intestinal barrier function in health and gastrointestinal disease: Review Article. *Neurogastroenterol. Motil.* 2012;24(9):889–889. Available at: <https://onlinelibrary.wiley.com/doi/10.1111/j.1365-2982.2012.01976.x>.
107. Ding JH, Jin Z, Yang XX, et al. Role of gut microbiota via the gut-liver-brain axis in digestive diseases. *World J. Gastroenterol.* 2020;26(40):6141–6162.
108. Han Y, Zhao T, Cheng X, et al. Cortical Inflammation is Increased in a DSS-Induced Colitis Mouse Model. *Neurosci. Bull.* 2018;34(6):1058–1066. Available at: <https://doi.org/10.1007/s12264-018-0288-5>.
109. Ferré JC, Shiroishi MS, Law M. Advanced techniques using contrast media in neuroimaging. *Magn. Reson. Imaging Clin. N. Am.* 2012;20(4):699–713.
110. Restrepo CS, Tavakoli S, Marmol-Velez A. Contrast-Enhanced Cardiac Magnetic Resonance Imaging. *Magn. Reson. Imaging Clin. N. Am.* 2012;20(4):739–760. Available at: <https://www.sciencedirect.com/science/article/pii/S1064968912000852>.
111. Serrano LF, Morrell B, Mai A. Contrast Media in Breast Imaging. *Magn. Reson. Imaging Clin.*

- N. Am. 2012;20(4):777–789. Available at: <https://www.sciencedirect.com/science/article/pii/S1064968912000839>.
112. Lin SP, Brown JJ. MR contrast agents: Physical and pharmacologic basics. *J. Magn. Reson. Imaging*. 2007;25(5):884–899.
113. Kanda T, Fukusato T, Matsuda M, et al. Gadolinium-based contrast agent accumulates in the brain even in subjects without severe renal dysfunction: Evaluation of autopsy brain specimens with inductively coupled plasma mass spectroscopy. *Radiology*. 2015;276(1):228–232.
114. Fritsch Fredin M, Vidal A, Utkovic H, et al. The application and relevance of ex vivo culture systems for assessment of IBD treatment in murine models of colitis. *Pharmacol. Res*. 2008;58(3–4):222–231.
115. Kim JJ, Shajib MS, Manocha MM, et al. Investigating intestinal inflammation in DSS-induced model of IBD. *J. Vis. Exp*. 2012;(60):1–6.
116. Margolis KG, Cryan JF, Mayer EA. The Microbiota-Gut-Brain Axis: From Motility to Mood. *Gastroenterology*. 2021;160(5):1486–1501.
117. Gracie DJ, Hamlin PJ, Ford AC. The influence of the brain–gut axis in inflammatory bowel disease and possible implications for treatment. *Lancet Gastroenterol. Hepatol*. 2019;4(8):632–642. Available at: <https://www.sciencedirect.com/science/article/pii/S2468125319300895>.
118. Craig CF, Filippone RT, Stavely R, et al. Neuroinflammation as an etiological trigger for depression comorbid with inflammatory bowel disease. *J. Neuroinflammation*. 2022;19(1):1–30. Available at: <https://doi.org/10.1186/s12974-021-02354-1>.
119. Anupriya Tripathi, Justine Debelius, David A. Brenner, Michael Karin, Michael Karin BS and RK. The gut-liver axis and the intersection with the microbiome. *Nat Rev Gastroenterol Hepatol*. 2018;176(3):139–148.
120. Corica D, Romano C. Renal involvement in inflammatory bowel diseases. *J. Crohn's Colitis*. 2015;10(2):1–10.
121. Ambruzs JM, Walker PD, Larsen CP. The histopathologic spectrum of kidney biopsies in patients with inflammatory bowel disease. *Clin. J. Am. Soc. Nephrol*. 2014;9(2):265–270. Available at: <https://pubmed.ncbi.nlm.nih.gov/24262508>.
122. Ambruzs JM, Larsen CP. Renal Manifestations of Inflammatory Bowel Disease. *Rheum. Dis. Clin. North Am*. 2018;44(4):699–714. Available at: <https://doi.org/10.1016/j.rdc.2018.06.007>.
123. Chang CJ, Wang PC, Huang TC, et al. Change in renal glomerular collagens and glomerular filtration barrier-related proteins in a dextran sulfate sodium-induced colitis mouse model. *Int. J. Mol. Sci*. 2019;20(6):1–13.
124. Di Gregorio E, Iani R, Ferrauto G, et al. Gd accumulation in tissues of healthy mice upon repeated administrations of Gadodiamide and Gadoteridol. *J. Trace Elem. Med. Biol*. 2018;48(April):239–245.
125. Frenzel T, Apte C, Jost G, et al. Quantification and assessment of the chemical form of residual gadolinium in the brain after repeated administration of gadolinium-based contrast agents comparative study in rats. *Invest. Radiol*. 2017;52(7):396–404.
126. Fretellier N, Granottier A, Rasschaert M, et al. Does Age Interfere With Gadolinium Toxicity and Presence in Brain and Bone Tissues? *Invest. Radiol*. 2019;54(2):61–71.
127. Rasschaert M, Emerit A, Fretellier N, et al. Gadolinium retention, brain T1 hyperintensity, and

endogenous metals A comparative study of macrocyclic versus linear gadolinium chelates in renally sensitized rats. 2018;53:328–337.

128. Berger F, Kubik-Huch RA, Niemann T, et al. Gadolinium Distribution in Cerebrospinal Fluid after Administration of a Gadolinium-based MR Contrast Agent in Humans. *Radiology*. 2018;288(3):703–709.

129. Le Fur M, Caravan P. The biological fate of gadolinium-based MRI contrast agents: a call to action for bioinorganic chemists. *Metallomics*. 2019;11(2):240–254.

130. Delfino R, Biasotto M, Candido R, et al. Gadolinium tissue deposition in the periodontal ligament of mice with reduced renal function exposed to Gd-based contrast agents. *Toxicol. Lett*. 2019;301(November 2018):157–167.

131. Clases D, Fingerhut S, Jeibmann A, et al. LA-ICP-MS/MS improves limits of detection in elemental bioimaging of gadolinium deposition originating from MRI contrast agents in skin and brain tissues. *J. Trace Elem. Med. Biol.* 2019;51(September 2018):212–218. Available at: <https://doi.org/10.1016/j.jtemb.2018.10.021>.

132. Lord ML, Chettle DR, Gräfe JL, et al. Observed deposition of gadolinium in bone using a new noninvasive in vivo biomedical device: results of a small pilot feasibility study. *Radiology*. 2018;287:96–103.

133. Erdene K, Nakajima T, Kameo S, et al. Organ retention of gadolinium in mother and pup mice : effect of pregnancy and type of gadolinium - based contrast agents. *Jpn. J. Radiol.* 2017;35:568–573.

134. Steger-hartmann T, Hofmeister R, Ernst R, et al. A review of preclinical safety data for Magnevist (gadopentetate dimeglumine ) in the context of nephrogenic systemic fibrosis. *Invest. Radiol.* 2010;45:520–528.

135. O’Connell KE, Mikkola AM, Stepanek AM, et al. Practical murine hematopathology: a comparative review and implications for research. *Comp. Med.* 2015;65(2):96–113. Available at: <http://www.ncbi.nlm.nih.gov/pubmed/25926395> <http://www.pubmedcentral.nih.gov/articlerender.fcgi?artid=PMC4408895>.

136. Caron A, Lelong C, Pascual M-H, et al. Miniaturized Blood Sampling Techniques to Benefit Reduction in Mice and Refinement in Nonhuman Primates: Applications to Bioanalysis in Toxicity Studies with Antibody–Drug Conjugates. *Jaalas*. 2015;54(2):145–152.

137. Kesava Raju CS, Cossmer A, Scharf H, et al. Speciation of gadolinium based MRI contrast agents in environmental water samples using hydrophilic interaction chromatography hyphenated with inductively coupled plasma mass spectrometry. *J. Anal. At. Spectrom.* 2010;25(1):55–61. Available at: [www.rsc.org/jaas](http://www.rsc.org/jaas).

138. Birka M, Wentker KS, Lusmo E, et al. Diagnosis of nephrogenic systemic fibrosis by means of elemental bioimaging and speciation analysis. *Anal. Chem.* 2015;87:3321–3328.

139. D’Onofrio G, Chirillo R, Zini G, et al. Simultaneous measurement of reticulocyte and red blood cell indices in healthy subjects and patients with microcytic and macrocytic anemia. *Blood*. 1995;85(3):818–23.

140. Hinks LJ, Clayton BE, Lloyd RS. Zinc and copper concentrations in leucocytes and erythrocytes in healthy adults and the effect of oral contraceptives. *J. Clin. Pathol.* 1983;36(9):1016–1021.

141. Herring WB, Leavell BS, Paixao LM, et al. Trace metals in human plasma and red blood cells: A Study of Magnesium, Chromium, Nickel, Copper and Zinc II. Observations of patients with some hematologic diseases. *Am. J. Clin. Nutr.* 1958:855–863.

142. Ferrauto G, Di Gregorio E, Dastrù W, et al. Gd-loaded-RBCs for the assessment of tumor vascular volume by contrast-enhanced-MRI. *Biomaterials*. 2015;58:82–92.
143. Reinhart WH, Pleisch B, Harris LG, et al. Influence of contrast media (iopromide, ioxaglate, gadolinium-DOTA) on blood viscosity, erythrocyte morphology and platelet function. *Clin. Hemorheol. Microcirc.* 2005;32(3):227–239.
144. Eylar EH, Madoff MA, Brody O V., et al. The contribution of sialic acid to the surface charge of the erythrocyte. *J. Biol. Chem.* 1962;237:1992–2000.
145. Kaur K, Gupta R, Saraf SA, et al. Zinc: The metal of life. *Compr. Rev. Food Sci. Food Saf.* 2014;13(4):358–376.
146. Rasschaert M, Idée JM, Robert P, et al. Moderate Renal Failure Accentuates T1 Signal Enhancement in the Deep Cerebellar Nuclei of Gadodiamide-Treated Rats. *Invest. Radiol.* 2017;52(5):255–264.
147. Hirano S, Suzuki KT. Exposure, metabolism, and toxicity of rare earths and related compounds. *Environ. Health Perspect.* 1996;104(suppl 1):85–95. Available at: <https://ehp.niehs.nih.gov/doi/10.1289/ehp.96104s185>.
148. Lancelot E. Revisiting the Pharmacokinetic Profiles of Gadolinium-Based Contrast Agents. *Invest. Radiol.* 2016;51(11):691–700. Available at: <https://journals.lww.com/00004424-201611000-00003>.
149. Schlatt L, Köhrer A, Factor C, et al. Mild Dissolution/Recomplexation Strategy for Speciation Analysis of Gadolinium from MR Contrast Agents in Bone Tissues by Means of HPLC-ICP-MS. *Anal. Chem.* 2021;93(33):11398–11405.
150. Freedman ND, Silverman DT, Hollenbeck AR, et al. Association between smoking and risk of bladder cancer among men and women. *JAMA - J. Am. Med. Assoc.* 2011;306(7):737–745. Available at: <https://jamanetwork.com/>.
151. Baker SC, Arlt VM, Indra R, et al. Differentiation-associated urothelial cytochrome P450 oxidoreductase predicates the xenobiotic-metabolizing activity of “luminal” muscle-invasive bladder cancers. *Mol. Carcinog.* 2018;57(5):606–618.
152. Lesseur C, Gilbert-Diamond D, Andrew AS, et al. A case-control study of polymorphisms in xenobiotic and arsenic metabolism genes and arsenic-related bladder cancer in New Hampshire. *Toxicol. Lett.* 2012;210(1):100–106. Available at: <http://dx.doi.org/10.1016/j.toxlet.2012.01.015>.
153. Murata N, Gonzalez-Cuyar LF, Murata K, et al. Macrocyclic and other non-group 1 gadolinium contrast agents deposit low levels of gadolinium in brain and bone tissue: Preliminary results from 9 patients with normal renal function. *Invest. Radiol.* 2016;51(7):447–453.
154. Cho SB, Lee AL, Chang HW, et al. Prospective Multicenter Study of the Safety of Gadoteridol in 6163 Patients. *J. Magn. Reson. Imaging.* 2020;51(3):861–868.
155. Jungblut M, Oeltze K, Zehnter I, et al. Preparation of Single-Cell Suspensions from Mouse Spleen with the gentleMACS Dissociator. *J. Vis. Exp.* 2008;(22). Available at: <http://www.jove.com/index/Details.stp?ID=1029>.
156. Beeton C, Chandy KG. Preparing T Cell Growth Factor from Rat Splenocytes. 2007. Available at: [www.jove.com?url=http://www.jove.com/video/402](http://www.jove.com?url=http://www.jove.com/video/402).
157. Liu X, Quan N. Immune Cell Isolation from Mouse Femur Bone Marrow. *BIO-PROTOCOL.* 2015;5(20).

158. Madaan A, Verma R, Singh AT, et al. A stepwise procedure for isolation of murine bone marrow and generation of dendritic cells. *J. Biol. Methods*. 2014;1(1):e1. Available at: <https://jbmmethods.org/jbm/article/view/12>.
159. Bussi S, Coppo A, Celeste R, et al. Macrocyclic MR contrast agents: evaluation of multiple-organ gadolinium retention in healthy rats. *Insights Imaging*. 2020;11(1). Available at: <https://doi.org/10.1186/s13244-019-0824-5>.
160. Layne KA, Wood DM, Dixon-Zegeye M, et al. Establishing Reference Intervals for Gadolinium Concentrations in Blood, Plasma, and Urine in Individuals Not Previously Exposed to Gadolinium-Based Contrast Agents. *Invest. Radiol*. 2020;Publish Ah(7):405–411. Available at: <https://journals.lww.com/10.1097/RLI.0000000000000657>.
161. Miltenyi B. Spleen (mouse). Available at: <https://www.miltenyibiotec.com/US-en/resources/mac-handbook/mouse-cells-and-organs/mouse-cell-sources/spleen-mouse.html#:~:text=The white pulp consists of,number of white blood cells>.
162. Bjurlin MA, Matulewicz RS, Roberts TR, et al. Carcinogen Biomarkers in the Urine of Electronic Cigarette Users and Implications for the Development of Bladder Cancer: A Systematic Review. *Eur. Urol. Oncol*. 2021;4(5):766–783. Available at: <https://doi.org/10.1016/j.euo.2020.02.004>.
163. Lewis SA. Everything you wanted to know about the bladder epithelium but were afraid to ask. *Am. J. Physiol. Physiol*. 2000;278(6):F867–F874. Available at: <https://www.physiology.org/doi/10.1152/ajprenal.2000.278.6.F867>.
164. Strzeminska I, Factor C, Robert P, et al. Speciation Analysis of Gadolinium in the Water-Insoluble Rat Brain Fraction After Administration of Gadolinium-Based Contrast Agents. *Invest. Radiol*. 2021;56(9):535–544. Available at: <https://journals.lww.com/10.1097/RLI.0000000000000774>.
165. Tang M, Wu X-R, Lee H-W, et al. Electronic-cigarette smoke induces lung adenocarcinoma and bladder urothelial hyperplasia in mice. *Proc. Natl. Acad. Sci*. 2019;116(43):21727–21731. Available at: <https://pnas.org/doi/full/10.1073/pnas.1911321116>.
166. Swerdlow SH. Disorders of the spleen, pathophysiology and management. *Hum. Pathol*. 1989;20(11):1134.
167. Bellomo A, Gentek R, Golub R, et al. Macrophage-fibroblast circuits in the spleen. *Immunol. Rev*. 2021;302(1):104–125.
168. Lokmic Z, Lämmermann T, Sixt M, et al. The extracellular matrix of the spleen as a potential organizer of immune cell compartments. *Semin. Immunol*. 2008;20(1):4–13.
169. Maas MC. Bones and Teeth, Histology of. In: *Encyclopedia of Marine Mammals*. Elsevier; 2009:124–129. Available at: <https://linkinghub.elsevier.com/retrieve/pii/B9780123735539000341>.
170. Darrah TH, Prutsman-Pfeiffer JJ, Poreda RJ, et al. Incorporation of excess gadolinium into human bone from medical contrast agents. *Metallomics*. 2009;1(6):479. Available at: <https://academic.oup.com/metallomics/article/1/6/479-488/6016731>.
171. Vidaud C, Bourgeois D, Meyer D. Bone as Target Organ for Metals: The Case of f-Elements. *Chem. Res. Toxicol*. 2012;25(6):1161–1175. Available at: <https://pubs.acs.org/doi/10.1021/tx300064m>.
172. Idée JM, Port M, Raynal I, et al. Clinical and biological consequences of transmetallation induced by contrast agents for magnetic resonance imaging: A review. *Fundam. Clin. Pharmacol*.

2006;20(6):563–576.

173. Kalra H, Adda CG, Liem M, et al. Comparative proteomics evaluation of plasma exosome isolation techniques and assessment of the stability of exosomes in normal human blood plasma. *Proteomics*. 2013;13:3354–3364. Available at: [www.proteomics-journal.com](http://www.proteomics-journal.com).

174. Mishra V, Heath RJ, Masi A Di. Molecular Sciences Structural and Biochemical Features of Human Serum Albumin Essential for Eukaryotic Cell Culture Protein Production Facility. 2021. Available at: <https://doi.org/10.3390/ijms22168411>.

175. Bücken P, Funke SKI, Factor C, et al. Combined speciation analysis and elemental bioimaging provide new insight into gadolinium retention in kidney. *Metallomics*. 2022;14(3).

176. White GW, Gibby WA, Tweedle MF. Comparison of Gd(DTPA-BMA) (Omniscan) Versus Gd(HP-DO3A) (ProHance) Relative to Gadolinium Retention in Human Bone Tissue by Inductively Coupled Plasma Mass Spectroscopy. *Invest. Radiol.* 2006;41(3):272–278. Available at: <http://journals.lww.com/00004424-200603000-00010>.

177. Gibby WA, Gibby KA, Gibby WA. Comparison of Gd DTPA-BMA (Omniscan) versus Gd HP-DO3A (ProHance) Retention in Human Bone Tissue by Inductively Coupled Plasma Atomic Emission Spectroscopy. *Invest. Radiol.* 2004;39(3):138–142. Available at: <https://journals.lww.com/00004424-200403000-00002>.